



University of
Stavanger

Faculty of Science and Technology

MASTER'S THESIS

Study program/ Specialization:

MSc in Well Engineering

Spring semester, 2014

Open / Restricted access

Writer: Farid Taghiyev

.....
(Writer's signature)

Faculty supervisor: Helge Hodne

External supervisor(s): Arild Saasen, Det norske oljeselskap ASA

Thesis title: Application of Thermo-Mechanically Treated Drill Cuttings as an Alternative to Bentonite in Spud Muds

Credits (ECTS): 30

Key words:

Petroleum engineering
Drilling engineering
Drilling fluid
Spud mud
Thermo-mechanically treated cuttings
TCC

Pages: 126

+ enclosure: 24

Stavanger, 22.05.2014

To my family and wife, for their endless love and support

Acknowledgement

I would like to express my utmost thankfulness to professors Arild Saasen and Helge Hodne for the advice they have given to me during the working process. I am also thankful to the highest degree for their contribution and follow up of my thesis work and not the least the productive discussions we have had.

I am very grateful to Mr. Jostein Tysse of Det Norske Oljeselskap ASA for suggesting the productive idea, which resulted in a whole spectrum of research.

I would like to thank Jorunn Vrålstad, Jostein Djuve, Andrea Bagi and other employees of drilling fluid laboratory for their precious help given to me during the laboratory testing.

I am thankful to the Department of Petroleum Engineering at UiS and the professors for providing me with this excellent opportunity to get the education in one of the best universities in Norway.

I would like to thank Mr. Vegard Haraldsen of TWMA for providing us with thermo-mechanically treated drill cuttings, which were used as the main material in the experimental part of this work.

I am thankful to professor Chandana Ratnayake of Tel-Tek for his help regarding determination of particle size distribution and Mr. Åsbjørn Dysvik of Rena Technology for the practical advice he has given.

Abstract

Drill cuttings recovered after drilling with OBM today are treated and deposited at onshore facilities. The TWMA Company offers a new technology, which recovers drilled subsurface materials together with oil and water rests. Due to the similarity between subsurface rock mineralogy and conventional bentonite used in the drilling fluid industry an extended laboratory study was carried out to evaluate the possibility of spud mud development using thermo-mechanically treated drill cuttings.

Prior to the main experiment a study of the material itself was performed to obtain particle size distribution of treated drill cuttings. Four groups of experiments were performed and 28 different spud mud compositions were designed (two commonly known traditional fluids are included here). The experiments were divided in the following way: fresh water and cuttings; fresh water, cuttings and polymers; seawater, cuttings, polymers and other additives; aging experiments. CMC Hi-Vis, PAC and xanthan gum polymers were tested as stabilizing agents, while CMC Lo-Vis and barite were tested for filter loss control and weighting. The fluids were mixed using standard drilling fluid laboratory equipment and tested in accordance with the API 13B-1 practices.

It was revealed that this batch of treated drill cuttings could not provide the required viscosity profile and the mixtures had very low gel strengths varying from 0 to 2 lb/100 ft². Moreover, hydration experiments demonstrated that the material was incapable of swelling even after long (10 days) exposure to fresh water. High chloride concentration (2400-4400 mg/l) and relatively low active clay content (21.4-35.6 kg/m³) in the prepared slurries were considered to be the main driving factors for this behavior. CMC Hi-Vis and PAC polymers provided unsatisfactory rheological improvements as low shear rate viscosity and gel strength remained very low. On the other hand, xanthan gum qualified as a robust stabilizing agent and stable spud mud compositions were designed. Effects of xanthan polymer concentration on the rheological properties of the fluids were studied and the obtained yield point calculated by Bingham model varied from 5.11 Pa to 12.8 Pa depending on the polymer concentration. Influence of cutting concentration on the plastic viscosity of stable spud mud compositions was studied with results varying from 6 cP to 12 cP. Effect of increased temperature on rheological properties was studied as well. CMC Lo-Vis demonstrated good filter loss control properties (10 ml API) even at concentrations as low as 2.86 kg/m³. The designed drilling fluids were as well capable of suspending heavy barite particles, which are often required during installation of casing.

Even though the treated drill cuttings alone were not capable of yielding required fluid properties a stable spud mud was developed as the result of this laboratory study. The designed composition satisfies existing spud mud properties criteria and might be implemented in a large-scale test.

Table of Contents

Acknowledgement	V
Abstract	VII
List of Tables	XIII
List of Figures	XV
Nomenclature	XIX
1 Introduction	1
2 Thesis Objective	3
3 What is a Drilling Fluid?	5
3.1 Functions of Drilling Fluids	5
3.1.1 Primary Well Control.....	5
3.1.2 Cutting Transport.....	6
3.1.3 Reduction of Fluid Losses to the Formation.....	7
3.1.4 Cooling and Lubrication of Drill String and Bit.....	7
3.1.5 Cutting Suspension	7
3.1.6 Other Functions of Drilling Fluid.....	8
3.2 Properties of Drilling Fluids	8
3.2.1 Density	8
3.2.2 Flow Properties.....	8
3.2.3 Filtration	12
3.2.4 pH.....	12
3.2.5 Cation Exchange Capacity.....	13
3.3 Drilling Fluid Types	13
3.3.1 Water-Based Drilling Fluids	13
3.3.2 Oil-Based Drilling Fluids	14
4 Spud Mud and Influence of Clays on Mud Properties	17
4.1 Composition and Types of Spud Mud	17
4.1.1 Types and Composition	17
4.1.2 Native Mud	18
4.2 Clay Minerals and Their Application in Drilling Fluid Technology	18
4.2.1 Clay Mineralogy.....	19
4.2.2 Clay Swelling Mechanism.....	21
4.2.3 Particle Association Forms.....	23
5 New Spud Mud Concept	25
5.1 Drill Cuttings and Bentonite Analogy	25
5.1.1 Sedimentary Rocks	25
5.1.2 Description and Mineralogy of Shales and Mudrocks	26
5.2 Drill Cuttings Treatment Technology	28
5.3 Benefits of the New Spud Mud Concept	29
5.4 Considerations Regarding Storage of Cuttings and Mud Mixing	30
6 Preliminary Material Testing	33
6.1 PSD Measurements	33

Table of Contents

6.1.1 Methods of PSD Determination	33
6.1.2 Laser Diffraction Principle	33
6.1.3 Measurement and Data Presentation	34
6.1.4 Results	36
7 Experiments	39
7.1 General Information	39
7.2 Materials	39
7.2.1 Base Fluids	39
7.2.2 Viscosifiers	40
7.2.3 Polymers	41
7.2.4 Weighting and Filter Loss Agents	42
7.3 Description of Experiments	43
7.3.1 Experiment 1 (E1). Water and Cuttings/Bentonite Spud Mud Systems	43
7.3.2 Experiment 2 (E2). Water, Cuttings and Polymers	44
7.3.3 Experiment 3 (E3). Aging Experiment. Hydration Test	46
7.3.4 Experiment 4 (E4). Seawater Based Spud Mud	46
7.4 Drilling Fluid Testing	48
8 Results	49
8.1 Experiment 1 (E1). Water and Cuttings/Bentonite Spud Mud Systems	49
8.2 Experiment 2 (E2). Water, Cuttings and Polymers	52
8.3 Experiment 3 (E3). Aging Experiment. Hydration Test	59
8.4 Experiment 4 (E4). Seawater Based Spud Mud	61
9 Discussion	71
9.1 Physical Properties	71
9.1.1 Density	71
9.1.2 Fluid Loss and Filter Cake Quality	72
9.1.3 Sand Content	75
9.2 Chemical Properties	77
9.2.1 Chloride Content	77
9.2.2 CEC and Bentonite Content	79
9.2.3 Other Chemical Properties	81
9.3 Rheological Properties	84
9.3.1 Performance of Drill Cuttings in Fresh Water	85
9.3.2 Effect of CMC and PAC Polymers on Rheological Properties	85
9.3.3 Effect of Xanthan Gum on Rheological Properties	87
9.3.4 Effect of Solids Concentration on Rheological Properties	92
9.3.5 Effect of Temperature on Rheological Properties	98
9.4 Economical Aspects of the New Spud Mud Concept	99
10 Conclusion	101
11 References	103
Appendix A. Paper Accepted for the Nordic Rheology Conference	107
Appendix B. Drilling Fluid Testing Procedures	117
Appendix C. Rheological Models	123
Appendix D. Correlation Coefficients of the Measured Viscometer Data	127

Appendix E. Zeta Potential Measurement Reports 129

List of Tables

Table 1. The summary of flow models based on the power law index value.....	11
Table 2. pH value as an indicator of solution acidity.....	13
Table 3. The summary of WBM used in the industry (from IPT, 2012).....	14
Table 4. Typical OBM composition and functions of the components (from Skjeggstad, 1989; Torbjørnsen, 1994 and IPT, 2012).....	15
Table 5. The overview over existing spud mud types (from Torbjørnsen, 1994).....	18
Table 6. Classification of sedimentary rocks (from Boggs, 2009).....	25
Table 7. The summary of the main PSD data for the cuttings and bentonite samples derived from laser diffraction analysis.....	36
Table 8. SW composition used in the experiments.....	40
Table 9. The chemical composition of the treated drill cuttings used in the experiments (from TWMA, 2012).....	40
Table 10. The summary of the prepared simple spud mud systems using bentonite and cuttings in experiment E1.....	44
Table 11. The summary of the prepared spud mud systems using bentonite, cuttings and polymers in experiment E2.....	45
Table 12. The summary of the prepared SW- based spud mud systems in experiment E4 using, cuttings, polymers and other additives.....	47
Table 13. The results of drilling fluid testing in E1.....	50
Table 14. The results of cuttings and polymer based fluids prepared in E2.....	53
Table 15. The results of cuttings and biopolymer based fluids in E2 (including the B CMC REF fluid).....	56
Table 16. The results of aging experiment E3.....	60
Table 17. The rheological measurements results at 20°C and calculated corresponding model parameters.....	62
Table 18. The rheological measurements results at 20°C and calculated corresponding model parameters (cont.).....	62
Table 19. The rheological measurements results at 50°C and calculated corresponding model parameters.....	63
Table 20. The rheological measurements results at 50°C and calculated corresponding model parameters (cont.).....	63
Table 21. The physical and chemical test results of spud mud compositions in E4.....	68
Table 22. The physical and chemical test results of spud mud compositions in E4 (cont.).....	69
Table 23. The comparison of the bentonite content and drill cuttings concentration in the designed fluids.....	80
Table 24. The assumed market prices for the materials used in laboratory testing.....	99
Table 25. The approximate prices for the drilling fluids designed in the experimental part.....	100
Table B-1. The correlations for determination of OH ⁻ , CO ₃ ²⁻ and HCO ₃ ⁻ ions concentration in mud filtrate.....	121
Table D-1. The summary of the linear correlation coefficients based on the different rheological models.....	127

List of Figures

Figure 1. Pore pressure plot with planned mud program (from Statoil, 2010).....	6
Figure 2. Laminar flow regime with imaginary fluid cylinders (from Caenn et al., 2011)	9
Figure 3. Consistency curves for different rheological models (from Caenn et al., 2011)	10
Figure 4. Apparent viscosity variation with increasing shear rate (from Caenn et al., 2011)	11
Figure 5. The octahedral layer structure. The white circles oxygen or hydroxyl; the black circles Al^{3+} , Mg^{2+} or other ions (from IPT, 2012).....	19
Figure 6. The tetrahedral layer structure. The white circles oxygen or hydroxyl; the black circles silica (from IPT, 2012)	20
Figure 7. The hexagonal framework of six tetrahedral structures (from IPT, 2012).....	20
Figure 8. The Hoffman structure with the tetrahedral and octahedral layers. The small black circles are silica, the large white circles are oxygen and the large black are circles either aluminum or magnesium (from Caenn et al., 2011).....	20
Figure 9. Framework of water molecules between tetrahedral layers in clay minerals (from Caenn et al., 2011).....	22
Figure 10. Forces acting between two unit layers (from Caenn et al., 2011)	23
Figure 11. The association forms of bentonite particles in drilling fluids (from IPT, 2012)	23
Figure 12. The principle of cuttings treatment used by TWMA (from Murray et al., 2008).....	29
Figure 13. The waste triangle (from the Norwegian Oil and Gas Association, 2004).....	30
Figure 14. The diffraction pattern from a particle (from Horiba, 2012).....	34
Figure 15. Mean, median and mode visualization (from Horiba, 2012).....	35
Figure 16. D10 and D90 visualization (from Horiba, 2012).....	36
Figure 17. PSD of the cuttings sample.....	37
Figure 18. PSD of the bentonite sample.....	37
Figure 19. The comparison of PSD of the cuttings and bentonite samples derived from laser diffraction analysis. The red line – bentonite PSD; the blue line – cuttings PSD	38
Figure 20. The principal structure of CMC (from IPT, 2012)	41
Figure 21. The principal structure of xanthan biopolymer (from IPT, 2012).....	42
Figure 22. B REF fluid viscosity curve based on the Herschel Bulkley model and the measured viscometer data of a standard bentonite spud mud containing 25 g bentonite per 350 ml of water	51
Figure 23. C75 fluid viscosity curve based on the Herschel Bulkley model and the measured viscometer data of a water-cuttings suspension containing 75 g cuttings per 350 ml of water	51
Figure 24. C100 fluid viscosity curve based on the Herschel Bulkley model and the measured viscometer data of a water-cuttings suspension containing 100 g cuttings per 350 ml of water.....	51
Figure 25. C125 fluid viscosity curve based on the Herschel Bulkley model and the measured viscometer data of a water-cuttings suspension containing 125 g cuttings per 350 ml of water.....	52
Figure 26. C150 fluid viscosity curve based on the Herschel Bulkley model and the measured viscometer data of a water-cuttings suspension containing 150 g cuttings per 350 ml of water.....	52
Figure 27. C75 CMC0.7 fluid viscosity curve based on the Herschel Bulkley model and the measured viscometer data of a fluid containing 75 g cuttings and 0.7 g CMC Hi-Vis polymer per 350 ml of water. 54	54
Figure 28. C75 CMC1.0 fluid viscosity curve based on the Herschel Bulkley model and the measured viscometer data of a fluid containing 75 g cuttings and 1.0 g CMC Hi-Vis polymer per 350 ml of water. 54	54
Figure 29. C75 CMC1.3 fluid viscosity curve based on the Herschel Bulkley model and the measured viscometer data of a fluid containing 75 g cuttings and 1.3 g CMC Hi-Vis polymer per 350 ml of water. 54	54
Figure 30. C75 CMC1.6 fluid viscosity curve based on the Herschel Bulkley model and the measured viscometer data of a fluid containing 75 g cuttings and 1.6 g CMC Hi-Vis polymer per 350 ml of water. 55	55
Figure 31. C75 PAC1.0 fluid viscosity curve based on the Herschel Bulkley model and the measured viscometer data of a fluid containing 75 g cuttings and 1.0 g PAC polymer per 350 ml of water	55
Figure 32. Bentonite/CMC reference fluid viscosity curve based on the Herschel Bulkley model and the measured viscometer data of a fluid containing 10.5 g bentonite, 0.7 g CMC polymer and 0.7 g Na_2CO_3 per 350 ml of water	57

List of Figures

Figure 33. C75 X1.0 fluid viscosity curve based on the Herschel Bulkley model and the measured viscometer data of a fluid containing 75 g cuttings and 1.0 g xanthan polymer per 350 ml of water.....	57
Figure 34. C75 X1.2 fluid viscosity curve based on the Herschel Bulkley model and the measured viscometer data of a fluid containing 75 g cuttings and 1.2 g xanthan polymer per 350 ml of water.....	57
Figure 35. C75 X1.4 fluid viscosity curve based on the Herschel Bulkley model and the measured viscometer data of a fluid containing 75 g cuttings and 1.4 g xanthan polymer per 350 ml of water.....	58
Figure 36. C75 X1.6 fluid viscosity curve based on the Herschel Bulkley model and the measured viscometer data of a fluid containing 75 g cuttings and 1.6 g xanthan polymer per 350 ml of water.....	58
Figure 37. C100 X1.2 fluid viscosity curve based on the Herschel Bulkley model and the measured viscometer data of a fluid containing 100 g cuttings and 1.2 g xanthan polymer per 350 ml of water....	58
Figure 38. C125 X1.2 fluid viscosity curve based on the Herschel Bulkley model and the measured viscometer data of a fluid containing 125 g cuttings and 1.2 g xanthan polymer per 350 ml of water....	59
Figure 39. C150 X1.2 fluid viscosity curve based on the Herschel Bulkley model and the measured viscometer data of a fluid containing 150 g cuttings and 1.2 g xanthan polymer per 350 ml of water....	59
Figure 40. C75 X1.0 SW fluid viscosity curve based on the Herschel Bulkley model and the measured viscometer data at 20°C of a fluid containing 75 g cuttings and 1.0 g xanthan polymer per 350 ml of SW	64
Figure 41. C75 X1.2 SW fluid viscosity curve based on the Herschel Bulkley model and the measured viscometer data at 20°C of a fluid containing 75 g cuttings and 1.2 g xanthan polymer per 350 ml of SW	64
Figure 42. C75 X1.4 SW fluid viscosity curve based on the Herschel Bulkley model and the measured viscometer data at 20°C of a fluid containing 75 g cuttings and 1.4 g xanthan polymer per 350 ml of SW	65
Figure 43. C75 X1.6 SW fluid viscosity curve based on the Herschel Bulkley model and the measured viscometer data at 20°C of a fluid containing 75 g cuttings and 1.6 g xanthan polymer per 350 ml of SW	65
Figure 44. C100 X1.2 SW fluid viscosity curve based on the Herschel Bulkley model and the measured viscometer data at 20°C of a fluid containing 100 g cuttings and 1.2 g xanthan polymer per 350 ml of SW	65
Figure 45. C125 X1.2 SW fluid viscosity curve based on the Herschel Bulkley model and the measured viscometer data at 20°C of a fluid containing 125 g cuttings and 1.2 g xanthan polymer per 350 ml of SW	66
Figure 46. C150 X1.2 SW fluid viscosity curve based on the Herschel Bulkley model and the measured viscometer data at 20°C of a fluid containing 150 g cuttings and 1.2 g xanthan polymer per 350 ml of SW	66
Figure 47. C75 X1.4 B SW fluid viscosity curve based on the Herschel Bulkley model and the measured viscometer data at 20°C of a fluid containing 75 g cuttings, 1.4 g xanthan polymer and 88.8 g barite per 350 ml of SW.....	66
Figure 48. C100 X1.4 B SW fluid viscosity curve based on the Herschel Bulkley model and the measured viscometer data at 20°C of a fluid containing 100 g cuttings, 1.4 g xanthan polymer and 68.1 g barite per 350 ml of SW.....	67
Figure 49. C75 X1.4 CMC LV SW fluid viscosity curve based on the Herschel Bulkley model and the measured viscometer data at 20°C of a fluid containing 75 g cuttings, 1.4 g xanthan polymer and 1.0 g CMC Lo-Vis per 350 ml of SW	67
Figure 50. Drilling fluid density as a function of cuttings concentration.....	72
Figure 51. Filter cake of the C100 X1.2 SW drilling fluid containing cuttings and xanthan gum.....	74
Figure 52. Filter cake of the C100 X1.4 B SW drilling fluid containing cuttings, xanthan and barite	75
Figure 53. Filter cake of the C75 X1.4 CMC LV SW drilling fluid containing cuttings, xanthan and CMC Lo-Vis fluid loss agent.....	75
Figure 54. Sand content of the freshwater based muds containing cuttings and xanthan (experiment E2)	76
Figure 55. Sand content of the SW based muds containing cuttings and xanthan (experiment E4)	77
Figure 56. The chloride content of the designed freshwater-based spud muds containing cuttings and xanthan as a function of cutting concentration (E2).....	78

Figure 57. The bentonite content of the freshwater based spud muds with cuttings and xanthan gum (E2).....	79
Figure 58. The bentonite content of the SW based spud muds containing cuttings and xanthan gum (E4).....	80
Figure 59. The lime content in the designed cuttings/xanthan containing spud muds (E2 corresponds to the freshwater-based muds and E4 to – the SW based).....	82
Figure 60. The Ca^{2+} concentration as a function of cuttings content of the freshwater-based spud muds containing cuttings and xanthan.....	83
Figure 61. The effect of CMC and PAC polymers concentration on the rheological properties of the designed freshwater-based spud muds with the cuttings concentration equal to 75 g per 350 ml water.....	86
Figure 62. The effect of xanthan gum, CMC and PAC polymers on the rheological properties of the designed freshwater-based spud muds with the cuttings concentration equal to 75 g per 350 ml water.....	88
Figure 63. The effect of the increasing xanthan gum concentration on the rheological properties of the freshwater-based spud muds with the cuttings concentration equal to 75 g per 350 ml water.....	89
Figure 64. The effect of the increasing xanthan gum concentration on the rheological properties of the SW based spud muds with the cuttings concentration equal to 75 g per 350 ml water.....	90
Figure 65. The comparison of the rheological properties of the freshwater-based mud C75 X1.6 and the identical SW based mud C75 X1.6 SW.....	91
Figure 66. The effect of the increasing cuttings concentration on the rheological properties of the freshwater-based spud muds containing cuttings and xanthan with the concentration equal to 1.2 g per 350 ml water.....	93
Figure 67. PV and τ_0 variation with the increasing cuttings concentration for the freshwater-based spud muds.....	94
Figure 68. The effect of the increasing cuttings concentration on the rheological properties of the SW based spud muds containing cuttings and xanthan with the concentration equal to 1.2 g per 350 ml water.....	95
Figure 69. The effect of barite on the rheological properties of spud mud C75 X1.4 SW containing cuttings and xanthan.....	97
Figure 70. The effect of CMC Lo-Vis fluid loss agent on the rheological properties of spud mud C75 X1.4 SW containing cuttings and xanthan.....	97
Figure 71. The temperature effect on the rheological properties of the SW based spud mud C75 X1.4 SW containing cuttings and xanthan (at 20°C and 50°C).....	98
Figure B-1. Mud balance used for density determination (from IPT, 2012).....	117
Figure B-2. The standard equipment for sand content test (from IPT, 2012).....	118
Figure E-1. Zeta potential measurement of the bentonite sample.....	129
Figure E-2. Zeta potential measurement of the cuttings sample.....	130

Nomenclature

List of Symbols:

$[Ca(OH)_2]$	estimated lime content in mud, kg/m ³
$[Ca^{2+}_{total}]$	total hardness as calcium in filtrate, mg/l
$[Ca^{2+}]$	calcium ion concentration, mg/l
$[Cl^-]$	chloride ion concentration in filtrate, mg/l
$[Mg^{2+}]$	magnesium ion concentration, mg/l
A	surface area of a cylinder, m ²
AV	apparent viscosity, cP
D_N	N% percentile (d_{10} , d_{16} , d_{50} , d_{84} and d_{90})
$D_{4,3}$	volumetric mean diameter, μm
D_i	geometrical mean diameter of a given interval, μm
F	force, N
F_w	water fraction of mud, ml/ml
g	free-fall acceleration, m/s ²
H	Depth, m
K	consistency index, Pa·s or lb/100ft ²
M_f	filtrate alkalinity in ml of H ₂ SO ₄ consumed, ml
n	power law index
P	pressure, Pa
P_f	filtrate alkalinity in ml of H ₂ SO ₄ consumed, ml
P_m	mud alkalinity in ml of H ₂ SO ₄ consumed, ml
PV	plastic viscosity, cP
R	linear correlation coefficient
V_{AgNO_3}	volume of silver nitrate consumed, ml
V_{EDTA}	volume EDTA consumed, ml
$V_{filtrate}$	volume of filtrate, ml
V_M	mud volume, cm ³
V_{MB}	volume of methylene blue consumed, cm ³
V_{mud}	total mud volume, ml
V_{water}	volume of water in mud, ml
X_n	N weight% percentile (X_{10} , X_{16} , X_{50} , X_{84} and X_{90})
YP	yield point, Pa
$\dot{\gamma}$	shear rate, 1/s
θ	shear stress, Pa
θ_0	zero gel strength, °
θ_N	reading on Fann viscometer at N RPM, °
μ	fluid's viscosity, Pa·s, mPa·s or cP
v_i	relative frequency of the particle size interval
ρ	density, SG or kg/m ³
τ	shear stress, Pa
τ_0	yield point/stress, Pa

List of Abbreviations:

API	American Petroleum Institute
AV	apparent viscosity
CEC	cation exchange capacity
CMC	carboxymethyl cellulose
ECD	equivalent circulating density
EDTA	ethylenediaminetetraacetic acid
MBT	methylene blue test
NCS	Norwegian Continental Shelf
OBM	oil-based mud
PAC	polyanionic cellulose
PSD	particle size distribution
PV	plastic viscosity
ROP	rate of penetration
SG	specific gravity
SW	seawater
SPE	Society of Petroleum Engineers
TCC	thermo-mechanical cuttings cleaner
TD	target depth
WBM	water-based mud
YP	yield point

1 Introduction

Drilling fluids play a central role in the drilling of exploration and development wells as the success of the project and its cost depends significantly on the type of fluids selected (Caenn et al., 2011). The authors mention that even though the drilling fluid itself may not be very expensive and comprises minor parts of the total cost, the performance of the fluid will have an impact on the cost of the project. Rate of penetration (ROP) and time needed to reach the target depth depends on the drilling fluid properties. Moreover, according to Bourgoyne et al. (1986) most of the problems encountered during drilling such as caving shales, stuck pipe and lost circulation are either directly or indirectly influenced by drilling fluids. In the worst case improper performance and wrong selection of drilling fluid may result in the abandonment of the well with following economical and possible environmental problems for the operating company.

Though drilling fluids have several primary and secondary functions its main function is to enable drilling process by transporting cuttings and rock fragments from the borehole to the surface (Caenn et al., 2011). It provides sufficient pressure against the borehole and stabilizes open hole sections, cools and lubricates the drill string and the bit and prevents formation fluids from entering the well. Not the least, the drilling fluid plays an important role in the collection of information about the subsurface formations and logging of drilled sections.

According to Skjeggstad (1989) history registers first application of simple drilling fluids as early as several centuries before the new era. The Chinese were using water to remove the cuttings when they were digging holes in the ground. Already in the 1910s it was common to add clays and weighting material to water in order to achieve desired properties – density and viscosity. Skjeggstad (1989) states in his book that the modern drilling fluid industry started with the development of bentonite mud and dates back to approximately 1935. Khodja et al. (2010) mention in their work that drilling fluid technology has constantly been in development starting with simple water and clay mixtures and ending up with complex water- and oil-based systems. Due to strict environmental regulations, today large amounts of drilling cuttings are cleaned from the mud and rests, discharged offshore, deposited onshore in special facilities or re-injected back to the formations. Since more than 75% of the drilled formations are shales (Huang et al., 2011), many of which contain great amounts of smectite and montmorillonite, it would be appropriate to try implementing cleaned drill cuttings to develop new spud muds (fluid used for drilling of top holes). Thus need for new onshore produced bentonite may be reduced significantly. However, no research has been carried out in this sphere of the petroleum industry so far. This work presents scientific laboratory research carried out to develop a new type of spud mud, which utilizes cleaned drill cuttings as a viscosifier. Based on the results of this work a paper has been written and accepted for the presentation at the Nordic Rheology Conference 2014. This paper is provided in Appendix A of this work.

2 Thesis Objective

Traditionally spud mud systems consist mainly of seawater and pre-hydrated bentonite clay used as main viscosifier. Main objective of this thesis was to study the possibility of developing a spud mud system using thermally treated drill cuttings recovered after drilling with oil-based mud systems. The purpose was to evaluate application of crushed cuttings in a new spud mud system, as a replacement for bentonite and obtain a stable drilling fluid with approximately the same properties as a conventional bentonite drilling fluid. Moreover, it was planned to carry out analysis of economical and other aspects of this new development. This investigation consisted of a literature study with theoretical background preparation and an extensive laboratory testing. The correct spud mud composition was planned to be found by mixing a number of mud compositions, including drill cuttings and other relevant additives. Analyses of the results were carried out using standard American Petroleum Institute (API) recommendations and adjustments of the properties to the desired levels following current mud properties.

3 What is a Drilling Fluid?

A drilling fluid is defined as “any number of liquid and gaseous fluids and mixtures of liquids and solids (as solid suspensions, mixtures and emulsions of liquids, gases and solids) used in operations to drill boreholes into the earth” (Schlumberger, 2014). The term drilling mud or just mud is often used in the petroleum industry to describe drilling fluids as well. Both of these terms will be used in the current work and have the same meaning. This section carries an introductory character and provides an overview over different functions of drilling fluids, their properties and types.

3.1 Functions of Drilling Fluids

A drilling mud has several functions in the process of drilling through the formations. However, Skjeggstad (1989) specifies the following three as the main functions:

1. Prevent formation fluids entering the well
2. Carry cuttings from the bottom of the well to the surface
3. Deposit thin impermeable filter cake on the borehole wall to reduce loss of drilling fluid into the formation.

In the following the main functions of mud will be described in more details.

3.1.1 Primary Well Control

It is necessary to have a higher pressure in the drilled wellbore than in the formation in order to prevent inflow of formation fluids to the well, which may result in well control problems (Caenn et al., 2011 and Skjeggstad, 1989). On the other hand, having too high wellbore pressure may be dangerous as this may lead to fracturing of the formations. This scenario results in excessive fluid loss to the formation and the reduction of the hydrostatic pressure in the wellbore (fluid level reduces due to the losses). In the worst case it may end up with lost circulation and influx (well control) problems at the same time, which is very difficult to treat (Aadnoy, 2010). Based on this information the density of the drilling fluid should balance the pore pressure at each depth, but not exceed the fracture gradient of the formation along the open hole section at the same time. Planned mud weight is shown in Figure 1 with a black line.

Mainly the hydrostatic pressure provided by the mud column performs the primary well control. Pressure at each depth depends on the mud density and the depth and can be calculated as the hydrostatic in the following way (Eq. 1, from Skjeggstad, 1989):

$$P = \rho \cdot g \cdot h \quad (\text{Eq. 1})$$

3 What is a Drilling Fluid?

where P is pressure in Pa, ρ is density in kg/m^3 , g is free-fall acceleration in m/s^2 and h is depth in m. During drilling and tripping the movement of the drill string and flow of the fluid will influence the pressure in the wellbore and the apparent density of the fluid may change. This is referred to in the literature as Equivalent Circulating Density (ECD) (Caenn et al. 2011).

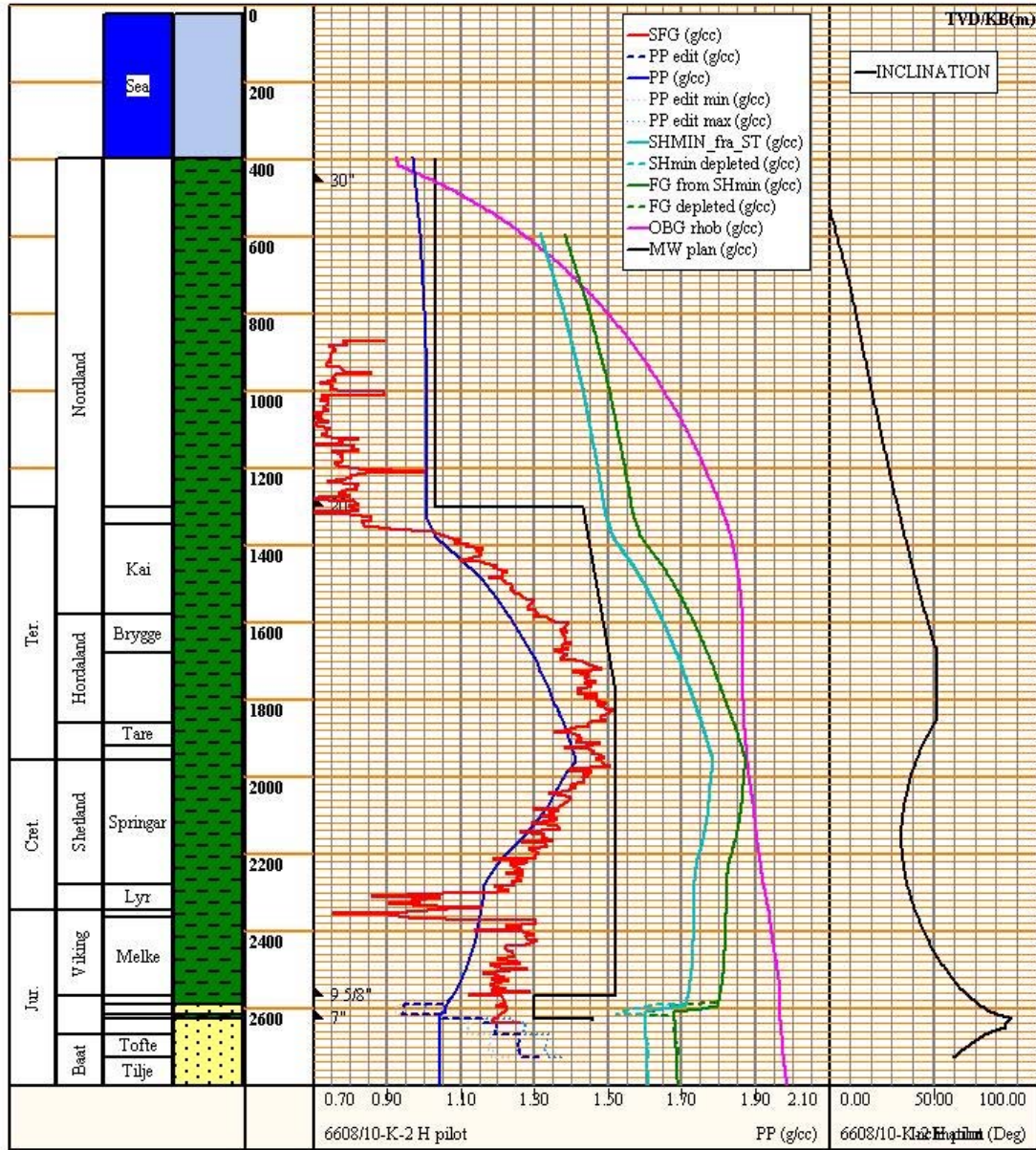


Figure 1. Pore pressure plot with planned mud program (from Statoil, 2010)

3.1.2 Cutting Transport

As mentioned in Section 3.1 transport of cuttings to the surface is considered to be the primary function of a drilling fluid. In addition, a drilling fluid should keep the drill bit clean by removing the drilled formation immediately. Torbjørnsen (1994) lists the following factors that influence the cutting transport efficiency: flow

velocity, drilling fluid rheological properties, cutting dimensions and weight as well as wellbore inclination. He mentions that wellbore inclinations between 40° and 60° are the most critical ones as the cuttings will tend to sliding along the wall and accumulating on the lower side of the wellbore. Two forces are acting on the cuttings: gravity forcing the particles to sink and drag force from the flowing fluid moving the particles upwards. Therefore the resultant velocity is the difference between sinking velocity and flow velocity (Skjeggstad, 1989). There are many factors influencing sinking velocity and Time (2009) provides an overview and a summary of several correlations.

According to Skjeggstad (1989) the viscosity of the mud needs to be low to remove the cuttings effectively away from the drill bit and transfer them to the annulus above. However, high viscosity of mud is required in order to lift the drill cuttings to the surface through the pipe-wellbore annulus in the vertical section. This sounds quite controversial, but it is possible to achieve by so called shear-thinning fluids. This phenomenon is described in details in Section 3.2.2.

3.1.3 Reduction of Fluid Losses to the Formation

Pressure in the well is kept above the formation pressure during drilling (Section 3.1.1). In the permeable rock intervals drilling fluids will therefore enter the formation due to this pressure differential. However, particles added to the drilling fluid (for example viscosifiers and weighting agents) are too large to pass through the pore openings and will gradually build a filter cake on the wall. A good drilling fluid should build a thin impermeable filter cake to reduce losses to the formation. Not only this is important with respect to fluid loss and filtrate invasion, but also a thick filter cake significantly influences logging data introducing challenges with regards to data interpretation and increases the chance of differential sticking (Skjeggstad, 1989).

3.1.4 Cooling and Lubrication of Drill String and Bit

During drilling processes heat is generated downhole due to friction between drilling bit and formation as the bit acts against the rocks. Torbjørnsen (1994) says that this heat may actually burn the drill bit. One of the functions of the drilling fluid is to cool the drill string and the bit during drilling by transporting the heat away. For this purpose cool mud is pumped from the surface through the drill string and the warmer mud returns on the annular side. The mud reduces the friction between the drill bit/string and the formation as well. To achieve supreme lubrication, friction reducing agents may be added in critical situations.

3.1.5 Cutting Suspension

Mud should keep the particles (weighting material, cuttings etc.) in suspension during pumping breaks in order to maintain the required qualities and avoid degradation of fluids. This function of the drilling fluid is especially important when drilling deep wells as tripping of the drill string may take long time (Skjeggstad, 1989). Drilling fluids therefore should develop a gel-like structure when it is under static condition. This property is called thixotropy and is described in more details in Section 3.2.2.

3.1.6 Other Functions of Drilling Fluid

Some of the main functions of the drilling mud were mentioned and described in Sections 3.1.1-3.1.5. However, these are not the only functions of muds. A drilling fluid should as well (Caenn et al., 2011, Skjeggstad, 1989 and Torbjørnsen, 1994):

- Provide buoyancy to drill string and to casing during installation to avoid high load on the lifting equipment of the rig
- Be non-corrosive and protect downhole drilling equipment from degradation
- Allow easy removal of cuttings from the drilling fluid on surface using standard equipment (shale shakers, centrifuges etc.)
- Allow data collection using existing logging techniques

3.2 Properties of Drilling Fluids

3.2.1 Density

Density is defined as weight per unit volume and is the main parameter to control hydrostatic pressure in the well (Caenn et al., 2011 and Skjeggstad, 1989). Density of the fluid is often expressed in specific gravity (SG), which is the density of the fluid relative to that of water. In addition to primary well control that drilling fluids delivers through correct density, this parameter is important to provide necessary borehole stability of the open hole sections (Caenn et al., 2011). While drilling through soft formations such as clays and salts the exerted pressure will restrict the inwards movement of the formation. Aadnoy (2010) introduces median line principle for mud weight to avoid wellbore stability problems. Avoiding too high density of the mud is necessary to avoid drilling related problems such as low ROP, hydraulic fracturing and differential sticking in porous formations.

3.2.2 Flow Properties

Rheology is defined as the “study of how matter deforms and flows including its elasticity, plasticity and viscosity” (Schlumberger, 2014) or said in a simpler way it describes flow properties of matter. Caenn et al. (2011) mention in their book that having correct drilling fluid properties is not only important to obtain good cutting transport, but also to avoid other possible problems.

Fluid flow regimes can be divided into two types dependent mainly on flow velocity (density, viscosity and pipe diameter as well) (Caenn et al. 2011):

- *Laminar flow*, where all the particles along the flow line move parallel to each other
- *Turbulent flow*, where particles flow in a chaotic manner forming eddies in the flow

Viscous properties of the fluids are important for the laminar flow, while inertial properties of the fluids are dominating in the turbulent flow regime.

Laminar flow can be described as flow of imaginary concentric fluid cylinders moving parallel to each other as shown in Figure 2. In this regard *shear rate* is

defined as the ratio of the difference in velocity of two such cylinders to the distance separating them (Caenn et al., 2011).

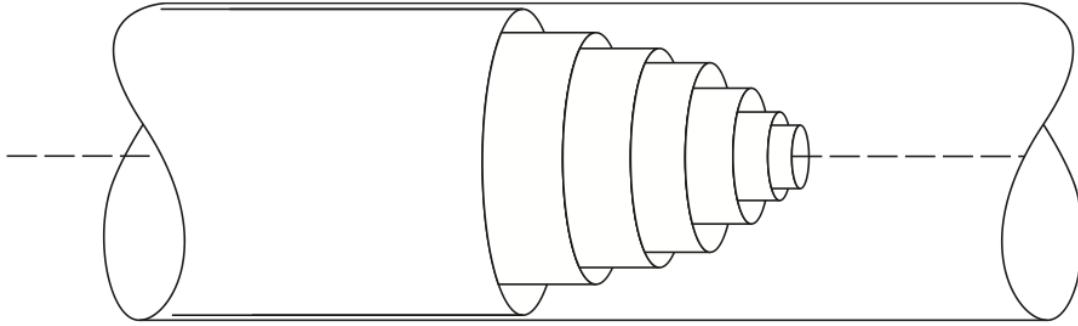


Figure 2. Laminar flow regime with imaginary fluid cylinders (from Caenn et al., 2011)

Each imaginary cylinder flowing parallel to the other exerts a certain axial force (parallel to the surface) on it. The ratio of this force to the surface area of the cylinder is defined as *shear stress*:

$$\tau = \frac{F}{A} \quad (\text{Eq. 2})$$

where τ is shear stress in Pa, F is force in N and A is surface area of a cylinder in m^2 .

Even though we use the term viscosity to describe resistance of the fluid against flowing, viscosity is scientifically defined as the ratio of shear stress to shear rate:

$$\mu = \frac{\tau}{\dot{\gamma}} \quad (\text{Eq. 3})$$

where μ is the viscosity in $\text{Pa}\cdot\text{s}$, τ is shear stress in Pa and $\dot{\gamma}$ is shear rate in $1/\text{s}$. In the petroleum industry the viscosity of drilling fluids is often denoted by $\text{mPa}\cdot\text{s}$ or centipoise (cP), which corresponds to $1/100$ of Poise. Poise in its turn is defined as the viscosity of the fluid when shear stress is equal to $1 \text{ dyne}/\text{cm}^2$ while shear rate is $1/\text{s}$. Skjeggstad (1989) mentions that the viscosity of the fluid depends on mechanical friction and electrical forces between the molecules, which in their turn contribute to the shear stress.

All the fluids can be divided into two major groups *Newtonian* and *non-Newtonian* based on their behavior with increasing shear rate (Caenn et al., 2011). Newtonian fluids have a constant viscosity, which is not dependent on the shear rate and the plot of shear stress against shear rate (called consistency curve) is a straight line that passes through the origin as shown in Figure 3.

Pure fluids as water, oil and salt solutions demonstrate Newtonian behavior and have a single viscosity value, which can be used in calculations. On the other hand, most of the drilling fluids demonstrate a non-Newtonian nature and several models

have been developed to match the shear stress/shear rate relationship of fluids (Figure 3).

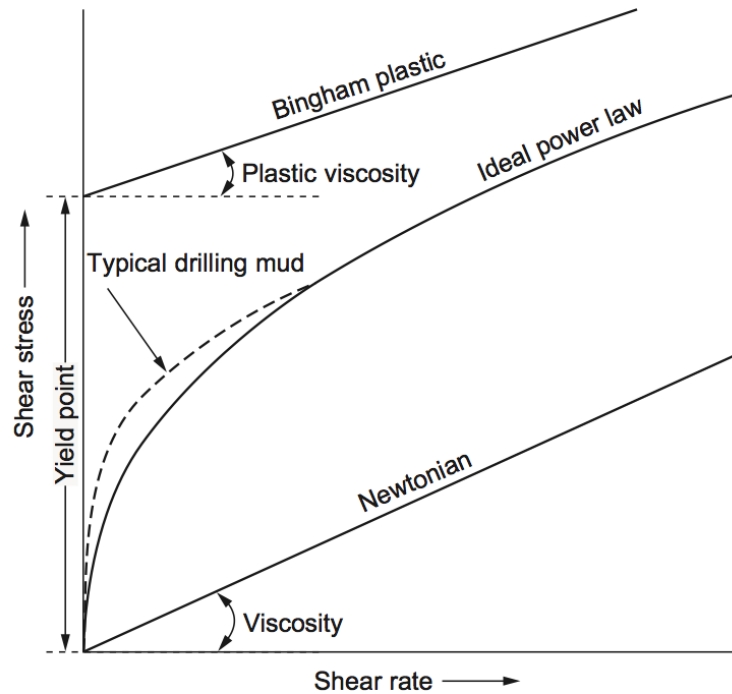


Figure 3. Consistency curves for different rheological models (from Caenn et al., 2011)

Simplest of these models is the *Bingham model* illustrated in Figure 3, which is characterized by two parameters:

- *Yield point* (YP), minimum shear stress required to initiate the flow
- *Plastic viscosity* (PV), additional shear stress required to maintain the flow at finite shear rate.

PV depends on the amount of solid particles, mechanical friction between the solids, solids and the fluid and friction between fluid molecules (Torbjornsen, 1994). YP occurs due to the electrical attraction forces between solid particles. For non-Newtonian fluids described by the Bingham model apparent viscosity (AV) decreases with increasing shear rate as shown in Figure 4. Fluids demonstrating this behavior are called shear thinning and this property is central for drilling fluids. At low velocities particles in the fluid are oriented in such way that attraction between them is highest resulting in high viscosity. With increasing shear rates particles will orient in the direction of flow and the attraction force reduces which results in a lower viscosity of the fluid (Skjeggstad, 1989). Shear thinning muds will have high viscosity at low shear rates in the pipe-wellbore annulus and a low viscosity when flowing through the bit nozzles, thus providing desired hole cleaning (Section 3.1.2).

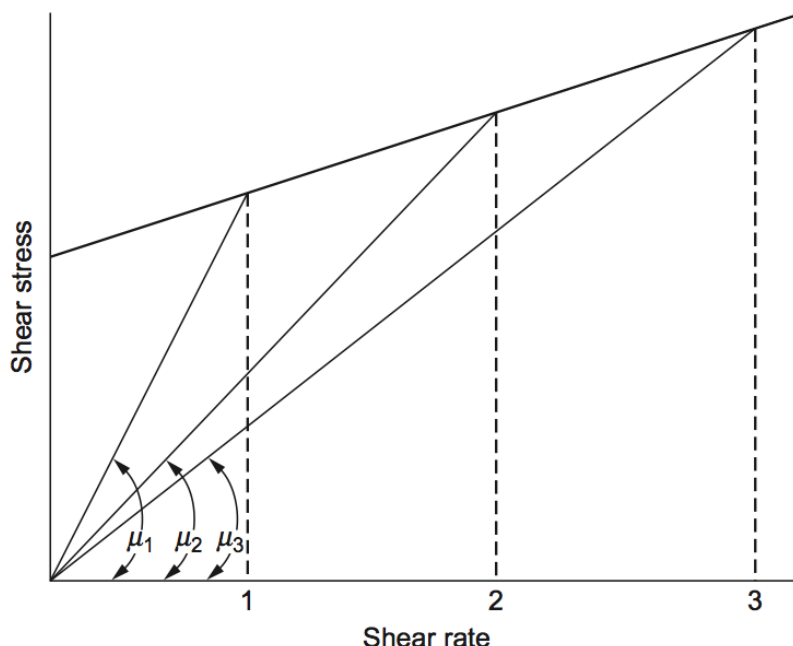


Figure 4. Apparent viscosity variation with increasing shear rate (from Caenn et al., 2011)

Another model often used to describe rheological behavior of a fluid is the so-called *power law model* for pseudo-plastic fluids (Figure 3) (Caenn et al., 2011). According to Skjeggstad (1989) this model is better than the Bingham model especially at low shear rates and is described by Eq. 4:

$$\tau = K \cdot (\dot{\gamma})^n \quad (\text{Eq. 4})$$

where τ is shear stress, $\dot{\gamma}$ is shear rate (as introduced earlier), K is a consistency index in $\text{Pa}\cdot\text{s}^n$, $\text{lb}/100\text{ft}^2$ or dynes/cm^2 and n is the power law index. The latter describes how viscosity changes with the shear rate or said in other words it is the measure for shear thinning. Table 1 summarizes different fluid flow models depending on the power law index values (Skjeggstad, 1989).

Table 1. The summary of flow models based on the power law index value

Power law index	Flow model
$0 < n < 1$	Shear thinning
$n = 1$	Newtonian
$n > 1$	Shear thickening (dilatant)

Another important property of muds is the so-called *gel strength*. It describes minimum required shear stress to initiate flow of a static fluid (Skjeggstad, 1989). As it was mentioned earlier in this section, electrically charged particles in drilling fluids (for example clays) attract each other with oppositely charged ends and build gel structures. Polymers are capable of building strong gel structures as well. Moreover, gel strength of drilling fluids increases with time at rest. This phenomenon is called *thixotropy*. Even though gel strength is often used to describe

YP, these are not totally the same since YP is not a time dependent parameter while gel strength is.

Though the power law model provides better description of rheological behavior of a non-Newtonian fluid it does not account for yield stress of the fluid, which will develop under static conditions. Thus, the model is not well suited for rheological characterization at low shear rates. It is reported that the Herschel Bulkley model introduced in 1926 yields best description of the measured data (IPT, 2012). This model is a modified version of the power law model, which is obtained by introducing a new parameter to the equation – yield stress/point as shown in Eq. 5.

$$\tau = \tau_0 + K \cdot \dot{\gamma}^n \quad (\text{Eq. 5})$$

where τ is shear stress in Pa, τ_0 is yield stress/point in Pa, K is the consistency index in $\text{Pa}\cdot\text{s}^n$, $\dot{\gamma}$ is the shear rate in $1/\text{s}$ and n is the power law index. In this model the consistency index gives information about the viscosity of the fluid at low shear rates and solid content at high shear rates (IPT, 2012).

3.2.3 Filtration

A filter cake is required to avoid continuous loss of drilling fluids to the formation (Caenn et al. 2011). As mentioned in Section 3.1.3 the mud enters the formation due to the positive pressure differential. Before the filter cake is formed on the borehole wall, particles smaller than the pore openings will penetrate the formation. This suspension of fine particles is called *mud spurt* and the initial loss of fluid to the formation is called *spurt loss*. Two types of filtration are mentioned in the literature (Skjeggstad 1989):

- *Static filtration*, which occurs under static conditions. Here the fluid is not being pumped and the thickness of the filter cake increases with time
- *Dynamic filtration*, filter cake is subjected to erosion due to flowing fluid or drill string working against the borehole wall. Here the thickness might decrease, increase or keep constant depending on the severity of erosion

According to the API standard filtration performance is measured by means of an API filter press and is presented as the volume of fluid loss during 30 minutes (API, 1990).

3.2.4 pH

pH is a common term used to describe acidity or alkalinity of a solution or liquid (Caenn et al., 2011). It is a measure of the hydrogen ion concentration in the solution presented as negative logarithm with base 10. It can be calculated using Eq. 6 (API, 1990).

$$pH = -\log [H^+] \quad (\text{Eq. 6})$$

The product of the hydrogen ion and the hydroxyl ion concentrations is constant and is equal to 10^{-14} mole/l. The pH parameter is often used to describe an

environment of solution as well (Table 2). Fresh water has a pH equal to 7, which means that concentration of H^+ ions is 10^{-7} .

Table 2. pH value as an indicator of solution acidity

Type of environment	pH value
Acidic	<7
Neutral	7
Basic	>7

Maintaining a high pH value of the mud is crucial to avoid corrosion, control solubility of contaminants and maximize performance of some additives for instance polymers (API, 1990).

3.2.5 Cation Exchange Capacity

Cation exchange capacity (CEC) is defined as “the quantity of positively charged ions (cations) that a clay mineral or a similar material can accommodate on its negatively charged surface, expressed as milli-ion equivalent per 100 g or more commonly as milliequivalent per 100 g” (Schlumberger, 2014). Montmorillonite, main mineral in bentonite, has much higher CEC than any other clay mineral and CEC measurements on drilling fluids provide rough estimates of the bentonite content. Methylene blue test (MBT) is performed on a drilling mud sample to determine CEC (API, 1990). Test procedure and calculation are given in Appendix B.

3.3 Drilling Fluid Types

All drilling fluids may be arranged into three main groups based on the continuous phase of the fluid: water-based, oil-based and gas-based (Caenn et al., 2011). Even though dry air and foam can be used for fast drilling in hard and stable formations gas-based drilling fluids are not often implemented in the oil industry and will not be described here.

3.3.1 Water-Based Drilling Fluids

Water-based drilling fluids have water as a continuous phase and contain clay minerals, polymers or combination of clay minerals and polymers to increase viscosity and YP (Torbjørnsen, 1994). Alkalis, salts, surfactants, droplets of emulsified oil and barite may be added to water-based muds (WBM). Choice of viscosifiers and other additives to the water-based drilling fluids depends on the exact downhole conditions. Torbjørnsen (1994) mentions that even though WBM is cheaper to prepare than oil-based, it might be difficult and expensive to maintain the desired properties of the fluid. There is a high number of water-based drilling fluid types, however, all of them can be divided into three major categories: fresh water WBM, seawater WBM and inhibitive WBM (IPT, 2012). Since the detailed analysis of existing WBM types is not the purpose of this thesis, only an overview over different types of WBM actively used in the industry is presented in Table 3.

3 What is a Drilling Fluid?

Table 3. The summary of WBM used in the industry (from IPT, 2012)

Subgroup	Mud type	Applications	Characteristics
Freshwater	Spud mud (bentonite mud)	Mainly for drilling of top holes (36" and 26")	<ul style="list-style-type: none"> Provides viscosity to carry cuttings at low velocities (large flow area) and fluid loss control. This type is not inhibitive and may cause problems with viscosity.
Seawater	Seawater mud	Drilling of salt formations and in general where appropriate	<ul style="list-style-type: none"> High salt content close to that of seawater Pre-hydrated bentonite are added continuously to maintain viscosity
Inhibitive	Polymer inhibition	Drilling of clay and salt formations	<ul style="list-style-type: none"> Polymers adsorb to clay particles and reduce clay minerals' contact with water
	Salt inhibition: <ul style="list-style-type: none"> Gypsum Lime KCL/NaCl/Multisalt Seawater+ lingsulfonate 	Used in clay and gumbo formations to avoid swelling. Drilling of salt formation layers	<ul style="list-style-type: none"> Salt ions replace ions in the clay's structure thus reducing its reactivity by binding two crystals together for example (Ca²⁺ ion) Polymers are added as well to build viscosity
	Alcohol inhibition	Drilling through shale formations	<ul style="list-style-type: none"> Here glycol and polymers are added to KCL drilling fluid to achieve good inhibition characteristics

3.3.2 Oil-Based Drilling Fluids

Oil-based drilling fluids have oil as a continuous phase and some water might be present as well (Caenn et al., 2011). Water might also be added on purpose to create so called invert emulsion oil-based muds (OBM), where water droplets are dispersed in a continuous oil phase (IPT, 2012). According to Caenn et al. (2011) approximately 50% of drilling jobs are performed using oil-based fluids. This type of drilling fluid has gained high popularity due to the number of advantages it gives as for example wellbore stability, shale inhibition, high lubricity, high temperature stability and absence of corrosion related problems. However, OBM is often dangerous for health and environment and strict regulations are applied when using this type of mud.

There are many commercial OBM products in the industry, but any invert emulsion drilling fluid basically consists of three main phases: oil phase, water phase and particles (IPT, 2012). In the early development of oil-based drilling fluids, diesel oil was used as a continuous phase. Today more environmentally friendly and less harmful mineral oils are the main component of OBM. Water phase in OBM is actually a salt solution with content varying between 5-50% all depending on the existing conditions. Type of salt used will depend on the exact formation fluid properties. Salt is added to the water phase of the oil-based drilling fluids to avoid osmosis and destabilization of the emulsion. The particle phase of OBM mainly

consists of weighting materials and cuttings. Summary over different oil-based drilling fluid components and their functions are provided in Table 4.

Table 4. Typical OBM composition and functions of the components (from Skjeggstad, 1989; Torbjørnsen, 1994 and IPT, 2012)

Component	Function
Mineral oil	<ul style="list-style-type: none"> • Continuous phase
Water	<ul style="list-style-type: none"> • Prevent filtrate invasion • Add plastic viscosity
Salt (CaCl ₂ , KCl, NaCl etc.)	<ul style="list-style-type: none"> • Avoid osmosis • Stabilize water phase
Surfactants	<ul style="list-style-type: none"> • Reduce surface tension and keep water phase in droplets. • Make solid particles oil wet to carry
Organophilic clay/maleated elastomers	<ul style="list-style-type: none"> • Add viscosity and increase carrying capacity
Fluid loss material	<ul style="list-style-type: none"> • Fluid loss control in high pressure high temperature conditions
Weighting agents	<ul style="list-style-type: none"> • Provide desired density
Lime (Ca(OH) ₂)	<ul style="list-style-type: none"> • Activate surfactants
Thinners	<ul style="list-style-type: none"> • Reduce fluid's viscosity

4 Spud Mud and Influence of Clays on Mud Properties

Any kind of drilling fluid or mud “used to drill a well from surface to a shallow depth” is defined as a spud mud (Schlumberger, 2014). Though a spud mud is used for drilling of very limited well sections (up to 1000-1500 m) in general, several performance criteria needs to be fulfilled. Torbjørnsen (1994) lists these criteria and points out that having a simple composition, being easy to prepare/maintain and economically viable are the most central ones.

As the main goal of this work was to develop a new fluid type to be used under top section drilling, more detailed information about the spud mud technology is presented in this section. Types of spud mud, their compositions and main principles behind viscosity and fluid loss control are of particular importance and in-depth analysis follows.

4.1 Composition and Types of Spud Mud

According to Torbjørnsen (1994) and Schlumberger’s Online Oilfield Glossary spud muds commonly contain freshwater, bentonite and polymers. Despite a small number of components used in spud muds several commercial mud types exist and are presented in Section 4.1.1.

4.1.1 Types and Composition

It was stated in Section 3.1 that hole cleaning and removal of drill cuttings were the main tasks of a drilling fluid and carrying capacity depended on the fluid properties (mainly viscosity) and its velocity. Upper sections drilled using spud mud have large diameters (36” and 26”), which results in a low transport velocity of cuttings. Low flow velocity needs to be balanced by high fluid viscosity at low shear rates to achieve a desired level of hole cleaning and to be able to reach target depth (TD) of the section (Torbjørnsen, 1994). These properties often are achieved when no special agents are added to the fluid. In this case clay minerals used to provide viscosity will be flocculated (see Section 4.2.3) yielding high flow resistance. High viscosity optimizes hole cleaning and minimizes washouts as well (Caenn et al., 2011).

Torbjørnsen (1994) in his book “Borevæsketeknologi (Drilling Fluid Technology)” provides an overview of different spud mud types used in the industry. These are summarized in Table 5. Sodium hydroxide is a common component for all types of spud muds. It is added to increase pH of the fluid and achieve better clay swelling. Moreover, at a higher pH negative influence of Mg^{2+} ions on bentonite is avoided. It is reported in several sources that bentonite reacts with freshwater (IPT, 2012 and Torbjørnsen, 1994). For this reason any spud mud based on seawater (SW) is prepared by adding pre-hydrated bentonite to the SW. Pre-hydrated bentonite needs to be added continuously since the properties will be lost with time (IPT, 2012). Guar gum mud is easy to prepare and exhibits good qualities both with regards to fluid loss control and viscous properties. However, degradation of the mud is an issue if bactericidal compounds are not present in the solution.

Table 5. The overview over existing spud mud types (from Torbjørnsen, 1994)

Type of spud mud	Main components	Content (kg/m ³ fluid)	
Freshwater	Freshwater and bentonite	K ₂ CO ₃	1.0-3.0
		NaOH	1.0-2.5
		Bentonite	70-12
Seawater	Seawater and bentonite	Dilution of freshwater spud mud with seawater	
Guar gum	Freshwater and guar gum	NaOH	0.5-1.0
		Guar gum	7.0-10
Bentonite and carboxymethyl cellulose (CMC)	Freshwater, bentonite and CMC	K ₂ CO ₃	1-3
		NaOH	0.5-2.5
		Bentonite	30-50
		CMC HIVIS	2.0-4.0

4.1.2 Native Mud

Another type of spud mud is the so-called *native mud*, which results when drilling top sections using clear water (Azar and Roberto Samuel, 2007). In native muds solids suspended in the fluid both clays and other particles are derived from the formations being drilled (Schlumberger, 2014). This mud is cost effective for drilling of top sections as no components are added here to achieve specific properties. Instead of drilling with fresh water through shallow formations, native muds can also be prepared at surface facilities by adding crushed clay containing cuttings to water.

4.2 Clay Minerals and Their Application in Drilling Fluid Technology

Spud mud is a rather simple drilling fluid system, where clay minerals and bentonite in particular very often is the only additive. Therefore, understanding clay mineralogy is central for drilling fluid technology as clay is used in almost all types of muds, both water-based and oil-based (Caenn et al., 2011).

Today bentonite is often used as viscosifier in drilling muds. Bentonite is a term that initially was used to describe a particular type of the clay found in Wyoming formed by weathering of volcanic ash (Skjeggstad, 1989). However, today this is a common term comprising any kind of clay mineral that demonstrates swelling properties when added to water and creates gel-like fluids. Actually bentonite consists mainly of the following clay minerals:

- Montmorillonite (Smectite)
- Kaolinite
- Chlorite

It may contain some non-clay minerals as well, for example quartz. Montmorillonite is the most abundant mineral in the bentonite structure and is responsible for the special viscous properties of the solutions.

Colloidal systems form when clay minerals are added to water. Caenn et al. (2011) point out that it is important to know that the term *colloid* is not used to describe a

matter, but rather refers to the particles smaller than 1 to 2 microns. It is as well reported that the largest clay particle size is equal to 2 microns, which means that clay can be regarded as colloid (Skjeggstad, 1989). In colloidal systems Brownian movement of water molecules keeps fine particles in suspension. Colloids have a high influence on the mud properties such as viscosity and sedimentation due to surface phenomena, as the particles are electrically charged and not balanced. To get a better understanding of how montmorillonite can influence fluid viscosity, a description of the mineral structure is given in Section 4.2.1

4.2.1 Clay Mineralogy

According to Skjeggstad (1989) most of the clay mineral structures consist of two main components:

1. *Octahedral layer* comprises either oxygen atoms or hydroxyls placed in the corners of an octahedral structure and an aluminum or a magnesium atom inside the structure, spaced equally away from the corners (Figure 5). Octahedral layer structures with aluminum atoms are called gibbsite, while those with magnesium – brucite (Caenn et al., 2011).
2. *Tetrahedral layer*, shown in Figure 6, consists of either oxygen atoms or hydroxyls placed in the corners of a tetrahedral structure with a silica atom located in the center of gravity of the structure. Several tetrahedral structures will share oxygen or hydroxyls in the corners to build a larger framework. Six silica tetrahedrons will often build a hexagonal structure with an open space in the middle as shown in Figure 7.

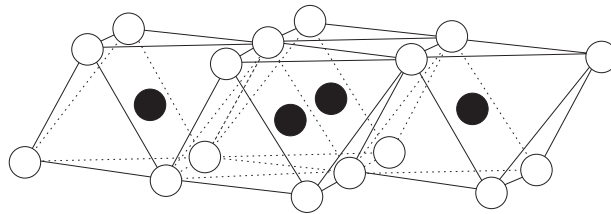


Figure 5. The octahedral layer structure. The white circles oxygen or hydroxyl; the black circles Al³⁺, Mg²⁺ or other ions (from IPT, 2012)

These two building blocks, octahedral and tetrahedral layers, are bound together to form a crystalline structure. Common oxygen atoms in the corners create chemical bonds between the layers. A montmorillonite mineral consists of two tetrahedral layers with a single octahedral layer in between. The top of the tetrahedral layer is connected to the octahedral as shown in Figure 8 and this formation is called the *Hoffman structure*. This is, however, not the only possible combination of arrangements and a single octahedral layer may be bound to a single tetrahedral like in kaolinite mineral. Any structure of this nature is called a unit layer. Several unit layers are piled up together to assemble what is called a *crystal lattice*. Caenn et al. (2011) states that strong covalent bonds exist within the unit layers, which makes this sub-structure rather firm. Contrary, weak van der Waals forces are holding unit layers together promoting cleavage along this plane.

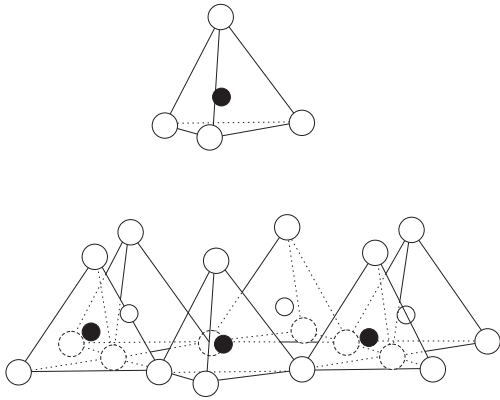


Figure 6. The tetrahedral layer structure. The white circles oxygen or hydroxyl; the black circles silica (from IPT, 2012)

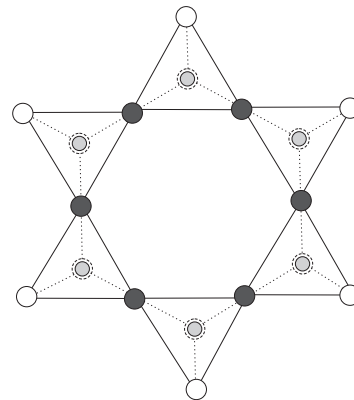


Figure 7. The hexagonal framework of six tetrahedral structures (from IPT, 2012)

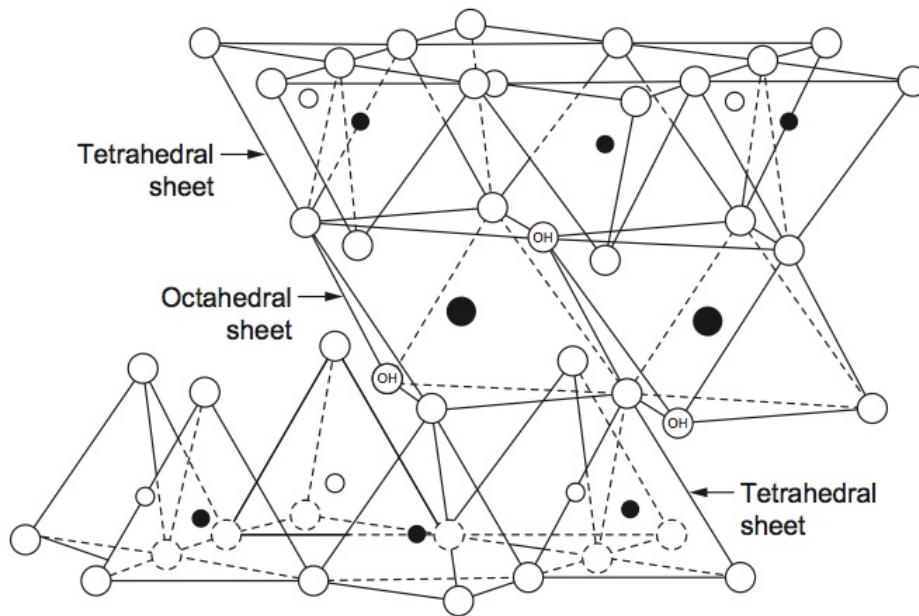
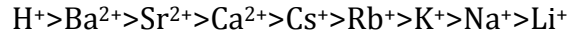


Figure 8. The Hoffman structure with the tetrahedral and octahedral layers. The small black circles are silica, the large white circles are oxygen and the large black are circles either aluminum or magnesium (from Caenn et al., 2011)

When silica atoms are present in the entire tetrahedral layer and aluminum atoms are present in the entire octahedral layer the crystal becomes electrically neutral. These electrically neutral minerals are not clay minerals, but their prototypes (Caenn et al., 2011). Talc and pyrophyllite are examples of such prototypes. Unlike their prototypes octahedral structures of clay minerals in the *smectite group* (where montmorillonite belongs) are not electrically neutral. In montmorillonite the misbalance often occurs due to substitution in the octahedral layer of Al^{3+} ion with Mg^{2+} ion resulting in a net negative charge spread nearly uniformly on the surface. The negative charge will attract positive ions to the surface, which can be later

exchanged with other cations when the mineral is added to water. These ions are often called *balancing ions*. Cations can be attracted to the edges of the mineral as well. Normally, polyvalent elements have a higher tendency to adhere to the crystals, stronger than monovalent. Hendricks et al. (1940) presented the relative ion attraction potential as:



The ability to swap cations was presented earlier in Section 3.2.5 as CEC and is used to describe colloidal activity of clay minerals. Montmorillonite, which has a high CEC value, will swell and create viscous fluids even at low concentrations (Caenn et al., 2011).

4.2.2 Clay Swelling Mechanism

Water can penetrate the space between the unit layers of montmorillonite and increase distance between them (Caenn et al., 2011). This happens both due to the weak van der Waals type of bonding and due to the repulsive force which stems from negative charged surfaces. The crystalline lattice expands leading to a larger surface area, which results in higher colloidal activity. Two swelling mechanisms of clays are reported in literature: *crystalline swelling* and *osmotic swelling* (Skjeggstad, 1989 and Caenn et al., 2011).

During crystalline swelling single molecular sheets of water adhere to the surface of the clay mineral in a structured way. Expanding lattice property of montmorillonite will allow adhesion of water both onto the external surface, which is in direct contact with bulk solution and onto the exposed internal layer surfaces as a result of expansion. Water molecules adsorb to the surface by means of hydrogen bonding, i.e. forces between oxygen atoms in the corners of tetrahedral layers and hydrogen in water molecules (Hendricks and Jefferson, 1938). Due to the similarities in the molecular structure of water and tetrahedral layer, water molecules will arrange themselves in the hexagonal fashion around the tetrahedral layer (Skjeggstad, 1989). When this structure is first in place other water molecules can build up on this framework as shown in Figure 9. It is important that this hexagonal water arrangement has slightly different properties than free water and its viscosity and density are reported to be higher (Caenn et al., 2011).

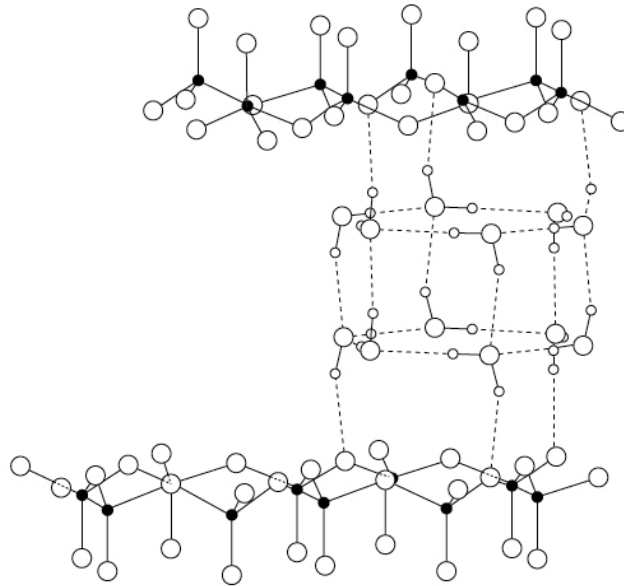


Figure 9. Framework of water molecules between tetrahedral layers in clay minerals (from Caenn et al., 2011)

Even though crystalline swelling occurs in all types of montmorillonite crystals independent of balancing ion type, osmotic swelling occurs mainly in the structures with Na^+ or Li^+ ions. Norrish (1954) studied the spacing between the crystals in the presence of different solutions and proposed the mechanism for initiation of osmotic swelling. Two forces are acting on the unit layers in opposite directions where one is the repellent swelling force due to the water molecule invasion and the other is the attracting electrical force from the balancing ions. These forces are shown in Figure 10. When balancing ions attached to the crystalline structure are Na^+ or Li^+ , swelling forces separating the unit layers from each other are sufficient to break the electrical bridging. This process promotes osmotic swelling on the surface of the clay particles. On the other hand, Skjeggstad (1989) points out that Ca^{2+} balancing ions can adhere to two unit layers simultaneously preventing separation and osmotic swelling will not occur here, as the attractive forces are strongest. Expansion of unit layers together with following separation may result in dissociation of metal ions, which move into the solution. Distribution of the metal ions near the crystalline surface is therefore much denser than in the surrounding water/solution. According to osmotic principles water will migrate from the regions with lower ion concentration to those with higher resulting in additional swelling and increased gap between the unit layers (Caenn et al., 2011). Skjeggstad (1989) reports that osmotic swelling is more significant and accounts for 80 to 90% of the total swelling in Na-montmorillonite. It is this property, which makes bentonite so attractive for the drilling fluid industry.

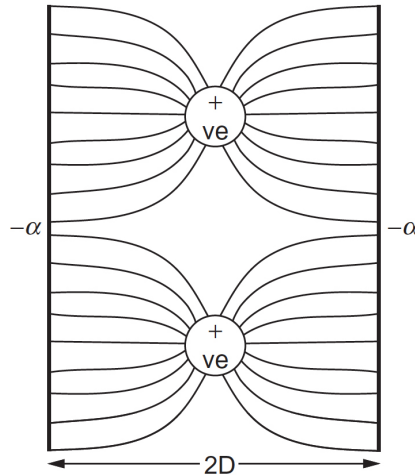


Figure 10. Forces acting between two unit layers (from Caenn et al., 2011)

4.2.3 Particle Association Forms

Generally bentonite particles may occur in four different association forms, when added to solution (Figure 11):

- Flocculated
- Deflocculated
- Aggregated
- Dispersed

	Flocculated	Deflocculated
Aggregated		
Dispersed		

Figure 11. The association forms of bentonite particles in drilling fluids (from IPT, 2012)

Skjeggstad (1989) indicates that the bentonite condition in the drilling fluid depends mainly on the electrostatic interactions between different particles. *Flocculation* is the term used to describe the association form where individual crystals are linked to each other *edge-to-edge* or *edge-to-basal surface*. The process depends on many different factors, which are covered in detail by Caenn et al.

(2011). Flocculation occurs normally in the solution with electrolyte since the electrical double layer of the particles will be reduced significantly (description of electrical double layer phenomena is, however, beyond the scope of this thesis). Electrolyte shrinks the electrical double layer around the clay particles and at high concentrations attractive forces start dominating. Moreover, it is required that bentonite particles have positive charge on the edges for flocculation to occur. This will result in the attraction between negatively charged basal surfaces and positively charged edges. Flocculation influences important drilling fluid properties as viscosity and filter loss. It results in a higher YP, gel strength and increased filter loss as well since flocculated particles will not build an impermeable filter cake on the borehole wall (Skjeggstad, 1989).

When bentonite is added to water to prepare spud mud it is very often that some of the particles will be in a flocculated condition. Total *deflocculation* is achieved normally only by addition of thinners as for example lignosulfonates and tannates. These materials are called *deflocculants* (Caenn et al., 2011). Deflocculants neutralize the positive charge on the edges of montmorillonite crystals thus preventing the attraction between the particles. The neutralization occurs as the result of the reaction between deflocculants and the ions exposed on the edges and formation of complex compounds incapable of dissolving.

Another term used to describe clay particles association in colloidal systems is *aggregation* or *aggregated condition*, which means that the bentonite particles are not in the form of single crystals, but are rather bounded in stacks (Figure 11). Caenn et al. (2011) describe the aggregation process as the opposite to what occurs during swelling. In this regard viscosity of the fluid decreases during aggregation due to the following two reasons:

1. Crystal external area exposed is now much smaller
2. The total number of crystals reduces as well since several crystals will coalesce with each other.

Dispersion is a term frequently used to depict the process of separating aggregated particles into individual sheets (Caenn et al., 2011). The desired condition of bentonite particles in spud mud is dispersed and slightly flocculated, as this mud will exhibit good properties both with regards to viscosity and filter loss control (Skjeggstad, 1989).

5 New Spud Mud Concept

The concept of native mud, where the only constituents are drill cuttings, was first introduced and defined in this thesis in Section 4.1.2. The new approach for preparation of spud mud is based on the idea that it could be possible to make a drilling fluid with required properties by mixing thermo-mechanically treated drill cuttings and available water at the installation. The basis for this idea lies in the possible similarity in chemical and mineralogical compositions of the drill cuttings and bentonite – often the only additive in a standard spud mud. Though this concept may seem rather unrealistic this chapter presents positive aspects of the concept and benefits this development may bring to the petroleum industry as a whole.

5.1 Drill Cuttings and Bentonite Analogy

Even though geologists define three main rock types: igneous, metamorphic and sedimentary, the petroleum industry is mainly interested in the latter type of rocks. Several sources report that sedimentary rocks cover up to 80% of the Earth crust and extend up to 2.2 km depth on average, which means that there is a number of sedimentary rocks found deeper than this (Boggs, 2009). Oil and gas deposits are found in sedimentary rocks as well and a short overview over these types of rocks is provided in Section 5.1.1.

5.1.1 Sedimentary Rocks

Sedimentary rocks are often defined as the rocks produced as the result of combination of weathering, transport, deposition and diagenesis on the earth surface under normal conditions (Boggs, 2009). All the sedimentary rocks can be classified into three main groups, whereas each of these groups may be subdivided according either to their composition or grain size. Boggs (2009) provides a classification of sedimentary rocks, which is shortly summarized in Table 6.

Table 6. Classification of sedimentary rocks (from Boggs, 2009)

Group	Grain size	Components	Examples
Siliciclastic	> 2mm	Rock fragments	Conglomerates
	1/16-2 mm	Silicate minerals and rock fragments	Sandstone
	<1/16 mm	Silicate minerals	Shale
Chemical/ biochemical rocks	Variable	Carbonate minerals	Limestone and dolomite
		Evaporite minerals	Rock salt and gypsum
		Chalcedony, opal	Chert
		Ferruginous minerals	Ironstone
		Phosphate minerals	Phosphorite
Carbonaceous rocks	Variable	Siliciclastic or chemical/biochemical components	Oil shales
		Carbonaceous residues	Humic coals

5.1.2 Description and Mineralogy of Shales and Mudrocks

The Petroleum industry is often interested in detailed studies and descriptions of sandstones and limestones as these two rock types contain a good deal of the world petroleum resources. However, here the description of shale rocks will be given, including their mineralogy, since this type of rock is the main component of the drill cuttings to be used in the development of the new spud mud.

Mudrock is another term used to describe fine-grained sedimentary rocks of siliciclastic origin. These types of sedimentary rocks are made of silt particles with their grain size varying from 1/256 to 1/16 mm and clay particles, which are smaller than 1/256 mm (Prothero and Schwab, 2004). Depending on the dominating grain size, rocks can fall into different categories as siltstone or claystone. In addition laminated mudrock types are called shales according to Prothero and Schwab (2004). On the other hand, Boggs (2009) points out that shale is often the term used by many to describe all the fine-grained siliciclastic sedimentary rocks. According to Boggs (2009) shales comprise 50% of all sedimentary rocks. The fact that these rocks are found mostly subsurface and are rarely found in form of outcrops increases the attractiveness of shales for this project. This is because of the simple aspect that drill cuttings are derived from subsurface.

As any other sedimentary rock mudrocks are formed as a result of several physical and chemical processes and are derived from the pre-existing rocks. Several sources provide a rough composition of shale rocks, but there has not been many scientific researches carried out to identify detailed mineralogical contents of this sedimentary rock in particular (Prothero and Schwab, 2004 and Boggs, 2009). These authors find the complexity of mudrocks, difficulties in application of conventional analysis methods, inaccessibility of clay rocks and vast variety in the rock composition as main reasons for the relatively low amount of information about the mineralogical contents of shales. On the other hand, it is commonly accepted that this type of sedimentary rocks consists of the following main building blocks (Boggs, 2009):

- Quartz
- Feldspar
- Mica
- Clay minerals
- Smaller amounts of oxides, carbonates and sulfur minerals

Boggs (2009) indicates that the amount of quartz versus clay minerals may notably vary depending on the depositional environment of the rock with clay mineral content reaching as high as 75%. The content of quartz minerals reduces in the marine environments when moving away from the shore. Prothero and Schwab (2004) mention that kaolinite, montmorillonite, illite, chlorite and gibbsite are the most abundant clay minerals in the sedimentary rocks and often a combination of

these minerals will be encountered. Even though the authors report that shales are very rich in illite it is worth paying attention to the presence of montmorillonite in the list over clay minerals given above. Montmorillonite is the main constituent of bentonite used actively in the drilling fluid industry. The fact that there is a high chance that drilled formations have some decent percentage of montmorillonite gives reason to believe that treated drill cuttings may exhibit similar properties as bentonite when added to water under correct conditions.

In spite of the difficulties regarding the mineralogical analysis of shale rocks several experimental and scientific works have been carried out to identify mineralogical composition of these rocks. Shaw and Weaver (1965) studied 96 samples of shale rocks derived mostly from Denver Basin, Gulf Coast and California. Several methods for analysis of shale rocks were used and the authors provided an average composition with clay minerals accounting approximately 61% of rock mass, while quartz, feldspars and carbonates comprised 30.5%, 4.5% and 3.5% respectively. Yaalon (1961) conducted an extensive research with the goal to reveal mineralogical content of clay. Instead of performing mineralogical analysis of the samples an average clay composition was derived from the chemical composition using correlations derived previously. The author concluded that shale rock consists of 59% clay, 20% quartz, 8% feldspars, 7% carbonates, 3% iron oxides and 2% other minerals and 1% organic matter. This analysis is therefore more detailed than the one performed by Shaw and Weaver (1965), though it may be more susceptible to uncertainty. Wilkinson et al. (2006) report that illite, smectite and kaolinite are the most abundant clay minerals in the shales from central and northern part of the North Sea. Smectite has also been found in the Paleocene sandstones acting as a cement material as well as in the shallow formations at the Veslefrikk Field. It is reported that fine-grained sedimentary rocks originating in the Viking and Central Grabens of the Jurassic and Paleogene ages are comprised mainly of an illite and smectite combination, with smectite being as high as 20%. Wilkinson et al. (2006) pointed out as well that smectite is more abundant in shallow formations rather than in deeper ones. The smectite content at the Gullfaks field may reach significant values varying from 70% to 100% of total clay amount. Wilkinson et al. (2006) reported that plenty of smectite is found in the Cretaceous and the upper Jurassic formations as well. Jones et al. (1989) carried out research and contributed with the detailed mineralogical analysis of shales from the Witch Ground Graben located in the central part of the northern North Sea. The analysis was performed on the cuttings from shale formations of the Cretaceous age. They concluded that mudrocks in this region consisted of clay minerals, calcite and a minor content of quartz and feldspar. Among the clay minerals smectite and illite were the most often occurring. Moreover, Na⁺ ions were found to be the most abundant in the shales of this origin. This fact is central for the analogy between shale formations in the North Sea and bentonite. Na-montmorillonite has good swelling properties and is responsible for the viscous properties water attains when bentonite is added (Section 4.2.2). According to the results provided by Jones et al. (1989) smectite concentration of shales varies from 15% to 40% as the upper limit, while that of illite from 4% to 22%. Non-clay minerals as quartz and calcite had average

concentrations of 12% and 40% respectively with some rare extremely high and low values. Good correlation between the amount of smectite and illite and the CEC of the shale rocks were observed. In addition, a correlation was documented between concentrations of Na⁺ ions and smectite mineral content, indicating possible presence of Na-montmorillonite. The presented summary of the scientific works carried out to reveal mineralogical composition of the shale rocks concludes that, not only these sedimentary rocks consist mainly of clay minerals; they may be abundant in the montmorillonite mineral, which is the main building block for the viscosity of drilling fluids. Therefore, the similarity in the mineralogical contents of bentonite and the cuttings derived from some subsurface formations in the North Sea may enable preparation of spud mud using treated cuttings.

5.2 Drill Cuttings Treatment Technology

High quality cutting treatment is required to enable preparation of spud mud using the recovered fragments of drilled formations. TWMA is a world leading service company in waste management and provides innovative environmental solutions for the petroleum industry. It has bases and operations in Europe, Americas, North Africa and the Middle East. TWMA provides technology for handling of oil-contaminated drill cuttings, which has already been successfully field-tested offshore on a semisubmersible rig on the UK Continental Shelf (Kirkness and Garrick, 2008). Cuttings provided by TWMA were used in the experimental part of this thesis.

The treatment process used by TWMA is based on the indirect thermal desorption principle. Here the cuttings are fed to a number of hammer mills connected in series and located in a housing. The mills consist of a rotor, rotating on a shaft with high RPM and a stator part as shown in Figure 12. This type of cutting treatment setup is known as thermo-mechanical cuttings cleaner (TCC). A significant heat amount is generated in the TCCs through conversion of mechanical energy provided by the rotor due to the friction (Murray et al., 2008). This principle does not apply any other form of energy but mechanical provided by the rotor to increase the treatment temperature. Drill cuttings are heated directly, which results in a quite fast process without implementation of complicated heating systems. This heat is high enough to convert liquid phases of oil and water into gaseous. Due to its fast rotating speed the rotor generates a centrifugal force, which pushes the material towards the walls of the stator. As the fluid phases evaporate they pass through several condenser sections, where both water and oil rests can be regained. Prior to this step fine particles following volatile fluids are removed by a setup of cyclones and separators.

Data achieved from the two field tests carried out on the UK Continental Shelf demonstrate quite positive results. Kirkness and Garrick (2008) report that the drill cuttings discharged to the North Sea had less than 0.1% by weight of hydrocarbon amount. Moreover, initial onshore trials demonstrated that water regained from the treatment process had less than 20 ppm of oil content. It is worth mentioning that according to the Norwegian Activity Regulations oil content of water should not exceed 30 mg of oil per liter of water, while oil content of cuttings should be lower than 10 g per kilogram of dry mass (Lovdata, 2014). Assuming density of seawater

to be 1030 kg/m^3 , 30 mg of oil per liter water corresponds to 29.12 ppm. Thus, the results provided by TMWA are well within the limit assigned by the Norwegian regulations, which makes the approach attractive for the industry. In addition to meeting all criteria there is a number of benefits when implementing cutting treatment technology for waste management in terms of reduced costs, less environmental impact, better safety and logistics.

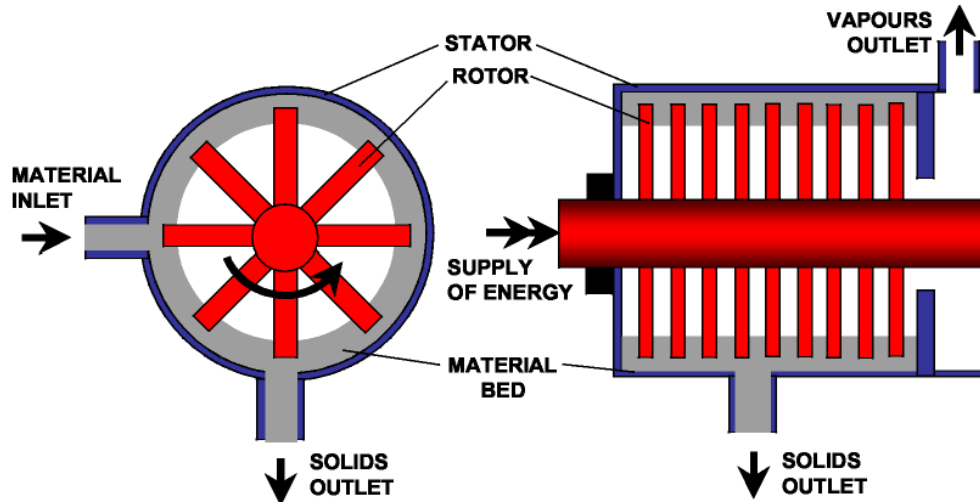


Figure 12. The principle of cuttings treatment used by TWMA (from Murray et al., 2008)

5.3 Benefits of the New Spud Mud Concept

The new approach to spud mud preparation using treated drill cuttings introduces a wide variety of benefits, where most of them can be classified into economical and environmental. According to the waste triangle shown in Figure 13 and presented in the Norwegian Oil and Gas Association "Recommended Guidelines for Waste Management in the Offshore Industry" (2004) it is desirable to avoid disposal of waste material on land. On the other hand, top priority is given to the prevention of waste occurrence at all or the reuse of the products. These options result both in reduced costs and serves as a significant advantage to the society and the environment. Currently drill cuttings with the rests of OBM are deposited onshore after having received a treatment and this approach does not lead to a lot of environmental benefits.

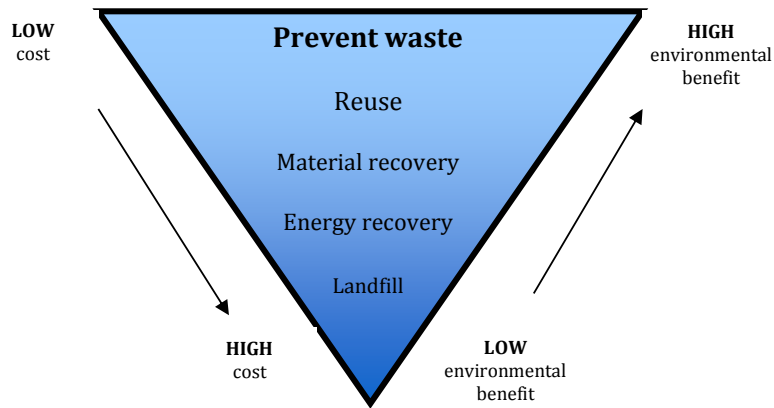


Figure 13. The waste triangle (from the Norwegian Oil and Gas Association, 2004)

Kirkness and Garrick (2008) emphasize, that sending drill cuttings to landfills results in the inevitable loss of oil, which could have otherwise been reused. Moreover, this results in additional marine transportation and pollution from cargo ships. According to the numbers provided by the authors as much as 50000 barrels of oil can be recovered from the cuttings coming from the UK Continental Shelf only using the TCC technology provided by TWMA. In addition to a decent environmental benefit, reuse of oil gives a significant economical reward, since the need for purchasing new oil will be reduced. The introduced new concept of the spud mud provides yet another reuse possibility in form of drill cuttings. This may reduce the volume of bentonite used on the yearly basis as well. This approach could turn drill cuttings, what actually have always been considered as a waste, into a useful material and this has a significant importance for the industry and the environment.

The treatment of drill cuttings can take place both at onshore facilities and directly offshore. The latter approach introduces a number of transport and safety related advantages. When processing the cuttings offshore the need for transportation of containers onshore is eliminated. This reduces the number of heavy lift operations and contributes to a safer work environment. Moreover, the need for transport operations during winter months is avoided as well (Kirkness and Garrick, 2008).

5.4 Considerations Regarding Storage of Cuttings and Mud Mixing

If an operator selects to mix a spud mud using thermo-mechanically treated drill cuttings recovered from TCC mills installed on a drilling rig offshore several considerations are required to be made in this regard. Due to this reason main aspects will be discussed in this section to provide a complete picture of the introduced concept. The most important features that will be discussed here are storage of treated drill cuttings offshore, pneumatic transfer of cuttings from bulk storage tanks to mud mixing area and mixing precautions.

When using drill cuttings as an alternative to bentonite in spud muds the required storage place for bentonite will be reduced, since volumes bentonite occupied are now replaced with treated drill cuttings. In this case drill cuttings treated by TCC on site can be stored in bentonite silos. These silos are placed normally in the legs of a

floating drilling rig or in the mixing rooms in case of a jack-up rig. Additional storage silos can be placed on the deck in case of available place and if this is required (Framnes, 1992).

Moreover, the process of pneumatic transfer of drill cuttings from bulk storage to the mixing equipment needs to be studied thoroughly and understood prior to the operations. Blow tanks are usually used to transfer barite or cement from silos to the mixing room. Dry powder material is fluidized in blow tanks by a membrane prior to further transfer. Ratnayake et al. (2008) emphasize that significant pressure drop may develop at the entry section of the blow tank during this process and it is therefore important to be able to predict the process behavior. Ratnayake et al. (2008) developed a simple model (using dimensional analysis) for scaling up entry pressure drop in blow tanks. This model could be implemented during initial testing, however, detailed discussion of this issue is beyond the scope of this thesis.

Several aspects need to be taken into consideration regarding the mixing of spud muds itself. As these cuttings are recovered after drilling with an OBM the rests of surfactants may be present on the material (Section 3.3.2). It is therefore important to keep an appropriate mixing speed to avoid significant vortex generation. Too aggressive agitation would result in entrained air in mud and foaming of the drilling fluid. According to ASME (2005) vertical baffles can be placed into the mixing tanks to avoid having air in mud pumps if this should be an issue.

6 Preliminary Material Testing

The idea behind and the main objective of this thesis were to develop a new type of water-based drilling fluid using treated drill cuttings (Section 2). The theoretical background for possible similarity between the main component of the conventional spud mud bentonite and the thermally treated drill cuttings was presented in Section 5.1. It was therefore of interest to conclude the expected resemblance between the materials by carrying out preliminary testing of central material properties. For this reason, particle size distribution (PSD) was studied both of bentonite and treated cuttings samples.

6.1 PSD Measurements

PSD curves demonstrate the relative distribution density of particles and provide understanding of what range of particles one is dealing with. It was mentioned in Section 4.2 that colloidal particles with a size of less than 2 microns had great influence on the fluids viscosity. Presence of particles in this size range might be important to obtain required drilling fluid properties when implementing drill cuttings instead of bentonite. Moreover, smaller particles contribute to better viscosity properties and particles with insignificantly spread distribution are less predisposed to sedimentation (Horiba, 2012). A laboratory study was carried out to compare the PSD of the conventional viscosifier and treated cuttings.

6.1.1 Methods of PSD Determination

A short literature review was conducted in order to evaluate existing methods of PSD determination so that the most convenient one could be selected based on the required detail level of the measurements and the time consumption. Caenn et al. (2011) present a summary of the particle size determination techniques commonly used in the industry. The authors present both simple methods as sieve or sedimentation tests and complex analysis technologies incorporating laser diffraction. One of the techniques for measurement of particles with size range of 0.6 to 400 microns approximately implements an instrument called Coulter counter. This type of device was recently received in the University laboratory and an attempt was made to determine PSD using Coulter counter instrument. However, the equipment was incapable of covering the entire particle size range of drill cuttings due to its limitations. The samples were therefore sent to the external laboratory Tel-Tek in Porsgrunn and analyzed using a laser diffraction technique.

6.1.2 Laser Diffraction Principle

Tel-Tek laboratory implements HELOS Laser Diffraction Sensor, which is capable of measuring the particles size in the total range of 0.1 to 8750 microns (Sympatec, 2014) and was therefore satisfactory for the selected purpose.

In general, the main principle of laser diffraction is based on the determination of the volume of particles based on the measurement of the diffracted light intensity. The size of particle influences the intensity of light scattered from the particle (Stojanovic and Markovic, 2012). When a particle is illuminated, the light will

scatter away from its surface creating what is called particle scattering pattern as shown in Figure 14. According to Stojanovic and Markovic (2012) this pattern depends on the ratio of the particle size to the wavelength of the light the particle is exposed to. Diffraction theory says that smaller particles scatter light at larger angles, but of weaker intensity, while larger particles scatter light of a higher intensity at reduced angles (Horiba, 2012). The entire particle range will produce a spectrum of diffracted light that can be used to convert the light intensity and angle values into the PSD.

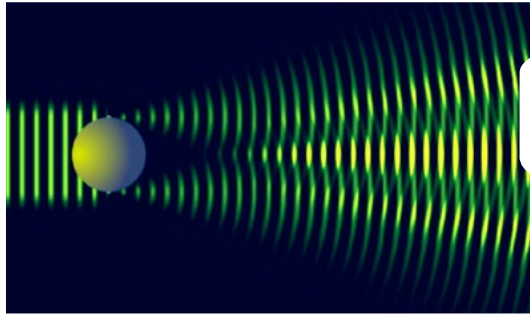


Figure 14. The diffraction pattern from a particle (from Horiba, 2012)

6.1.3 Measurement and Data Presentation

Laser diffraction measurements carried out by the Tel-Tek laboratory were performed in accordance with the ISO 13320:2009 Standard and the reader is referred to this standard for detailed procedure description. A dry test was performed for PSD of cuttings and a wet test for that of bentonite. This was done to disperse dry aggregated bentonite particles. However, this chapter presents a detailed description of main statistical data that is presented in Section 6.1.4 as well to provide better understanding of the obtained results.

Number and Volumetric Distribution

PSD statistical data can be presented in a numerical and a volumetric form (Horiba, 2012). In the former method particle distribution is given in a curve or histogram form with particle size on the x-axis and the frequency of these particles on the y-axis. This presentation form is more intuitive as each particle size receives equal weight coefficient. On the other hand, in volumetric PSD the x-axis still has the same values, while on the y-axis the volumetric percentage of total volume any particular size accounts for is represented. In this case larger particles can constitute a large part of the total volume, so the distribution will look differently. Since laser diffraction technique measures the volume of particles and not their linear dimensions it is commonly accepted to provide results in volumetric distribution fashion. Even though it is possible to recalculate the results to obtain a numerical distribution, it is reported that significant error sources may be introduced in this process (Horiba, 2012). Moreover, the samples were expected to have lognormal volumetric distribution as well.

Mean, Median, Mode and Percentile Values

When dealing with any kind of distribution it is not sufficient to state a single value, as this value does not tell much about the distribution itself (Horiba, 2012). Statistical parameters are commonly used to give more detailed description of PSD. The meanings of several statistical parameters used to describe the data in Section 6.1.4 are provided here.

Mean is a term often used as a synonym of average. Though when dealing with particle distributions mean is not always the sum of all sizes divided by the number of particles. In volumetric distributions volumetric mean is often calculated according to Eq.7 (Horiba, 2012):

$$D_{4,3} = \frac{\sum_1^n D_i^4 \cdot v_i}{\sum_1^n D_i^3 \cdot v_i} \quad (\text{Eq.7})$$

where, $D_{4,3}$ is volumetric mean diameter in μm , D_i is geometrical mean diameter of a given interval in μm and v_i is a relative frequency of this interval.

Median is the term used to describe the value where 50% of measurements are smaller and 50% are larger than the given value (Horiba, 2012). In case of symmetrical distributions mean and median values will coincide.

Mode is used to refer to the most often occurring value in the distribution i.e. the highest point on the diagram (Horiba, 2012). This parameter is of lesser interest when dealing with single mode distributions. However, in bimodal distributions the difference in the values can describe data spreading. Mean, mode and median terms are visualized in Figure 15.

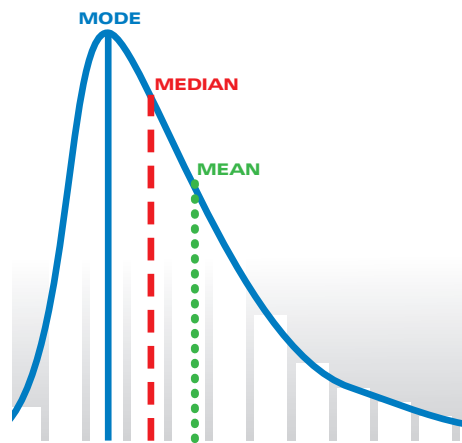


Figure 15. Mean, median and mode visualization (from Horiba, 2012)

In addition to the statistical values introduced in this section percentile values are often used to describe the width of PSD. D_{10} and d_{90} values represent particle size at lower and upper ends of distribution respectively as shown in Figure 16. 10% of the particles have dimensions smaller than d_{10} value, while 90% of the particles are

smaller than d_{90} . On the other hand, d_{16} and d_{84} percentile values are used in the oil industry on the common basis (Datta et al., 2007). In case of a normal distribution, these two percentiles would be one standard deviation away from the mean value and therefore have a distinct statistical meaning. These values are included in the results as well (Section 6.1.4).

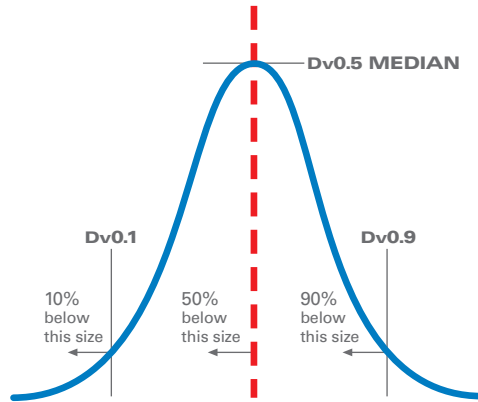


Figure 16. D10 and D90 visualization (from Horiba, 2012)

6.1.4 Results

Five runs were carried out for each sample in order to determine the PSD of bentonite and treated cuttings samples. The obtained results in each run demonstrated good correspondence with each other and the main statistical parameters as X_{10} , X_{16} , X_{50} , X_{84} , X_{90} , mean and mode had only slight variations. Due to this reason averaged data for the runs is presented in this section. Here X_n value has similar statistical meaning as D_n value introduced in Section 6.1.3. X_n is the value where n weight% of the mixture has size smaller than X_n . Table 7 contains statistical data of cutting and bentonite samples PSD. Graphical representations of PSD of the analyzed samples are shown in Figure 17 and Figure 18.

Table 7. The summary of the main PSD data for the cuttings and bentonite samples derived from laser diffraction analysis

Sample	Statistical Data						
	X_{10} , μm	X_{16} , μm	X_{50} , μm	X_{84} , μm	X_{90} , μm	Mean, μm	Mode, μm
Cuttings	1.03	1.35	5.12	46.1	69.7	21.2	2.30
Bentonite	1.06	1.40	4.10	24.3	49.2	15.6	4.00

Both samples demonstrated lognormal distribution as expected (Figure 17 and Figure 18). It is important to mention that the bentonite sample has a median value of 4.10 microns. This means that approximately 50% of the bentonite particles are of colloidal nature, which is in correspondence with expectations as well (Section 4.2). However, the results of the bentonite particle distribution measurements are quite elevated. According to Skjeggstad (1989) d_{90} value of bentonite should be approximately equal to 2 microns. And the rest of the distribution is flat with the particles in the range from 2 microns to 100 microns. As it can be seen from

Figure 18 the shape of the distribution is similar to that described by Skjeggstad, with flat line at higher values. On the other hand, d_{90} is much higher than 2 microns. That bentonite particles are in aggregated form in dry condition means that several particles are bound together forming large flakes. Even though wet measurements were performed by Tel-Tek, poor and insufficient dispersion of bentonite during sample preparation was probably the reason for the observed deviation from the expectations. However, given that the treated drill cuttings material was not aggregated and did not hydrate either (Section 8.3) dry test results were acceptable for this application and the cuttings PSD was considered to be correct.

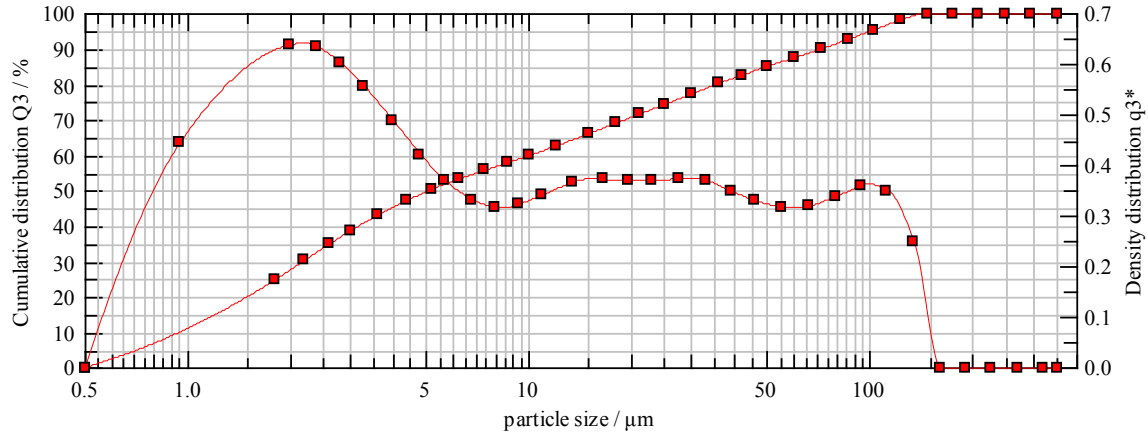


Figure 17. PSD of the cuttings sample

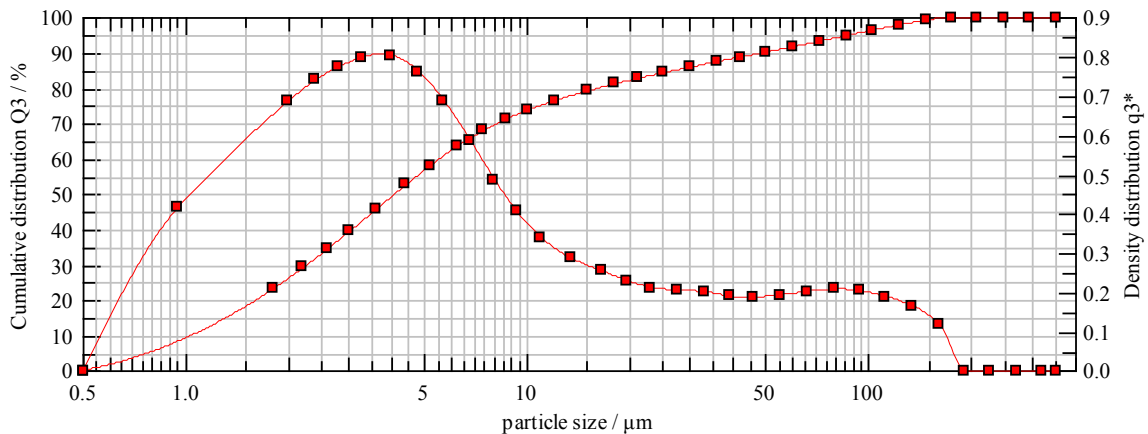


Figure 18. PSD of the bentonite sample

It can be seen from Table 7 that bentonite and treated cuttings have quite similar PSDs at the lower end. The lowermost 10% of the particles have approximately the same size distribution, as the X_{10} values are almost equal. Moreover, the X_{50} values, of the samples are of comparable range as well. Median particle size of the drill cuttings is only 24.9% larger than that of the bentonite. Though this number might sound significant on the relative scale, on absolute scale this corresponds to the 1.02 microns difference. The statistical distribution obtained from the PSD testing supports the expectations that the materials might have comparable dimensions.

However, there are more particles of a larger size in the cuttings sample as mean is approximately 36% larger than that of the bentonite sample. This is seen on the diagram provided in Figure 19 as well.

The overall distribution curve shapes of the two samples are quite similar. However, bentonite sample has much higher percentage of particles less than 10 microns in size. At the same time percentage of the particle size larger than 10 microns is almost double as high for the cuttings sample. These differences are reflected in Figure 19.

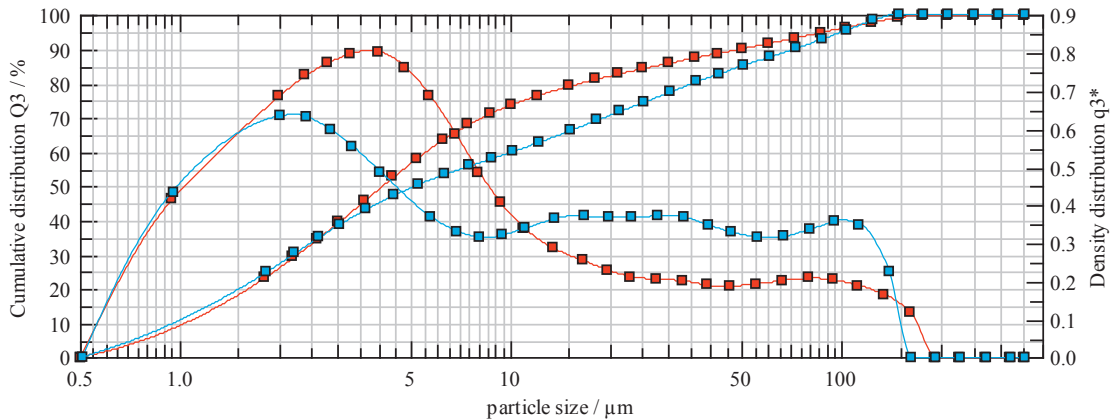


Figure 19. The comparison of PSD of the cuttings and bentonite samples derived from laser diffraction analysis. The red line – bentonite PSD; the blue line – cuttings PSD

It is important to emphasize here that during mixing of drilling fluids bentonite particles will be dispersed and result in a different PSD with smaller particles dominating in the distribution. However, keeping this in mind, comparison of the PSD of drill cuttings and bentonite leads to the conclusion that high viscosity of spud mud will be required at low shear rates in order to keep high amounts of large solid cuttings in suspension and to provide required yield for cutting transport at low flow velocities. On the other hand, particles in the colloidal range were observed in the cuttings sample as well as the result of the testing. These particles might theoretically contribute to the viscous properties of the fluid. PSD measurements partially confirmed the expected similarities in the size distribution of cuttings and bentonite (since the shapes of the distributions are similar though the values are quite different) and yielded the required precautions that were used during the main development of spud muds.

7 Experiments

7.1 General Information

Main objective of the experimental part of this thesis was to evaluate and test in practice the possibility of preparing a stable spud mud using thermo-mechanically treated drill cuttings as a replacement for bentonite (Section 2). Theoretical description of how clay minerals residing in cuttings especially montmorillonite may contribute to the generation of high viscous fluids was presented in Section 4.2. Several drilling fluid mixing experiments were conducted to study the efficiency of treated cuttings and to identify correct drilling fluid composition that yields the required properties. Two reference drilling fluids commonly used in the industry today and reported in the literature (Torbjørnsen, 1994 and IPT, 2012) were prepared as well. These fluids were tested in order to provide a baseline for the experiments conducted. All the mixed drilling muds were tested in accordance with the standard API procedures (API, 1990).

7.2 Materials

All the materials used in the experimental part of this thesis can be divided into four main groups:

- Base fluid
- Solid viscosifiers
- Polymers
- Weighting and filter loss agents

Even though polymers are often used as viscosifiers in drilling fluids, they are presented in a separate group in this work. This is due to the reason that we were mainly interested in investigating the viscosifying properties of thermally treated cuttings. Weighting and filter loss agents are not very common in the composition of spud muds and were therefore combined in one group as well. Though the former can be used during casing running to provide buoyancy and the latter to combat expected fluid losses while drilling through shallow permeable zones.

7.2.1 Base Fluids

Fresh water

Bentonite and active clay minerals in general neither hydrate nor yield high viscosity in high saline environments. Due to this reason the tests were initially conducted using fresh water from the tap at ambient room temperature.

Seawater

Normally the base fluid of a spud mud used offshore is SW since plenty of it is easily available offshore. Drilling fluid compositions that demonstrated stable rheological properties with fresh water were tested with SW as a base fluid as well. SW was

prepared artificially by mixing in the laboratory at the University of Stavanger according to the composition given in Table 8.

Table 8. SW composition used in the experiments

Salt	Concentration, g/l solution
NaCl	23.38
Na ₂ SO ₄	3.41
NaHCO ₃	0.17
KCl	0.75
MgCl ₂ ·6H ₂ O	9.05
CaCl ₂ ·2H ₂ O	1.91

7.2.2 Viscosifiers

Bentonite

MI-Swaco Norge supplied bentonite used for the experiments. According to the datasheet following the sample, it contained 60-100% of bentonite and less than 5% crystalline quartz (MI-Swaco, 2010). Specific gravity of this material is 2.5.

Treated Drill Cuttings

TWMA supplied 50 kg of drill cuttings from a well recently drilled on the Norwegian Continental Shelf (NCS) and treated by the TCC in the facilities at Mongstad. The cuttings were supplied in the powder form. The material is reported to have a density approximately equal to 2.5 SG. Chemical composition of the sample provided by TWMA is given in Table 9.

Table 9. The chemical composition of the treated drill cuttings used in the experiments (from TWMA, 2012)

Component	Content, %
SiO ₂	20-40
BaSO ₄	5-30
Al ₂ O ₃	<10
Fe ₂ O ₃	<10
CaO	<10
MgO	<5
Na ₂ O	<5
K ₂ O	<5
TiO ₂	<1
MnO ₂	<1
P ₂ O ₅	<0.5
SrO	<0.5

Relatively high content of barium sulfate in the drill cuttings composition can be explained by the fact that barite was present in the OBM which was used to drill the well. Presence of phosphorus (V) oxide can be ascribed to possible polyphosphates, which were used as a dispersing agent in the original mud. Other oxides are commonly present in the subsurface shale and clay structures that are encountered during drilling. Grim (1968) provides chemical composition of different clay

minerals and the main constituents are quite similar. In addition to this, the material contained 2247 mg/kg oil, 178 mg/kg aromatic compounds and 1.1 mg/kg of polycyclic aromatic hydrocarbons.

7.2.3 Polymers

Three types of polymers commonly implemented in the industry for different needs were used during the experimental testing of the properties of the drilling fluids. Polymers are often used to provide required viscosity and/or to reduce losses of the fluid to the formation. The effect of different types of polymers and their concentrations on the cutting-based drilling fluid was studied.

Carboxymethyl Cellulose (CMC) Hi-Vis

The CMC polymer shown in Figure 20 can be used to satisfy several needs as fluid loss control, viscosity and inhibition of clay materials (IPT, 2012). The radical group denoted by R is CH_2COONa in a CMC polymer structure (Figure 20). This type of polymer consists of glucose molecules connected in chains and is delivered in two modifications: short and long polymer chains. The former type of CMC gives low viscous effects, though the latter provides a high increase in viscosity. High viscosity type of the polymer was tested during the experiments as CMC is often used as a viscosifier and filter loss control material in spud muds (Section 4.1.1). This polymer type is reported to have relatively low Ca^{2+} ion and salt tolerance, 2000 ppm and 50000 ppm respectively (IPT, 2012).

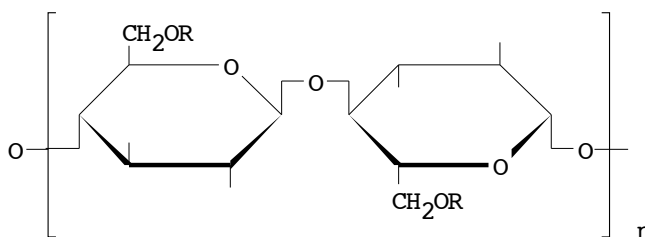


Figure 20. The principal structure of CMC (from IPT, 2012)

Polyanionic Cellulose (PAC)

This type of polymer has similar structure as CMC and can be used for the same purposes. However, PAC is reported to have better salt and Ca^{2+} ion tolerance and is more durable with regards to bacterial degradation (IPT, 2012). High viscosity modification of the PAC polymer was tested in the experiments. PAC is often implemented in the industrial drilling fluids as well to inhibit clay minerals and to provide additional viscosity.

Xanthan Gum

The xanthan gum biopolymer type Duo-Vis Plus NS supplied by MI-Swaco was used in the experiments. This polymer was available at the University of Stavanger drilling fluid laboratory. Generally xanthan polymers have a complex structure with cellulose molecules as the main chain and mannose, glucose and monosaccharide attached to it as shown in Figure 21 (IPT, 2012).

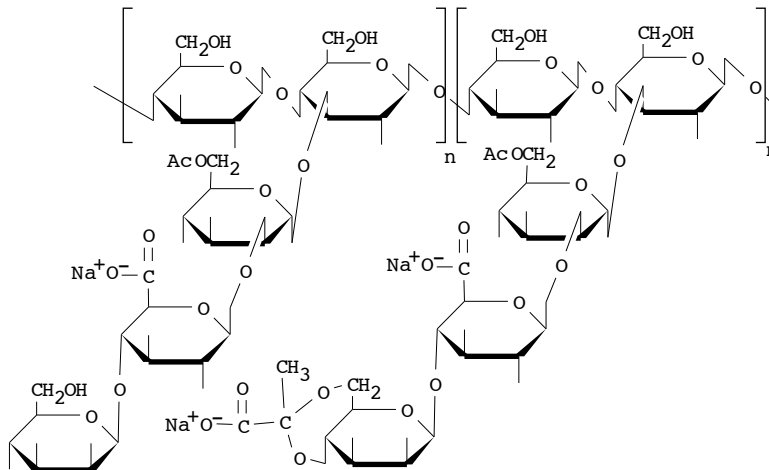


Figure 21. The principal structure of xanthan biopolymer (from IPT, 2012)

As a rule xanthan polymers are quite good with regards to viscosity generation, but not as effective as other polymers with regards to filter loss control (IPT, 2012). According to the product sheet provided by MI-Swaco, Duo-Vis Plus NS is particularly effective to increase low shear rate viscosity values, yield notable gel strength and give good cutting transport (MI-Swaco, 2004). The supplier reports that the material can be used both in fresh and saline water systems with either low or high solid contents. The resulting fluid has significant shear thinning properties, which are desirable during drilling (Section 3). The fact that xanthan gum polymers give the stated characteristics to a drilling fluid was the driving factor behind choosing this particular polymer for analysis. Standard concentrations of Duo-Vis Plus NS used in drilling fluids may vary from 1.0 kg/m³ to 4.0 kg/m³ and concentrations up to 9 kg/m³ can be used if required according to MI-Swaco (2004).

7.2.4 Weighting and Filter Loss Agents

Barite

Weighting agents are commonly added to drilling fluids in order to increase its density to the desired level with regards to the control of pore pressures and other drilling related issues (Section 3.1.1). These agents are normally minerals such as hematite, ilmenite, calcite, galena and siderite with very high specific gravity varying from 2.7 SG up to 7.0 SG (IPT, 2012). However, the most popular of all weighting agents used is barite. It is composed mainly of barium sulfate (BaSO₄), small amounts of barium carbonate (BaCO₃) and other impurities. Its density is equal to

4200 kg/m³. This material is non-reactive and can yield high fluid density even at low concentrations. Barite was added to the drilling fluid in order to study the ability of mud to suspend heavy solid particles and to evaluate how this would affect the fluid properties. Moreover, this allowed investigating the possibility to increase the density of spud mud prior to casing running.

CMC Low-Vis

Since xanthan gum polymer is not as effective as other types with regards to fluid loss, short chain length CMC (Figure 20) was tested as a fluid loss material in spud muds with xanthan gum. It is often used as a filter loss agent and is reported to have high efficiency in water based mud systems with salt concentrations lower than 50000 ppm (Chilingarian and Vorabutr, 1983). This material was selected for filter loss controlling purpose since it is easily available and is relatively cheap in comparison with other polymers.

7.3 Description of Experiments

A number of different drilling fluid compositions were mixed and tested to attain a mud with stable properties implementing drill cuttings. The experimental part of this work is divided into three sub-groups. Initially two reference drilling fluids were mixed i.e. bentonite and bentonite/CMC spud mud. Performance of thermally treated drill cuttings when added to water was studied in the first stage of the experimental work as well. This test carried more of an introductory character, which enabled a better evaluation of the situation and provided basis for further adjustments. Based on the results of the initial testing, influence of different kind of polymers, weighting and fluid loss agents were studied at a later stage. The effect of temperature on drilling fluid viscosity profile was studied on the stable drilling fluids. This chapter contains description of experiments, all the drilling fluid compositions prepared and points out procedures for the preparations and any precautions, which were of interest.

The sample naming convention used in this thesis was based on the two main principles. Here the letters were used to describe a specific component, while the number following these letters reflected the concentration of this particular component in grams per 350 ml of water. So, C stands for cuttings, X for xanthan, B for barite, CMC LV for CMC Lo-Vis and SW indicated if the drilling fluid was prepared using SW as the base fluid. CMC and PAC abbreviations were used in the same way where applicable. For example, C75 X1.4 fluid contained 75 g cuttings and 1.4 g xanthan per 350 ml of water.

7.3.1 Experiment 1 (E1). Water and Cuttings/Bentonite Spud Mud Systems

Simple spud fluids consisting only of fresh water from the tap at room temperature and a specific amount of bentonite or treated cuttings were mixed in the first stage. Table 10 summarizes compositions of the prepared muds. When mixing the spud mud with the highest cutting concentration (C150) the amount of water and cuttings needed to be reduced in order to avoid splashing of the fluid during mixing

in a standard Hamilton Mixer as the obtained volume was close to the mixing cup volume. This was done accordingly as 129 g of cuttings in 300 ml of water is the same concentration as 150 g of cuttings in 350 ml of water. This made the achieved results totally comparable.

Table 10. The summary of the prepared simple spud mud systems using bentonite and cuttings in experiment E1

Drilling Fluid Name	Component	Amount (g or ml)
B REF	Water, ml	350
	Bentonite, g	25
C75	Water, ml	350
	Cuttings, g	75
C100	Water, ml	350
	Cuttings, g	100
C125	Water, ml	350
	Cuttings, g	125
C150	Water, ml	300
	Cuttings, g	129

As shown in Table 10 much higher concentrations of cuttings were used than that of the bentonite reference fluid (B REF). Compositional difference between the materials was the main reason. It was given in Table 9 that the treated drill cuttings contained up to 30% barite. Moreover, the rest of the material was not necessarily active clay minerals and might not hydrate. Due to this reason 3, 4, 5 and 6 times higher concentrations of cuttings were tested to compensate for these differences. It was important to add drill cuttings to water in batches as the powder flew easily when added in large amounts at once. The water-cutting mixtures were mixed in the standard Hamilton Mixer for 12 minutes. Mixing of cuttings and water resulted in a vortex even at the lowest mixing speed and the fluid could easily take up air. Thus, when adding treated drill cuttings to water under mixing considerable amounts of foam were generated. This foam was actually difficult to break and high amounts of foam breakers needed to be implemented. Delfoam V14 supplied by MI-Swaco was efficient to break the foam. On the other hand, DF5001 of MI-Swaco did not result in any positive effect. Up to 10 drops of antifoam agent were transferred to the mixing cup to combat this effect depending on the drill cuttings concentration. It is worth mentioning that it is recommended to disperse foam breaker in the fluid manually using a spoon and not in the mixer as this will drive in more air.

7.3.2 Experiment 2 (E2). Water, Cuttings and Polymers

Experiments with fresh water, cuttings and polymers were carried out as well to evaluate the influence of these compounds on the overall drilling fluid properties. Bentonite/polymer reference mud (B CMC REF) was mixed during these experiments as well. Three types of polymers were tested together with drill cuttings. This included CMC, PAC and xanthan gum. The polymers were added to the newly prepared water/cuttings mixtures as in the E1 experiment to yield comparable data. When the correct type of polymer was identified upon the analysis of the results, the effect of cutting and polymer concentration on the spud mud

properties was tested as well. Table 11 reflects the summary over the spud mud compositions mixed in E2.

Table 11. The summary of the prepared spud mud systems using bentonite, cuttings and polymers in experiment E2

Drilling Fluid Name	Component	Amount (g or ml)
B CMC REF	Water, ml	350
	Na ₂ CO ₃ , g	0.7
	Bentonite, g	10.5
	CMC HiVis, g	0.7
C75 CMC 0.7	Water, ml	350
	Na ₂ CO ₃ , g	0.7
	Cuttings, g	75
	CMC HiVis, g	0.7
C75 CMC 1.0	Water, ml	350
	Na ₂ CO ₃ , g	0.7
	Cuttings, g	75
	CMC HiVis, g	1.0
C75 CMC 1.3	Water, ml	350
	Na ₂ CO ₃ , g	0.7
	Cuttings, g	75
	CMC HiVis, g	1.3
C75 CMC 1.6	Water, ml	350
	Na ₂ CO ₃ , g	0.7
	Cuttings, g	75
	CMC HiVis, g	1.6
C75 PAC 1.0	Water, ml	350
	Cuttings, g	75
	Drispac, g	1.0
C75 X 1.0	Water, ml	350
	Cuttings, g	75
	Xanthan gum, g	1.0
C75 X 1.2	Water, ml	350
	Cuttings, g	75
	Xanthan gum, g	1.2
C75 X 1.4	Water, ml	350
	Cuttings, g	75
	Xanthan gum, g	1.4
C75 X 1.6	Water, ml	350
	Cuttings, g	75
	Xanthan gum, g	1.6
C100 X 1.2	Water, ml	350
	Cuttings, g	100
	Xanthan gum, g	1.2
C125 X 1.2	Water, ml	350
	Cuttings, g	125
	Xanthan gum, g	1.2
C150 X 1.2	Water, ml	300
	Cuttings, g	129
	Xanthan gum, g	1.03

It is important to emphasize that polymers need to be added after the cuttings have been added to water. This step was found to be important with regards to possible hydration of cuttings since presence of polymers in the fluid may hinder the hydration. After addition of each component the fluid was mixed for 10 minutes at the lowest speed.

In the case with the highest cutting concentration, C150 X1.2 fluid, again lower volumes of the components were used as in E1 due to the volume limitations of a standard mixing cup. However, the cutting concentration ratio increased here to obtain comparable data as well. The comment regarding foam formation during mixing was given in Section 7.3.1. The foam-breaking agent was transferred to the mixtures twice during mixing of muds. Ten drops of antifoam were transferred when cuttings had been added and mixed for 10 minutes and then after having transferred polymers to the cup and mixed 10 more drops were transferred. Again the antifoam agent was dispersed in the fluid by manual agitation.

7.3.3 Experiment 3 (E3). Aging Experiment. Hydration Test

Hydration tests were carried out to identify whether the hydration degree of the treated drill cuttings would change with time. For this purpose simple water-cuttings slurries C75, C100, C125 and C150 compositions used in E1 and presented in Table 10 were mixed again using the same procedure and stored at ambient conditions for 10 days. C75 X1.2 fluid sample was as well prepared to study stability of the designed spud mud composition. The samples were tested accordingly after 10 days to compare the results from both experiments. Rheological measurements and visual observations of the conditions of samples were carried out to conclude on the hydration capability of the material.

7.3.4 Experiment 4 (E4). Seawater Based Spud Mud

Based on the results of the E2 and the E3 experiments the most stable drilling fluid compositions were tested using SW as the base fluid as well. The composition of the artificially prepared SW is given in Table 8. This experiment was of interest to investigate the possibility of quick spud mud preparation using easily available SW offshore. The results of E2 (Section 8.2) demonstrated that biopolymer alone was not efficient enough to combat possible fluid losses to porous formations. This observation is in line with the literature as well (IPT, 2012). Even though losses were significantly reduced with the application of biopolymer this was still twice as high as Statoil's requirements in the drilling program (Statoil, 2010). Due to this an additional drilling fluid composition was designed where a CMC Lo-Vis polymer was added to provide required fluid loss control. It is also common in the oil industry to increase the density of drilling fluids prior to casing installation. This is done to provide an extra buoyancy force and reduce load on rig equipment. Normally fluid density can be increased up to 1.30 SG (Statoil, 2012). Two compositions using varying concentrations of barite and cuttings were mixed to evaluate the performance of weighted spud muds.

In this experiment larger volumes of drilling fluids were prepared to provide sufficient amounts for both physical and chemical testing. Due to this the fluids in E4

were mixed using a Silverson L4RT-A mixer in a 2 l beaker. Mixing procedure was developed based on the best practice experience and included the following steps:

1. Drill cuttings were added slowly to the water and mixed at 3200 RPM for 4-5 minutes.
2. Depending on the drill cuttings concentration 5-10 drops of antifoam were added. The mixture was mixed at 2500 RPM until most of the foam disappeared.
3. Polymers were added slowly in batches to avoid large polymer lumps on fluid surface. Mixing speed was increased gradually from 2500 RPM to 4200 RPM as the fluid started to get more viscous. The mixture was mixed for 5 more minutes.
4. 5-10 drops of antifoam may be added during mixing process to combat foam immediately.

Table 12. The summary of the prepared SW- based spud mud systems in experiment E4 using, cuttings, polymers and other additives

C75 X 1.0 SW	SW, ml	700
	Cuttings, g	150
	Xanthan gum, g	2.0
C75 X 1.2 SW	SW, ml	700
	Cuttings, g	150
	Xanthan gum, g	2.4
C75 X 1.4 SW	SW, ml	700
	Cuttings, g	150
	Xanthan gum, g	2.8
C75 X 1.6 SW	SW, ml	700
	Cuttings, g	150
	Xanthan gum, g	3.2
C100 X 1.2 SW	SW, ml	700
	Cuttings, g	200
	Xanthan gum, g	2.4
C125 X 1.2 SW	SW, ml	700
	Cuttings, g	250
	Xanthan gum, g	2.4
C150 X 1.2 SW	SW, ml	700
	Cuttings, g	300
	Xanthan gum, g	2.4
C75 X 1.4 B SW	SW, ml	700
	Cuttings, g	150
	Xanthan gum, g	2.8
	Barite, g	177.6
C100 X 1.4 B SW	SW, ml	700
	Cuttings, g	200
	Xanthan gum, g	2.8
	Barite, g	136.1
C75 X 1.4 CMC LV SW	SW, ml	700
	Cuttings, g	150
	Xanthan gum, g	2.8
	CMC Low-Vis, g	2.00

In the cases with barite and CMC Lo-Vis the materials were added and mixed for 5 more minutes. Table 12 summarizes the prepared spud mud compositions in E4.

7.4 Drilling Fluid Testing

Drilling fluids prepared in experiments E1, E2, E3 and E4 were tested in accordance with the API procedures provided in Recommended Practice 13B-1 (API, 1990). Both physical and chemical tests were carried out in order to identify drilling fluid properties, which were influencing its behavior. However, the rheological properties of fluids were considered the most central parameter. Due to this the samples, which did not demonstrate the required properties, were not qualified for the extended physical and chemical analysis. As there were no deviations from the procedures provided by API (1990) the detailed testing procedures will not be given in this work and the reader is referred to 13B-1 practices. Short description of the tests, their principles and overview of implemented equations are, however, provided in Appendix B and Appendix C.

8 Results

Results of all the conducted experiments are provided in this section. The shear stress and shear rate values presented in the tables with the results in this section are given in lb/100ft² and RPM respectively. These values have been converted to the SI units when plotting the viscosity curves and the shear stress is given in Pa while shear rate is given in 1/s. This chapter carries the informative character and the explanations of the obtained results together with corresponding discussions are provided in the designated chapter (Section 9). All the calculated parameters in Section 8 are derived from the existing models and equations presented in Appendix B and Appendix C.

Prior to building the viscosity curves and selecting a rheological model, applicability of different models were studied by calculating linear correlation coefficients for every designed fluid using Eq. C-10, Eq. C-11 and Eq. C-12 given in Appendix C. These coefficient values are summarized in Table D-1 in Appendix D. For most of the designed fluids the Herschel Bulkley model provided the best data matching. However, in five cases the Bingham model gave a higher correlation coefficient. This occurred in cases with simple water-cutting slurries and the drilling fluids with either CMC Hi-Vis or PAC polymers. According to the theory the Bingham plastic model describes fluids with solid suspensions and a given YP the best (IPT, 2012). Even though water-cutting slurries did not have any significant YP, these mixtures can be definitely classified in a solid suspension group. The Bingham model yields poor description of the low shear rate viscosity as it is based only on 300 and 600 RPM measurements. Thus, when applying the Bingham model to the shear thinning fluids a significant error will be introduced. However, the fluids with CMC Hi-Vis and PAC polymers did not show good shear thinning properties, had poor low shear rate viscosity and a high power law index thus resulting in rather linear data points. Due to this reason the Bingham model gave best coefficient of correlation for some of these fluids. On the other hand, addition of xanthan gum to the mud compositions yielded far better shear thinning properties. As a result for xanthan gum containing spud muds, coefficient of correlation for the Herschel Bulkley model was significantly better than the two other models. This occurred since the Herschel Bulkley model is better than the Bingham model for describing shear stresses at low shear rate values (IPT, 2012). Moreover, the Herschel Bulkley model incorporates the YP parameter, when the power law model does not. Even though for a minor number of results the Bingham model provided a better data matching, all the viscosity curves were built using the Herschel Bulkley model to make the results comparable with each other and thus to simplify the discussion part.

8.1 Experiment 1 (E1). Water and Cuttings/Bentonite Spud Mud Systems

Overview of the samples prepared during this experiment is provided in Table 10. Fluid samples with drill cuttings did not demonstrate the desired rheological properties and yielded poor viscous parameters. Thus, chemical tests were not performed and some of the physical characteristics were not measured in this regard.

In this preliminary experiment spud mud systems, which consisted exclusively of fresh water and varying cutting concentrations, were tested for rheological properties, filtrate loss and pH value. Density measurements were attempted as well. However, large particles quickly settled out from the suspension. This phenomenon had significant influence on the measured density value. Moreover, the prepared spud mud samples demonstrated absolutely no fluid loss control. Filtrate started producing immediately after C75, C100, C125 and C150 spud mud systems were transferred to the test cell without applying any pressure. The resulted filter cake was thick, rough and quite porous.

In addition to the four water-cutting mixtures, a bentonite reference spud mud was mixed and tested for density, filtrate loss, pH and rheological properties. The obtained drilling fluid test results are reflected in Table 13. The viscosity curves for each of the drilling fluid compositions presented in Table 13 were constructed using MS Excel based on the Herschel Bulkley model assumption. These curves are shown in Figure 22, 23, 24, 25 and 26 together with the measured data points. These viscosity curves show how rheological properties of the designed fluids changed with increase of cutting concentration together with the curve of B REF standard bentonite spud mud.

Table 13. The results of drilling fluid testing in E1

Measured Parameters	Drilling Fluid Type				
	B REF	C75	C100	C125	C150
Rheology (RPM)					
600	35	5	8	11	14
300	27	4	5	7	10
200	24	3	3	5	9
100	21	2	2	4	7
6	14	1	2	3	3
3	13	1	1	2	2
GEL 10s	14	0	1	2	3
Density, SG ¹	1.04	1.12	1.15	1.19	1.22
pH	9.45	11.2	11.2	11.25	11.2
API Filter Loss, ml	12	N/A	N/A	N/A	N/A
Bingham Parameters					
PV, cP	8	1	3	4	4
YP, Pa	9.71	1.53	1.02	1.53	3.07
AV, cP	17.5	2.50	4	5.5	7
Herschel-Bulkley Parameters					
τ_0 , Pa	6.13	0.511	0	0.511	0.511
n	0.616	0.415	0.678	0.737	0.530
K, Pa·s ⁿ	0.164	0.115	0.0374	0.0311	0.1686

¹ Theoretical density value is provided in the table (except of B REF)

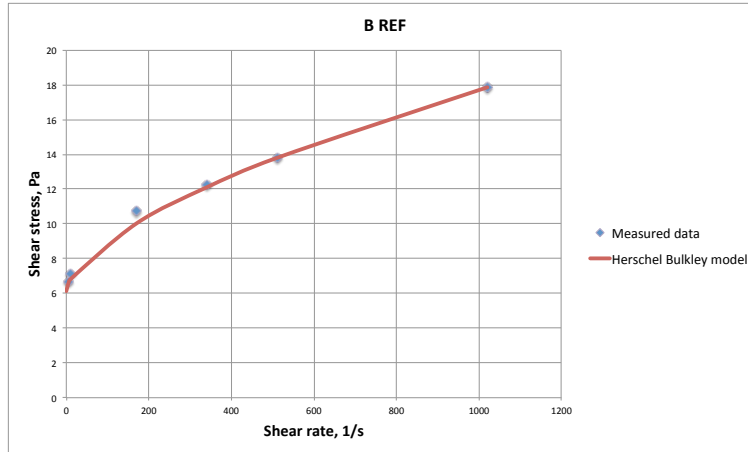


Figure 22. B REF fluid viscosity curve based on the Herschel Bulkley model and the measured viscometer data of a standard bentonite spud mud containing 25 g bentonite per 350 ml of water

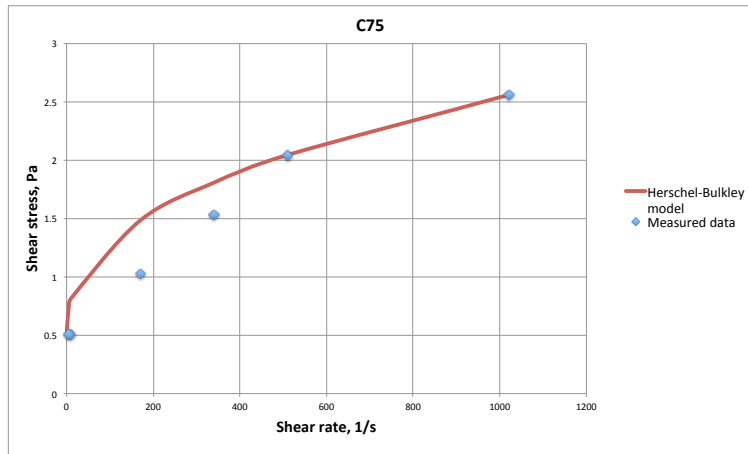


Figure 23. C75 fluid viscosity curve based on the Herschel Bulkley model and the measured viscometer data of a water-cuttings suspension containing 75 g cuttings per 350 ml of water

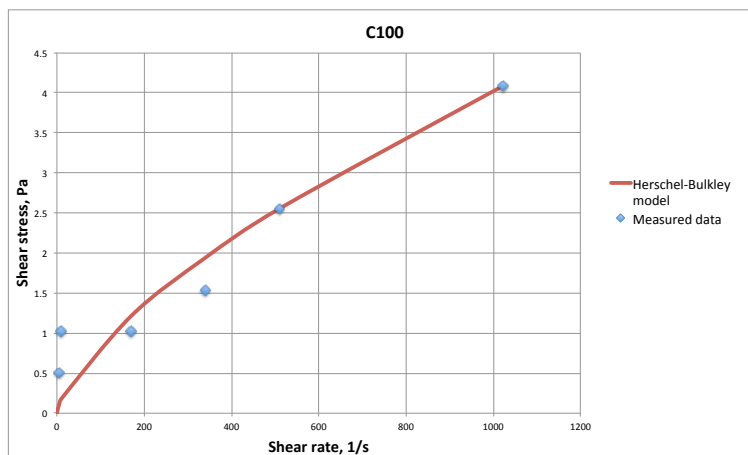


Figure 24. C100 fluid viscosity curve based on the Herschel Bulkley model and the measured viscometer data of a water-cuttings suspension containing 100 g cuttings per 350 ml of water

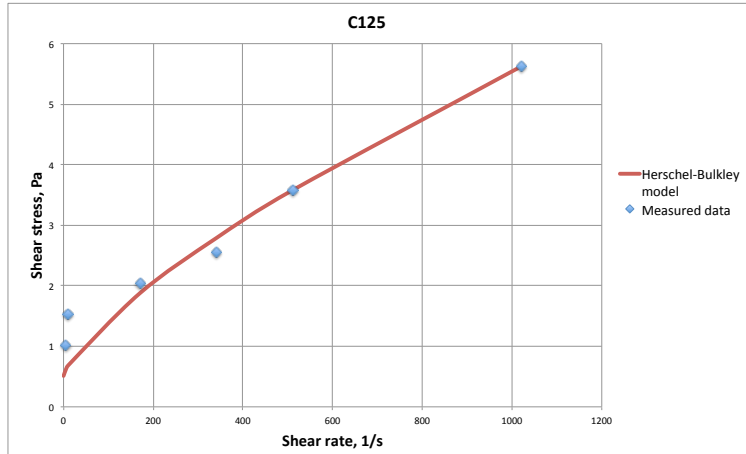


Figure 25. C125 fluid viscosity curve based on the Herschel Bulkley model and the measured viscometer data of a water-cuttings suspension containing 125 g cuttings per 350 ml of water

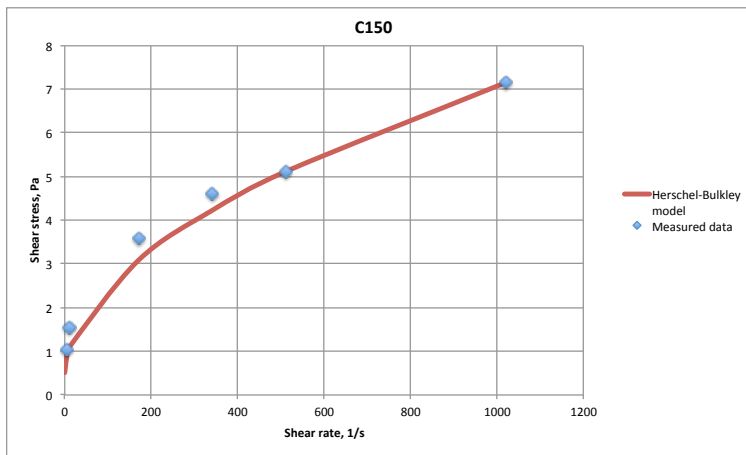


Figure 26. C150 fluid viscosity curve based on the Herschel Bulkley model and the measured viscometer data of a water-cuttings suspension containing 150 g cuttings per 350 ml of water

8.2 Experiment 2 (E2). Water, Cuttings and Polymers

None of the tested fluids containing only cuttings demonstrated similar performance parameters to those of the bentonite reference spud mud. Moreover, there was observed a severe mismatch between single studied properties. Based on the results of E1, where simple water-cutting slurries were analyzed, it was concluded that this batch of thermo-mechanically treated drill cuttings alone was not capable of providing the desired drilling fluid properties.

It is common practice in the industry to use the combination of bentonite and polymers in drilling fluids (Section 4.1). Due to this it was decided that the designed drilling fluids could be stabilized by addition of polymers. The performances of three types of polymers on the water-cutting slurries were tested. Oil well service companies commonly implement these polymers. This included: CMC Hi-Vis, PAC and a xanthan gum type biopolymer.

Fluid testing revealed that only the biopolymer was capable of generating the desired fluid properties of water-cutting slurries. Drilling fluids containing xanthan gum were therefore tested extensively. This included most common chemical tests in the combination with full physical testing (these tests are reflected in Appendix B). Due to this the results are presented in two separate tables: Table 14 contains measured parameters of spud drilling fluids with either CMC Hi-Vis or PAC and Table 15 summarizes properties of fluids where xanthan gum was used as a stabilizing polymer. Table 14 and Table 15 reflect how the type of selected polymer and the concentration affected the rheological properties and the fluid loss characteristics of the fluids. Here the numbers in the drilling fluid names represent the concentration of cuttings/polymers in grams per 350 ml of water. A reference bentonite/CMC drilling fluid (B CMC REF) was mixed in this experiment. Physical properties of this mud are presented in Table 15 as well.

Table 14. The results of cuttings and polymer based fluids prepared in E2

Measured parameters	Drilling Fluid Type				
	C75 CMC 0.7	C75 CMC 1.0	C75 CMC 1.3	C75 CMC 1.6	C75 PAC 1.0
Rheology (RPM)					
600	9	13	18	23	17
300	6	9	11	14	10
200	4	6	8	11	8
100	3	3	5	6	4
6	1	1	2	1	1
3	1	1	1	1	1
GEL 10s	1	1	1	1	1
Density, SG	1.12	1.12	1.11	1.12	1.10
pH	11.4	11.4	11.8	11.55	11.15
API Filter Loss, ml	30	23	13	8	15
Bingham Parameters					
PV, cP	3	4	7	9	7
YP, Pa	1.53	2.56	2.04	2.56	1.53
AV, cP	4.5	6.5	9	11.5	8.5
Herschel-Bulkley Parameters					
τ_0 , Pa	0.511	0.511	0	0.511	0.511
n	0.678	0.585	0.710	0.759	0.830
K, Pa·s ⁿ	0.0374	0.107	0.0671	0.0586	0.0261

Viscosity curves calculated using the Herschel Bulkley model based on the fluid data presented in Table 14 are shown together with the measured viscometer data in Figure 27 through Figure 31. The figures are arranged in an increasing CMC Hi-Vis polymer concentration order, while Figure 31 shows viscosity curve of a PAC based fluid.

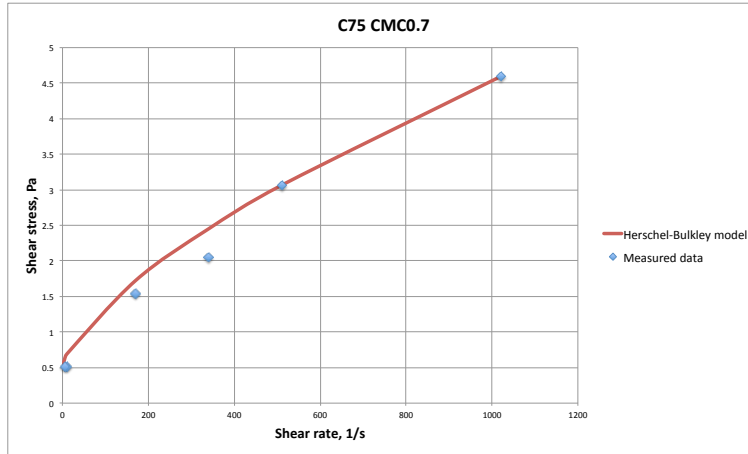


Figure 27. C75 CMC0.7 fluid viscosity curve based on the Herschel Bulkley model and the measured viscometer data of a fluid containing 75 g cuttings and 0.7 g CMC Hi-Vis polymer per 350 ml of water

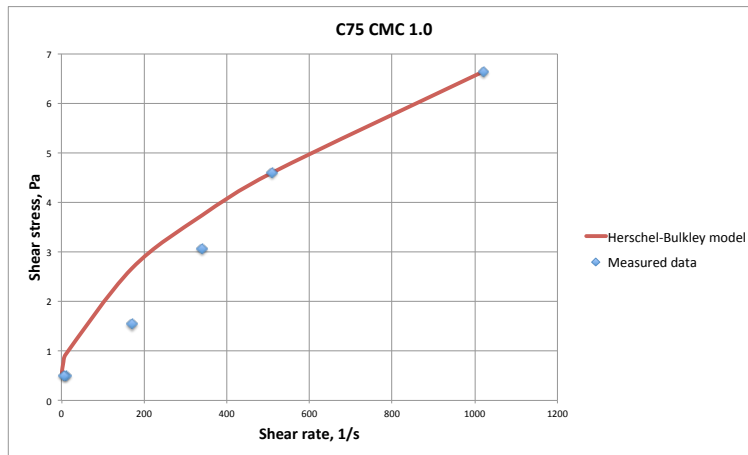


Figure 28. C75 CMC1.0 fluid viscosity curve based on the Herschel Bulkley model and the measured viscometer data of a fluid containing 75 g cuttings and 1.0 g CMC Hi-Vis polymer per 350 ml of water

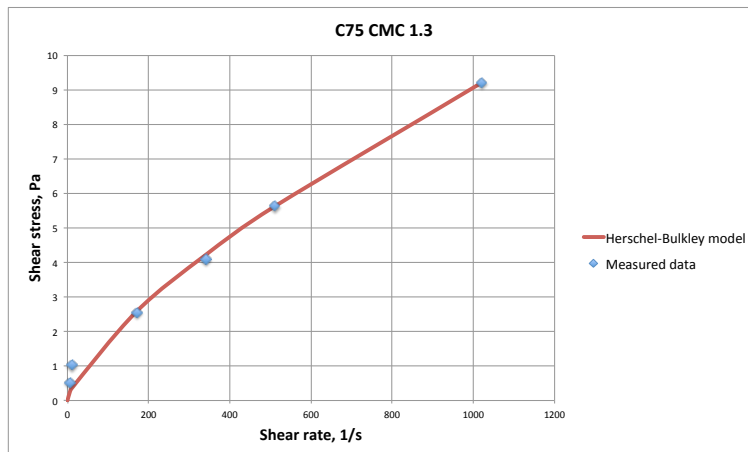


Figure 29. C75 CMC1.3 fluid viscosity curve based on the Herschel Bulkley model and the measured viscometer data of a fluid containing 75 g cuttings and 1.3 g CMC Hi-Vis polymer per 350 ml of water

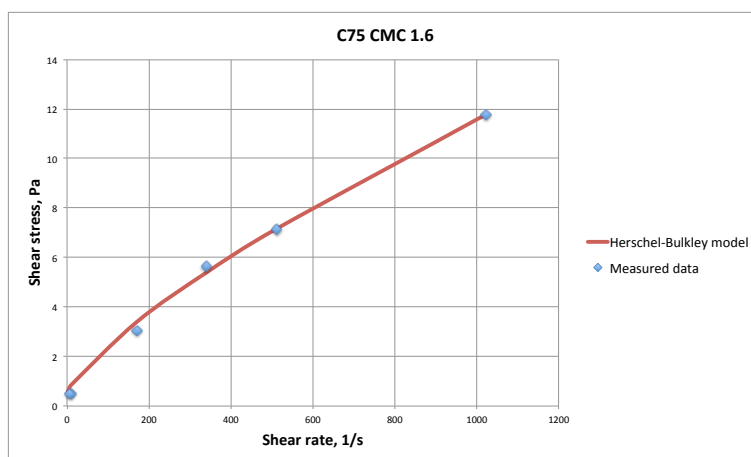


Figure 30. C75 CMC1.6 fluid viscosity curve based on the Herschel Bulkley model and the measured viscometer data of a fluid containing 75 g cuttings and 1.6 g CMC Hi-Vis polymer per 350 ml of water

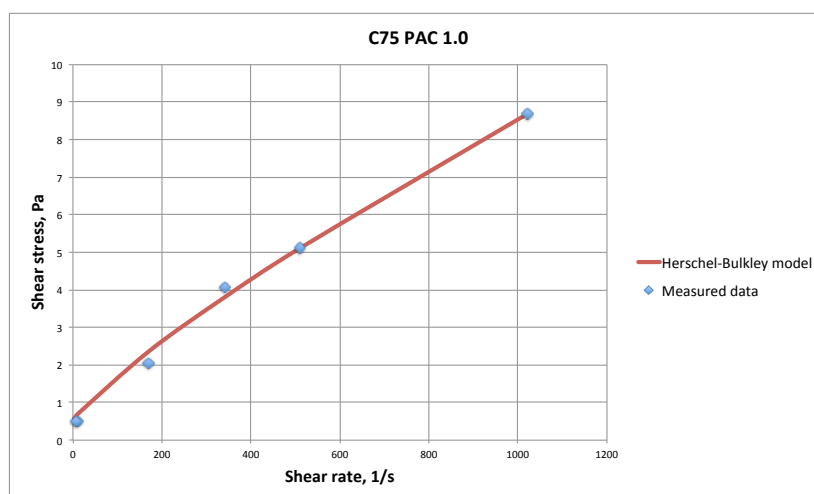


Figure 31. C75 PAC1.0 fluid viscosity curve based on the Herschel Bulkley model and the measured viscometer data of a fluid containing 75 g cuttings and 1.0 g PAC polymer per 350 ml of water

The concentration of xanthan gum polymers was not considered to be the influencing factor on any of the achieved results from the chemical testing. The influence of cutting concentration on the chemical properties of the fluid was, however, of more interest. Due to this chemical tests were run on four of the spud mud compositions with varying cuttings content (Table 15). However, a full range of chemical testing was carried out in a later stage of the work. The compositions were tested extensively to confirm the expectations (Section 8.4).

The viscosity curves based on the Herschel Bulkley model for the spud drilling fluids containing xanthan gum and summarized in Table 15 are shown in Figure 32 through Figure 39 together with the measured viscometer data. The viscosity curve of the B CMC REF reference fluid is shown in Figure 32 to provide an insight to a standard curve for a polymer-based spud mud. The effect of increased xanthan gum concentration can be observed when comparing curves shown in Figure 33 through Figure 36, while the effect of cutting concentration can be seen in Figure 37 through Figure 39.

8 Results

Table 15. The results of cuttings and biopolymer based fluids in E2 (including the B CMC REF fluid)

Measured parameters	Drilling Fluid Type							
	B CMC REF	C75 X1.0	C75 X1.2	C75 X1.4	C75 X1.6	C100 X1.2	C125 X1.2	C150 X1.2
Rheology (RPM)								
600	25	22	29	32	35	31	33	36
300	19	16	22	24	27	22	23	25
200	15	13	19	21	23	19	19	21
100	12	10	14	17	20	16	16	16
6	7	5	8	10	12	8	8	8
3	6	4	7	9	11	7	7	7
GEL 10s	10	5	9	11	13	8	8	8
GEL 10min		8	13	14	15	12	12	34
Density, SG	1.02	1.12	1.12	1.12	1.12	1.16	1.20	1.22
API Filter Loss, ml	11	28	20	18	16	20	24	31
Sand, %			1.50			1.60	2.50	2.80
Bingham Parameters								
PV, cP	6	6	7	8	8	9	10	11
YP, Pa	6.64	5.11	7.67	8.18	9.71	6.64	6.64	7.15
AV, cP	12.5	11	14.5	16	17.5	15.5	16.5	18
Herschel-Bulkley Parameters								
τ_0 , Pa	2.56	1.53	3.07	4.09	5.11	3.07	3.07	3.07
n	0.514	0.547	0.523	0.585	0.556	0.644	0.667	0.659
K, Pa·s ⁿ	0.290	0.219	0.313	0.214	0.271	0.148	0.136	0.160
Chemical Tests								
pH	10.2	11.25	11.55	11.2	11.2	11.55	11.3	11.8
P _m , ml H ₂ SO ₄			2.40			3.85	5.20	7.15
P _f , ml H ₂ SO ₄			0			0	0	0
M _f , ml H ₂ SO ₄			0.55			0.70	0.80	0.80
V _{mb} , ml			1.50			2.00	2.50	2.50
V _{AgNO3} , ml			2.40			2.95	3.80	4.40
Total hardness								
V _{EDTA} , ml			1.50			2.20	2.70	3.40
Calcium								
V _{EDTA} , ml			1.47			2.15	2.65	3.40
Calculated chemical parameters								
Bentonite, kg/m ³			21.4			28.5	35.6	35.6
[Cl ⁻], mg/l			2400			2950	3800	4400
[Ca ²⁺ _{total}], mg/l			600			880	1080	1360
[Cl ²⁺], mg/l			580			860	1060	1360
[Mg ²⁺], mg/l			12			12	12	0
[Ca(OH) ₂], kg/m ³			1.78			2.85	3.85	5.30
[HCO ₃ ⁻], mg/l			671			854	976	976
[OH ⁻], mg/l			0			0	0	0
[CO ₃ ²⁻], mg/l			0			0	0	0

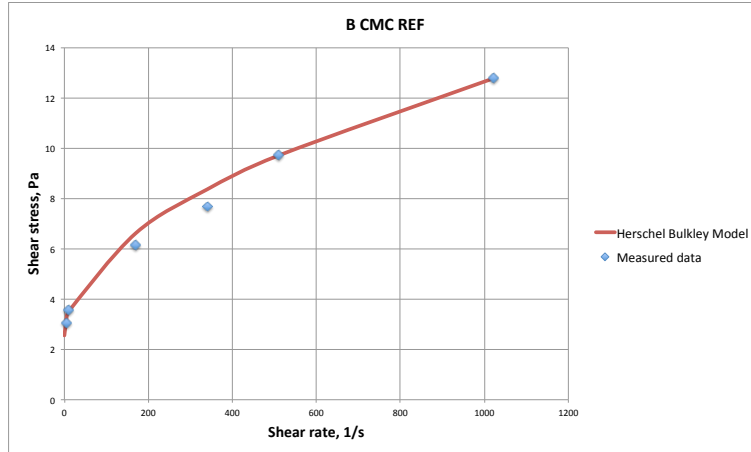


Figure 32. Bentonite/CMC reference fluid viscosity curve based on the Herschel Bulkley model and the measured viscometer data of a fluid containing 10.5 g bentonite, 0.7 g CMC polymer and 0.7 g Na_2CO_3 per 350 ml of water

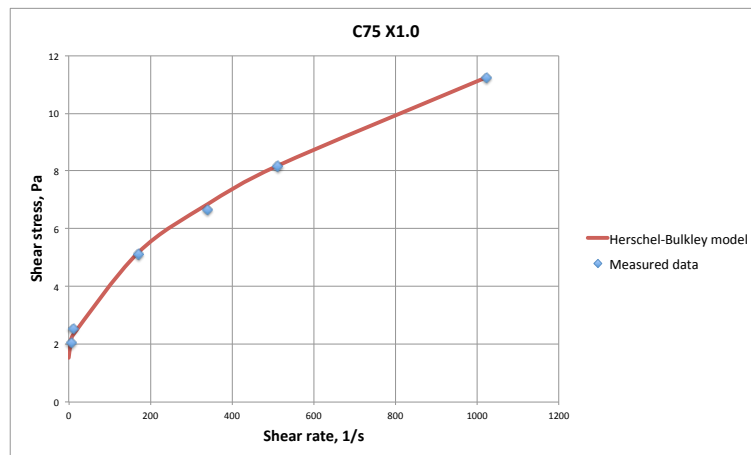


Figure 33. C75 X1.0 fluid viscosity curve based on the Herschel Bulkley model and the measured viscometer data of a fluid containing 75 g cuttings and 1.0 g xanthan polymer per 350 ml of water

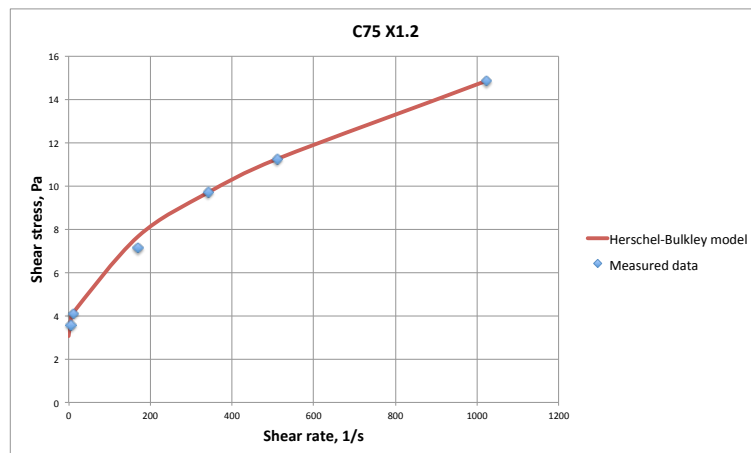


Figure 34. C75 X1.2 fluid viscosity curve based on the Herschel Bulkley model and the measured viscometer data of a fluid containing 75 g cuttings and 1.2 g xanthan polymer per 350 ml of water

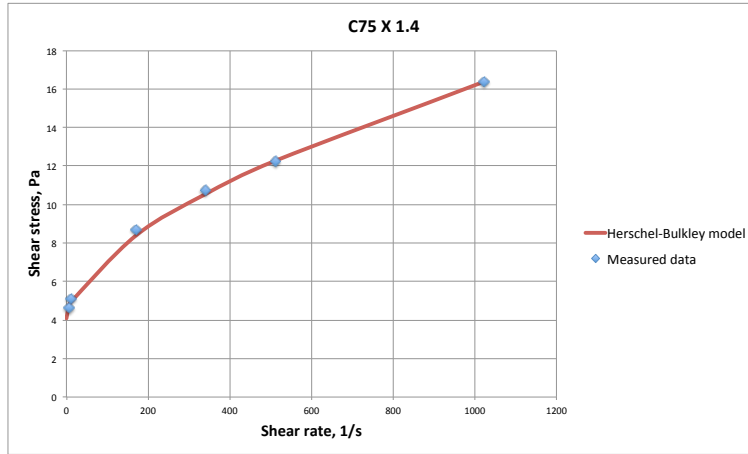


Figure 35. C75 X1.4 fluid viscosity curve based on the Herschel Bulkley model and the measured viscometer data of a fluid containing 75 g cuttings and 1.4 g xanthan polymer per 350 ml of water

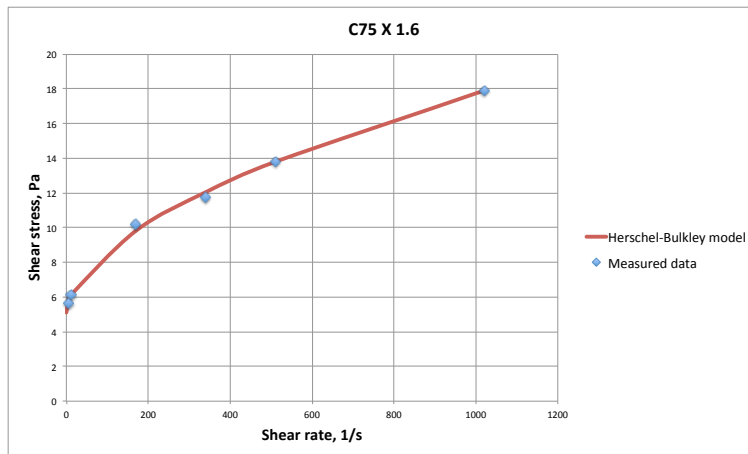


Figure 36. C75 X1.6 fluid viscosity curve based on the Herschel Bulkley model and the measured viscometer data of a fluid containing 75 g cuttings and 1.6 g xanthan polymer per 350 ml of water

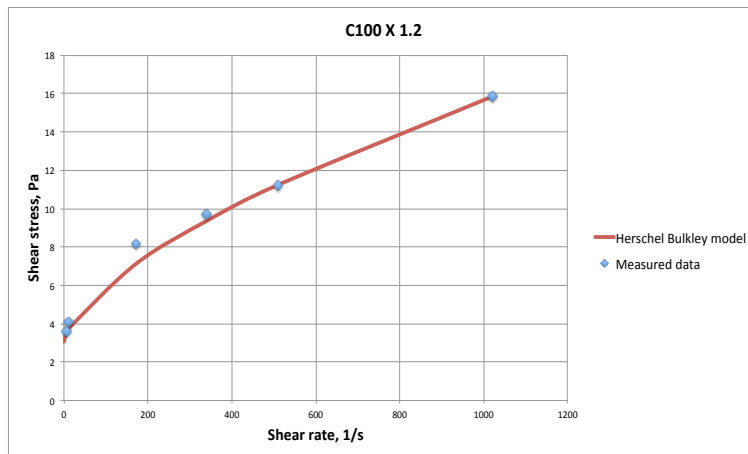


Figure 37. C100 X1.2 fluid viscosity curve based on the Herschel Bulkley model and the measured viscometer data of a fluid containing 100 g cuttings and 1.2 g xanthan polymer per 350 ml of water

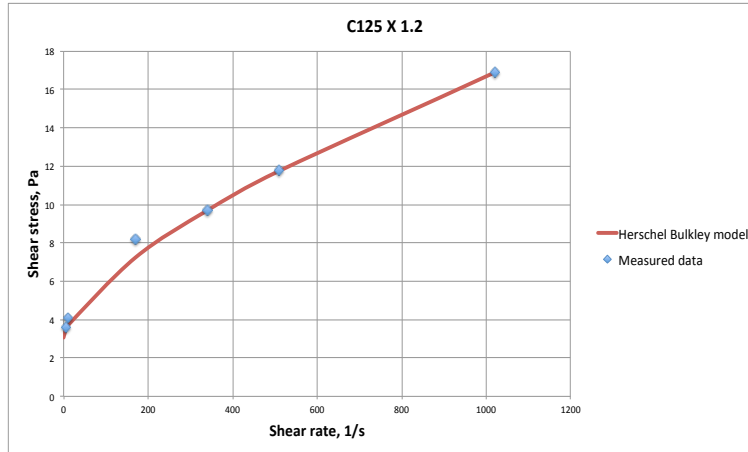


Figure 38. C125 X1.2 fluid viscosity curve based on the Herschel Bulkley model and the measured viscometer data of a fluid containing 125 g cuttings and 1.2 g xanthan polymer per 350 ml of water

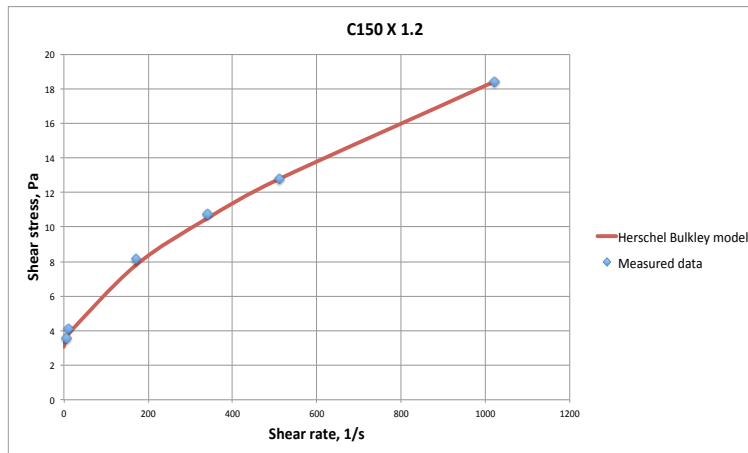


Figure 39. C150 X1.2 fluid viscosity curve based on the Herschel Bulkley model and the measured viscometer data of a fluid containing 150 g cuttings and 1.2 g xanthan polymer per 350 ml of water

In these experiments with the fluids containing cuttings and polymers the influence of the polymers on the rheological properties of the fluids was studied and it was revealed that the spud muds containing xanthan gum demonstrated rheological parameters close to those of the reference fluids (Table 15). Depending on the concentration of polymers and cuttings the yield stress as high as 5.11 Pa was registered, while the highest YP calculated based on the Bingham model was 9.71 Pa. The criterion of low PV was satisfied simultaneously as this parameter varied from 6 cP to 9 cP for most of the compositions, which was similar to the corresponding parameters of the reference mud. No segregations of the solid and liquid phases were observed even after storing one of the samples for 10 days (Section 8.3).

8.3 Experiment 3 (E3). Aging Experiment. Hydration Test

Water-cutting slurries identical to those in the E1 experiments containing 75/100/125/150 g of cuttings per 350 ml water were tested for the same physical properties after having been aged at ambient conditions for 10 days in transparent bottles. The xanthan gum containing stable drilling fluid, C75 X 1.2, was stored for 10 days under the same conditions as well.

Severe separations of the solid and liquid phases of the water-cutting slurries were observed. The solids were firmly packed on the bottom and the bottles were intensively shaken for several minutes to disperse particles in the mixture again. Moreover, a soft porous “cap” floated on the top of the mixture. Initially this cap was incorrectly assumed to be the swelled clay minerals. After having performed thorough analysis of the substance at a later stage it was revealed to be the foam generated during the mixing process, which had aggregated on the top of the bottle due to its lighter density. This foam occurred probably due to the rests of surfactants, which have followed drill cuttings after the thermo-mechanical treatment, as significant amounts of surfactants are used to obtain invert emulsion in OBM (Section 3.3.2). Even after repeated mixing and dispersion, the aged slurries were still incapable of suspending large particles, which deposited on the bottom of mixing cup quite quickly. This testing revealed no observable significant change in the viscosity of the fluids, which has been confirmed with viscometer measurements shown in Table 16. Due to this, the rheological profiles of the fluids are not presented in this section, as they would look quite similar to those in Section 8.1.

Table 16. The results of aging experiment E3

Measured parameters	Drilling Fluid Type				
	C75A ²	C100A	C125A	C150A	C75 X 1.2A
Rheology (RPM)					
600	5	8	9	13	29
300	4	5	5	9	22
200	3	4	4	6	19
100	2	3	3	5	14
6	1	1	2	3	8
3	1	1	1	2	7
GEL 10s	0	1	2	2	9
Density, SG	1.12	1.15	1.19	1.22	1.12
pH	11.2	11.2	11.25	11.2	11.55
API Filter Loss, ml	N/A	N/A	N/A	N/A	20
Bingham Parameters					
PV, cP	1	3	4	6.5	7
YP, Pa	1.53	1.02	0.511	2.56	7.67
AV, cP	2.5	4	4.5	4	14.5
Herschel-Bulkley Parameters					
τ_0 , Pa	0.511	0.511	0	0.511	3.07
n	0.415	0.807	0.848	0.585	0.523
K, Pa·s ⁿ	0.115	0.0134	0.0130	0.107	0.313

Aging of C75 X1.2 drilling fluid, comprising only cuttings and xanthan gum, did not have any effect on its rheological characteristics as the same viscometer values were

²A stands for aged

obtained after 10 days. This can be seen when comparing the C75 X1.2 column in Table 15 and the C75 X1.2A column in Table 16. Severe gel structure was built as the result of the aging experiment. However, this pattern was easy to break by agitating the fluid with a spoon. After having mixed the fluid for a couple of minutes the initial rheological qualities were recovered. Based on this experiment it was concluded that the current fluid composition was quite stable.

As a bottom-line, the hydration/aging experiment pointed out that the treated drill cuttings were not capable of hydration under long exposure to fresh water. Even after 10 days of exposure, which is already considered too long for a quick offshore application, no hydration effects were observable. Moreover, the material did not build any gel structure and had negligible low shear rate viscosity. Therefore, possible pre-hydration of drill cuttings would have been unnecessary. Based on these results it was made a decision to perform the experiments with SW as the base fluid.

8.4 Experiment 4 (E4). Seawater Based Spud Mud

After having achieved successful results with xanthan biopolymer in E2, same fluid compositions were mixed and tested using SW as the base fluid instead of fresh water. The overview and compositions of the designed drilling fluids in this experiment are given in Table 12. This experiment was conducted to evaluate the expectations of similar drilling fluid behavior independently of the salinity of the base fluid. In this experiment all spud muds were tested both for physical and chemical properties to provide the descriptive summary of the designed fluids. This testing was expected to justify the observed trends in main characteristics of the fluid. Two standard API rheological tests were carried out at 20°C and 50°C to study the temperature effect. The results obtained from the rheological tests conducted at 20°C are summarized in Table 17 and 18, while those conducted at 50°C in Table 19 and 20. Here the same principle was used for the drilling fluid type nomenclature. The letter corresponds to the type of the component and the numbers following the letters reflect the concentration of this component in grams per 350 ml water. Here C stands for cuttings, X for xanthan, B for barite and CMC LV for CMC Lo-Vis.

8 Results

Table 17. The rheological measurements results at 20°C and calculated corresponding model parameters

Measured parameters	Drilling Fluid Type				
	C75 X1.0SW	C75 X1.2SW	C75 X1.4SW	C75 X1.6SW	C100 X1.2SW
Rheology at 20°C (RPM)					
600	26	32	36	41	38
300	20	24	28	31	27
200	17	20	24	27	23
100	14	16	19	22	18
6	7	8	11	13	9
3	6	7	10	11.5	8
GEL 10s	7	8	11	12.5	9
GEL 10min	10	11	14	15	12
Bingham Parameters					
PV, cP	6	8	8	10	11
YP, Pa	7.15	8.18	10.2	10.7	8.18
AV, cP	13	16	18	20.5	19
Herschel-Bulkley Parameters					
τ_0 , Pa	2.56	3.07	4.60	5.11	3.58
n	0.485	0.530	0.507	0.562	0.632
K, Pa·s ⁿ	0.372	0.337	0.412	0.324	0.199

Table 18. The rheological measurements results at 20°C and calculated corresponding model parameters (cont.)

Measured parameters	Drilling Fluid Type				
	C125 X1.2SW	C150 X1.2SW	C75 X1.4 B SW	C100 X1.4 B SW	C75 X1.4 CMC LV SW
Rheology at 20°C (RPM)					
600	42	44	48	49	41
300	30	32	36	37	31
200	26	27	31	31	26
100	20	20	24	24	20
6	10	10	12	13	10
3	9	9	11	12	9
GEL 10s	10	10	12	12	11
GEL 10min	14	15	13	14	14
Bingham Parameters					
PV, cP	12	12	12	12	10
YP, Pa	9.20	10.2	12.3	12.8	10.7
AV, cP	21	22	24	24.5	20.5
Herschel-Bulkley Parameters					
τ_0 , Pa	4.09	4.09	5.11	5.62	4.09
n	0.628	0.585	0.547	0.547	0.521
K, Pa·s ⁿ	0.225	0.320	0.438	0.438	0.458

Table 19. The rheological measurements results at 50°C and calculated corresponding model parameters

Measured parameters	Drilling Fluid Type				
	C75 X1.0SW	C75 X1.2SW	C75 X1.4SW	C75 X1.6SW	C100 X1.2SW
Rheology at 50°C (RPM)					
600	24	28	32	35	32
300	18	22	25	27	24
200	15	19	21	23	20
100	12	15	18	20	16
6	6.5	8	10	12	9
3	6	7	9	11	8
GEL 10s	7	8	10	12	8.5
GEL 10min	8	10	12	13	10
Bingham Parameters					
PV, cP	6	6	7	8	8
YP, Pa	6.13	8.18	9.20	9.71	8.18
AV, cP	12	14	16	17.5	16
Herschel-Bulkley Parameters					
τ_0 , Pa	2.81	3.07	4.09	5.11	3.58
n	0.565	0.459	0.497	0.556	0.556
K, Pa·s ⁿ	0.188	0.467	0.391	0.271	0.271

Table 20. The rheological measurements results at 50°C and calculated corresponding model parameters (cont.)

Measured parameters	Drilling Fluid Type				
	C125 X1.2SW	C150 X1.2SW	C75 X1.4 B SW	C100 X1.4 B SW	C75 X1.4 CMC LV SW
Rheology at 50°C (RPM)					
600	37	41	41	44	34
300	27	29	31	33	25
200	23	24	27	28	21
100	19	19	22	22	17
6	9	9	11	12	10
3	8	8	10	10	9
GEL 10s	9	8	11	11	10
GEL 10min	13	14	12	14	12
Bingham Parameters					
PV, cP	10	12	10	11	9
YP, Pa	8.69	8.69	10.7	11.2	8.18
AV, cP	18.5	20.5	20.5	22	17
Herschel-Bulkley Parameters					
τ_0 , Pa	3.58	3.58	4.60	4.09	4.09
n	0.585	0.628	0.540	0.526	0.613
K, Pa·s ⁿ	0.267	0.225	0.387	0.482	0.191

The viscosity curves based on the Herschel Bulkley model together with the measured viscometer data for these ten drilling fluid compositions are presented in Figure 40 through Figure 49. Figure 40 through Figure 43 include the spud mud compositions with increasing xanthan gum concentration, thus this effect can be studied by comparing these curves. Figure 44 through Figure 46 reflect the effect of increasing cutting concentration on the designed SW based fluids. The influence of barite and CMC Lo-Vis on viscous properties of three of the designed spud muds is shown in Figure 47 through Figure 49. These curves were built based on the data obtained at 20°C. However, the separate evaluation of temperature effect on spud mud rheological properties has been performed and presented in Section 9.3.5.

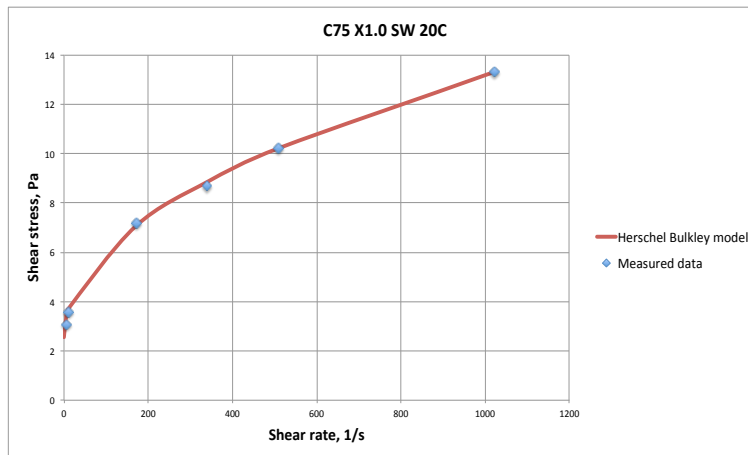


Figure 40. C75 X1.0 SW fluid viscosity curve based on the Herschel Bulkley model and the measured viscometer data at 20°C of a fluid containing 75 g cuttings and 1.0 g xanthan polymer per 350 ml of SW

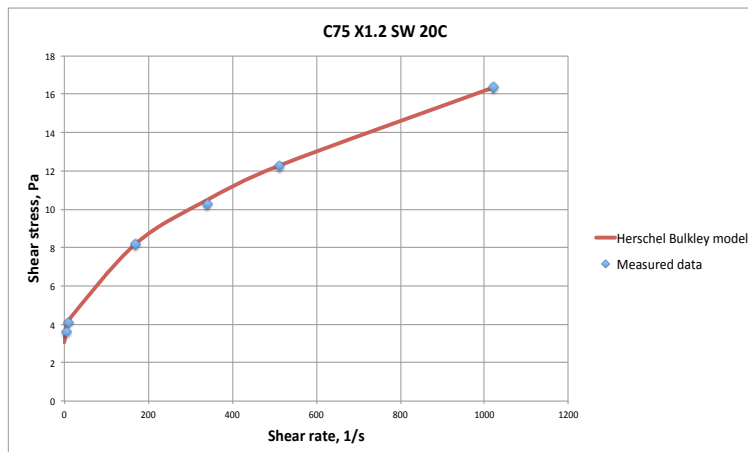


Figure 41. C75 X1.2 SW fluid viscosity curve based on the Herschel Bulkley model and the measured viscometer data at 20°C of a fluid containing 75 g cuttings and 1.2 g xanthan polymer per 350 ml of SW

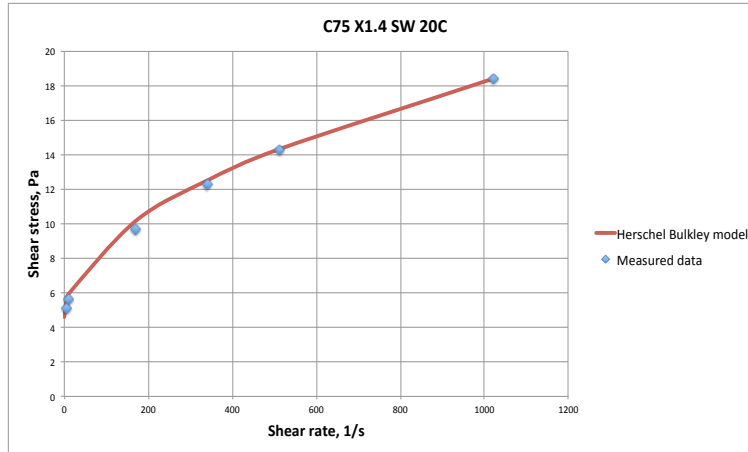


Figure 42. C75 X1.4 SW fluid viscosity curve based on the Herschel Bulkley model and the measured viscometer data at 20°C of a fluid containing 75 g cuttings and 1.4 g xanthan polymer per 350 ml of SW

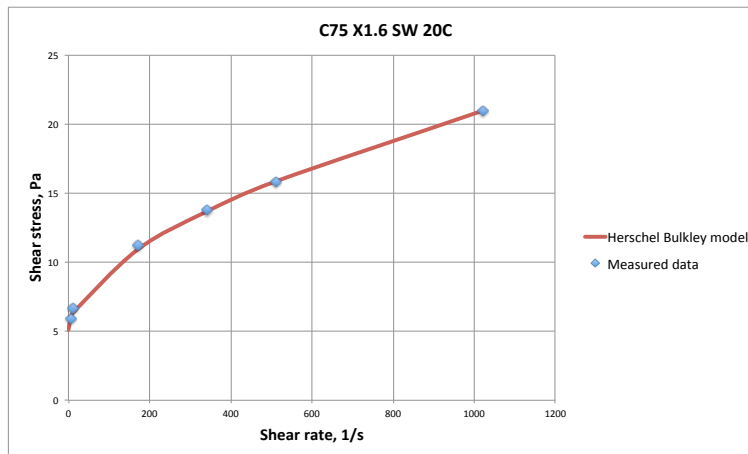


Figure 43. C75 X1.6 SW fluid viscosity curve based on the Herschel Bulkley model and the measured viscometer data at 20°C of a fluid containing 75 g cuttings and 1.6 g xanthan polymer per 350 ml of SW

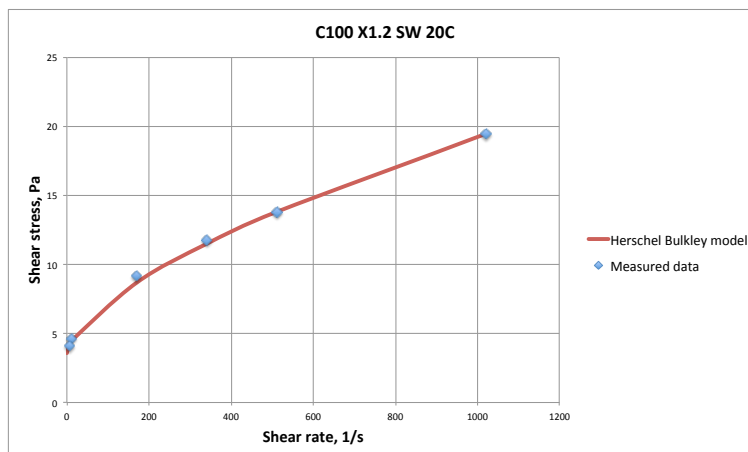


Figure 44. C100 X1.2 SW fluid viscosity curve based on the Herschel Bulkley model and the measured viscometer data at 20°C of a fluid containing 100 g cuttings and 1.2 g xanthan polymer per 350 ml of SW

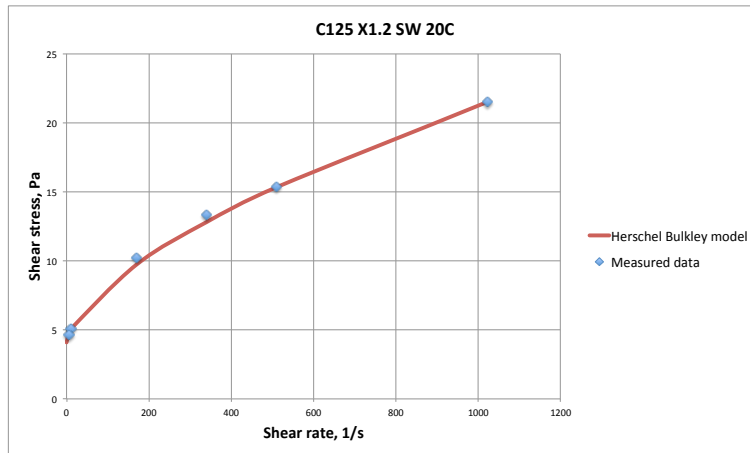


Figure 45. C125 X1.2 SW fluid viscosity curve based on the Herschel Bulkley model and the measured viscometer data at 20°C of a fluid containing 125 g cuttings and 1.2 g xanthan polymer per 350 ml of SW

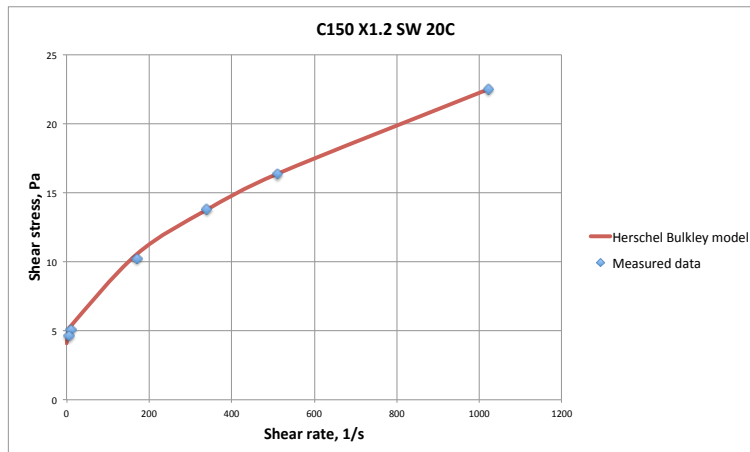


Figure 46. C150 X1.2 SW fluid viscosity curve based on the Herschel Bulkley model and the measured viscometer data at 20°C of a fluid containing 150 g cuttings and 1.2 g xanthan polymer per 350 ml of SW

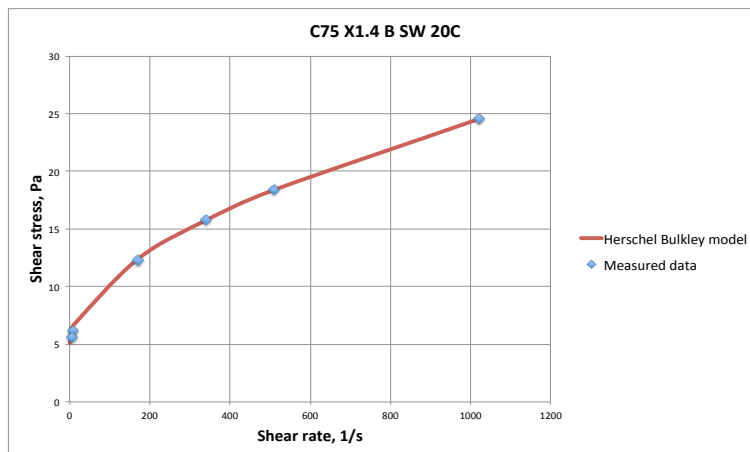


Figure 47. C75 X1.4 B SW fluid viscosity curve based on the Herschel Bulkley model and the measured viscometer data at 20°C of a fluid containing 75 g cuttings, 1.4 g xanthan polymer and 88.8 g barite per 350 ml of SW

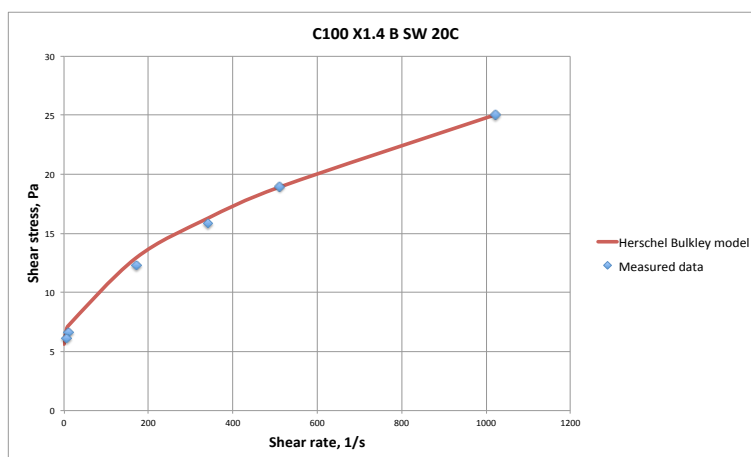


Figure 48. C100 X1.4 B SW fluid viscosity curve based on the Herschel Bulkley model and the measured viscometer data at 20°C of a fluid containing 100 g cuttings, 1.4 g xanthan polymer and 68.1 g barite per 350 ml of SW

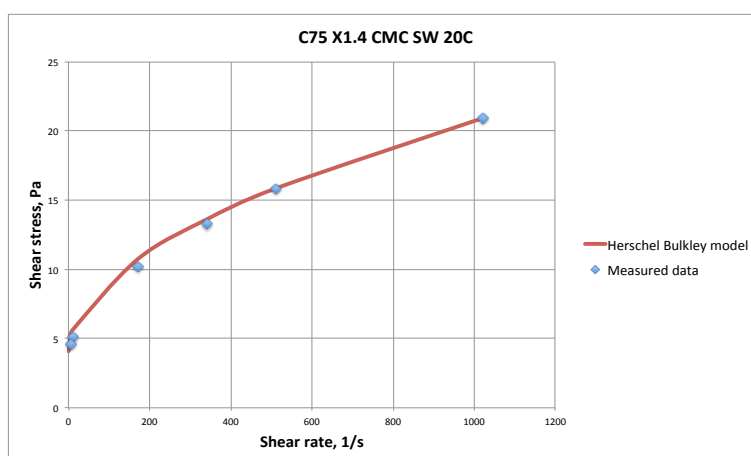


Figure 49. C75 X1.4 CMC LV SW fluid viscosity curve based on the Herschel Bulkley model and the measured viscometer data at 20°C of a fluid containing 75 g cuttings, 1.4 g xanthan polymer and 1.0 g CMC Lo-Vis per 350 ml of SW

The rest of the obtained physical and chemical data of the designed spud mud compositions in this experiment are presented in Table 21 and 22. These tables provide the insight of how increasing xanthan gum and cutting concentration influenced the main physical and chemical properties of the designed fluids. Moreover, Table 22 shows the effect of barite and CMC Lo-Vis on the main physical properties (barite was added to increase fluid density to 1.30 SG).

8 Results

Table 21. The physical and chemical test results of spud mud compositions in E4

Measured parameters	Drilling Fluid Type				
	C75 X1.0 SW	C75 X1.2 SW	C75 X1.4 SW	C75 X1.6 SW	C100 X1.2 SW
Physical tests					
Density, SG	1.14	1.14	1.14	1.14	1.18
API Filter Loss, ml	22	21	19.5	18	21
Sand, %	1.50	1.50	1.50	1.6	3.00
Chemical tests					
pH	10.15	10.15	10.1	10.15	10.15
P _m , ml H ₂ SO ₄	0.55	0.60	0.60	0.60	1.30
P _f , ml H ₂ SO ₄	0.00	0.00	0.00	0.00	0.00
M _f , ml H ₂ SO ₄	0.40	0.45	0.45	0.45	0.55
V _{mb} , ml	1.50	1.50	1.50	1.50	2.00
V _{AgNO₃} , ml	20.5	20.5	20.6	20.5	21.4
Total hardness					
V _{EDTA} , ml	7.60	7.60	7.55	7.55	7.90
Calcium					
V _{EDTA} , ml	7.05	7.10	6.55	7.05	7.50
Calculated chemical parameters					
Bentonite, kg/m ³	21.4	21.4	21.4	21.4	28.5
[Cl ⁻], mg/l	20500	20500	20600	20500	21400
[Ca ²⁺ total], mg/l	3040	3040	3020	3020	3160
[Ca ⁺], mg/l	2820	2840	2620	2820	3000
[Mg ²⁺], mg/l	132	120	240	120	96
[Ca(OH) ₂], kg/m ³	0.408	0.445	0.445	0.445	0.963
[HCO ₃ ⁻], mg/l	480	549	549	549	671
[OH ⁻], mg/l	0.00	0.00	0.00	0.00	0.00
[CO ₃ ²⁻], mg/l	0.00	0.00	0.00	0.00	0.00

Table 22. The physical and chemical test results of spud mud compositions in E4 (cont.)

Measured parameters	Drilling Fluid Type				
	C125 X1.2 SW	C150 X1.2 SW	C75 X1.4 B SW	C100 X1.4 B SW	C75 X1.4 CMC LV SW
Density, SG	1.20	1.24	1.30	1.30	1.14
API Filter Loss, ml	24	24	20	21.0	10
Sand, %	3.00	3.50	2.00	2.50	1.90
Chemical tests					
pH	10.25	10.35	10.30	10.40	10.15
P _m , ml H ₂ SO ₄	1.90	2.90			
P _f , ml H ₂ SO ₄	0.00	0.00			
M _f , ml H ₂ SO ₄	0.60	0.70			
V _{mb} , ml	2.00	2.50			
V _{AgNO3} , ml	22.1	23.8			
Total hardness					
V _{EDTA} , ml	8.40	9.45			
Calcium					
V _{EDTA} , ml	8.10	9.10			
Calculated chemical parameters					
Bentonite, kg/m ³	28.5	35.6			
[Cl ⁻], mg/l	22100	23800			
[Ca ²⁺ total], mg/l	3360	3780			
[Ca ⁺], mg/l	3240	3640			
[Mg ²⁺], mg/l	72	84			
[Ca(OH) ₂], kg/m ³	1.41	2.15			
[HCO ₃ ⁻], mg/l	732	854			
[OH ⁻], mg/l	0.00	0.00			
[CO ₃ ²⁻], mg/l	0.00	0.00			

It is worth mentioning here that the standard chemical tests were not performed on drilling fluids containing barite and CMC Lo-Vis. According to literature (IPT, 2012) barite is insoluble in water and has very low chemical activity. Therefore the addition of this material to the drilling fluid would not influence any of the earlier measured chemical properties. Since organic CMC polymer neither was capable of adjusting any of the chemical fluid qualities it was decided not to perform extensive fluid analysis on the mentioned samples.

The results of these experiments, where the SW based fluids were tested, confirmed the existing prior to the execution expectations. The designed drilling fluid compositions demonstrated the similar rheological behavior to the corresponding spud muds in E2, where fresh water was used as the base fluid. The fluid compositions were otherwise absolutely identical. Moreover, all of the designed fluids satisfied rheological requirements, without having unnecessary high fluid

density. Here the density varied between 1.14 to 1.24 SG depending on the drill cuttings concentration. These values were slightly higher than those achieved in the E2 experiment (with fresh water as the base fluid) due to the higher base fluid density (SW had approximately 1.03 SG density). The SW based drilling fluids had comparable rheological properties with the tested bentonite reference fluids as well. CMC Lo-Vis polymer was concluded to provide the required fluid loss control even when added in relatively small concentrations (2.86 kg/m^3). The designed fluids were capable of suspending heavy barite particles as well when the density was increased to 1.30 SG. This may be required during casing installation. As this section was meant to introduce the reader to the obtained results from the spud mud testing, no critical result evaluation is given here. Reader is referred to Section 9 for in depth analysis of the obtained results.

9 Discussion

This chapter introduces the analysis of the results presented in Section 8 and tries to explain the trends observed in the measurements. Here the analysis is divided into three main groups based on the drilling fluid properties. Therefore physical, chemical and rheological properties of the designed drilling fluids are evaluated separately. The rheological characteristics of fluids are often regarded as the most important ones, as they play a central role for the realization of many of the functions of spud muds. The rheological properties of fluids, in their turn, depend on physical and chemical properties of the fluid. Due to this the rheological properties of the designed fluids are discussed in one of the last chapters of this section. Economical aspects of this development are as well considered in this section.

9.1 Physical Properties

Physical properties as density, fluid loss, filter cake quality and sand content of the designed drilling fluids are discussed in this section.

9.1.1 Density

The density of spud mud is one of the central parameters as it is the main means of controlling pressure in the well during drilling (Section 3.1.1). On the other hand, spud mud is used to drill through shallow formations, which are often weak and loosely consolidated. In these intervals (up to 1500 m), depending on the geological regime, fracture gradients can be as low as 1.45 SG and sometimes overburden gradient can have even lower values, as was shown in Figure 1. In cases where the overburden gradient has the lowest value, excessive wellbore pressure will result in horizontal fractures around the wellbore and uplifting of the formation. It is important to keep in mind that during circulation the apparent density of fluid will increase due to the additional friction pressure loss as well. For this reason it is important to be able to keep the density of the spud mud as low as possible to avoid drilling related problems as fractured formations. A theoretical correlation curve between the density of a drilling fluid and its treated drill cuttings concentration was built using MS Excel and is shown in Figure 50.

The curve in Figure 50 is based on the assumptions that SW is used as the base fluid and treated drill cuttings have the density of 2.5 SG. Any concentration of drill cuttings larger than 326 kg/m^3 will result in the drilling fluid density higher than 1.20 SG (Figure 50). It is undesirable to exceed this density limit as sometimes either overburden or fracture gradient may have the value as low as 1.30 SG (Figure 1). Given that the fluid is pumped with a high flow rate during drilling of top holes to provide sufficient hole cleaning and lifting capacity, ECD can approach the critical fracture gradient value resulting in excessive fluid losses and wellbore stability related problems. In addition to this, added polymers may have a minor influence on density. However, since the amount of polymers added during the experiments and its density (1.5 SG according to the datasheet) are significantly lower than those of drill cuttings this aspect was regarded of less importance and was therefore omitted during the analysis.

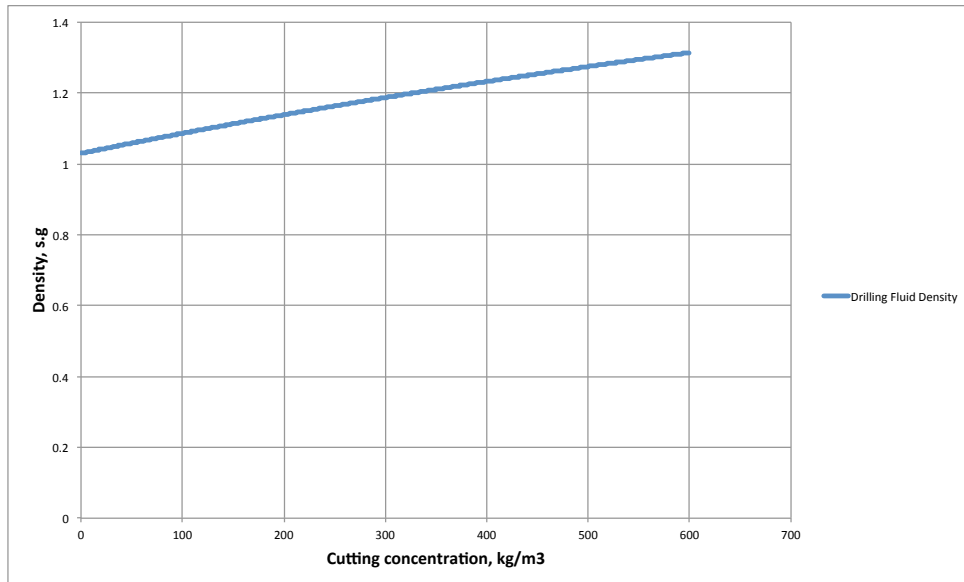


Figure 50. Drilling fluid density as a function of cuttings concentration

Cutting concentration of 326 kg/m³ corresponds approximately to 114 g of cuttings per 350 ml of SW. This means that spud muds containing xanthan gum and 75-100 g of cuttings per 350 ml of water would be the most appropriate from the density point of view only. Still this conclusion is very case dependent and higher concentrations may be implemented in stronger geological formations with higher subsurface pressure gradients. In cases where high fluid density is required prior to the installation of casing strings it is recommended to use a high barite amount rather than a high drill cuttings amount to increase density to 1.30 SG. According to the API requirements (IPT, 2012), barite contains less than 3% of particles larger than 74 microns. On the other hand, PSD testing revealed that 10 to 15% of drill cuttings are larger than this value (Figure 17). Larger particles result in more severe erosion during pumping operations and rougher filter cake, which may cause problems during cementing of the well. It is therefore recommended to increase the density using barite.

The highest drill cutting concentration mixed in the experiments was 150 g per 350 ml, which corresponds to 428.6 kg/m³. In this case the measured density was 1.24 SG, while that calculated theoretically using Excel Worksheet was equal to 1.245 SG. This difference corresponds to 0.4% error between the theoretical and the measured values, which justifies the assumption that drill cuttings had the density of approximately 2.5 SG (density of SW was measured to be 1.03 SG).

9.1.2 Fluid Loss and Filter Cake Quality

Another important physical drilling fluid property is fluid loss to the formation (Section 3.1.3). According to the results of experiment E1 with simple water-cuttings slurries, pure drill cuttings and water mixtures did not provide any fluid loss control at all. Filtrate started to flow even at ambient pressure conditions resulting in a very thick and porous filter cake. Though the designed drilling fluid

compositions containing CMC Hi-Vis polymer had filter loss value as low as 8 ml API filter loss, these spud muds did not demonstrate the desired rheological properties (Table 14). On the other hand, stable from a rheological point of view spud mud compositions with application of xanthan gum had relatively high values of API filter loss (Table 15). The results of the initial experiments with xanthan gum (E2 experiment) revealed that increasing xanthan concentration would reduce fluid loss to the formation. Thus, when 1 g of xanthan was added per 350 ml of water the drilling fluid had filtrate loss equal to 28 ml, however, when, xanthan amount was increased to 1.6 g the loss reduced to 18 ml. On the other hand, this reduction is not very efficient, since one needs to increase the polymer concentration by 60% to achieve a filter loss reduction of only 43%. Contrary, an increase in drilling cuttings concentration resulted in the increased filtrate loss. As it is reflected in Table 15, with 75g of cuttings per 350 ml of water in case of the C75 X1.2 spud mud the fluid loss was equal to 20 ml. On the other hand, when cutting concentration was doubled (keeping the same xanthan gum concentration) in case of the C150 X1.2 mud this value increased to 31 ml. This corresponds to the significant increase equal to 55%. This increase in fluid loss may be ascribed to the increased solid particle concentration, which results in more porous filter cake allowing easier filtrate loss. High particle concentration resulted in a thicker filter cake as well, which is also undesirable. Similar trends regarding polymer and cutting concentrations were observed in experiments, where identical drilling fluids were mixed based on SW (E4 experiment). Thus, the SW based drilling fluid with the lowest cutting concentration 75g/350 ml water had the lowest filtrate loss value equal to 18 ml (Table 21). Increase in cutting concentration up to 150g/350 ml water resulted in an increased API filter loss varying from 21 to 24 ml as well.

According to Statoil's Drilling Program (2010) the API filter loss value for drilling of 26" hole should not exceed 10 ml. Due to this an additional drilling fluid composition, containing fluid loss agent was designed. This fluid is referred as C75 X1.4 CMC LV SW and contained CMC Lo-Vis in addition to cuttings and xanthan. The results demonstrated that even low amounts of CMC Lo-Vis polymers were quite efficient to combat fluid losses. So, 2 g of CMC Lo-Vis filter loss agent per 700 ml of SW (2.86 kg/m^3) was sufficient to reduce the losses to 10 ml (Table 22). It is important to mention that an otherwise similar fluid, but without CMC Lo-Vis had a filtrate loss equal to 19.5 ml. This corresponds to a reduction approximately by a factor of 2. Two drilling fluid compositions were designed using barite as weighting material to increase the density to 1.30 SG as well (Table 12). The results of the experiments with barite demonstrated that barite does not have any influence on the performance of the fluid filtrate loss as the observed deviations were insignificant and within the experimental uncertainty. Thus, when barite was added to the cuttings/xanthan mud, C75 X1.4 SW, fluid loss increased from 19.5 ml to 20 ml, which is basically within the experimental uncertainty.

Based on the discussion regarding filtrate loss of the designed spud muds, high cutting concentration is undesirable from this point of view as well as it would result in higher losses to the formation. However, this conclusion depends on the

application as well. Shallow formation layers often consist entirely of impermeable shale formations, as was shown in Figure 1. In this case fluid loss control properties of the fluid is of less importance and other parameters may play more important roles for the fluid design process. This means that designed spud muds with high cutting concentration may be still applicable in some cases. Nevertheless, if one expects to drill through permeable sand formations, fluid loss property will become of high importance.

Another characteristic of drilling fluids, which is closely related to the API filter loss, is filter cake quality. As it was mentioned in Section 3.1.3 it is required to achieve a thin and impermeable filter cake during the drilling process. Filter cake analyses were carried out only on the stable spud mud compositions containing xanthan gum biopolymers. Drilling fluids consisting only of cuttings and biopolymers had very similar filter cake properties regardless of the base fluid, cuttings and polymer concentrations. The filter cake in these cases shown in Figure 51 was thin, rough with visible large solid particles and rather porous. Porosity of the filter cake was considered the main reason for relatively high filter loss. The thickness of the filter cakes was equal to 1 mm. Thickness of 1 mm is quite low and is acceptable for top hole drilling. However, in case with the highest cuttings concentration (150 g/350 ml of water), the thickness increased to 1.5 mm.

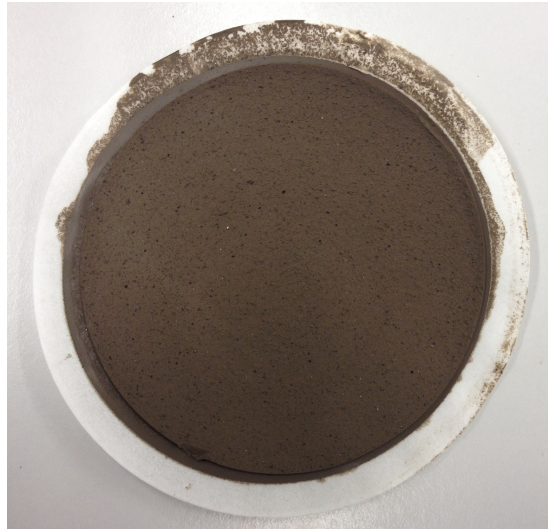


Figure 51. Filter cake of the C100 X1.2 SW drilling fluid containing cuttings and xanthan gum

In the case of barite containing drilling fluids the obtained filter cakes had similar properties. They were rough with large solid particles and porous. However, the filter cake took a slightly lighter color due to the presence of barite as shown in Figure 52.



Figure 52. Filter cake of the C100 X1.4 B SW drilling fluid containing cuttings, xanthan and barite

On the other hand, the filter cake of the spud mud containing fluid loss control material was thin and non-porous, having much less permeability resulting in a reduced API filter loss equal to 10 ml. The thickness of the filter cake was still equal to 1 mm, which qualified CMC Lo-Vis material as a recommended fluid loss control agent for this application. This filter cake is shown in Figure 53 and comparing it to Figure 51 and Figure 52 a significant reduction in porosity can be observed.



Figure 53. Filter cake of the C75 X1.4 CMC LV SW drilling fluid containing cuttings, xanthan and CMC Lo-Vis fluid loss agent

9.1.3 Sand Content

Sand content was measured for stable spud mud compositions containing drill cuttings, xanthan gum, barite and CMC Lo-Vis using a standard API sand test. This included fresh water based muds in E2 and SW based muds in E4. It was important to determine sand content of the designed fluids, as too much large solid particles would result in several negative effects on the equipment and the drilling process

itself. Skjeggstad (1989) reports that any measured sand content above 1% should not occur at the installation if solid control equipment (i.e. shale shakers or cyclones) functions properly. Higher content would result in excessive erosion, wearing of pipes and pumping equipment. Moreover, too high solid content during drilling would result in reduced ROP, increased filter cake thickness and possible logging related problems (Section 3.1.3).

None of the designed stable drilling fluids with cuttings and xanthan gum had sand content as low as 1% (Table 15, Table 21 and Table 22). Nevertheless, most of the drilling fluid compositions with the lowest drill cutting concentration (75g/350 ml water) had sand volume equal to 1.5% or 1.6%. This value can still be considered as low enough for a spud mud application, as the operations are concluded quite fast and the equipment will not be exposed to this slightly high solid content of the fluid. The results of the experiments revealed that increase in drill cutting concentration had direct influence on the volumetric content of sand in the designed fluid as shown in Figure 54 and Figure 55. Cutting concentration of the fluids shown in Figure 54 increases, while polymer concentration was kept the same.

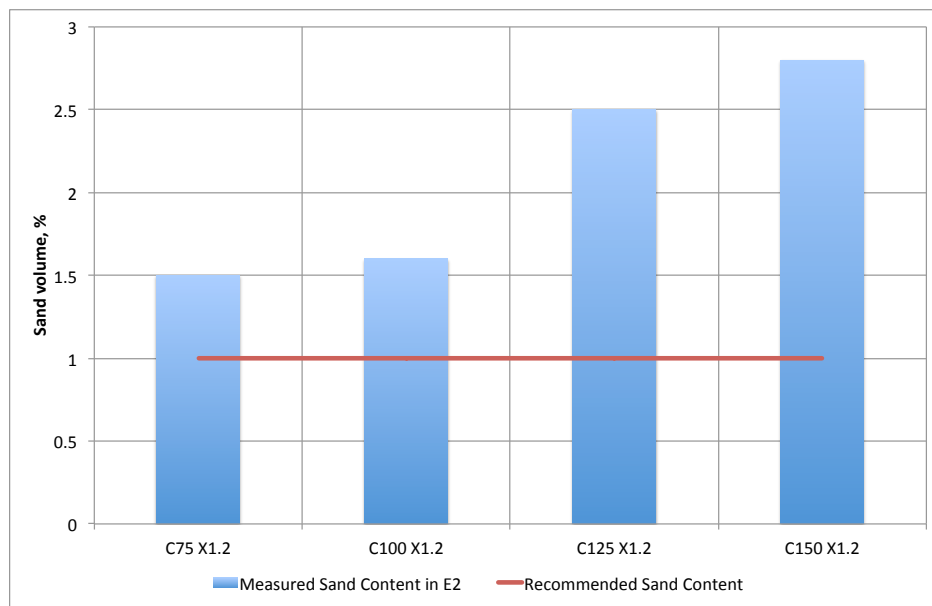


Figure 54. Sand content of the freshwater based muds containing cuttings and xanthan (experiment E2)

From this point of view it is recommended to choose low concentration of drill cuttings as well when designing spud mud based on this approach to avoid possible problems. However, when pumped through bit nozzles, particles may be reduced in size due to the high shear rate.

Addition of barite to the drilling fluid resulted in a higher sand content as well. This can be seen when comparing sand content of the fluid without barite (C75 X1.4 SW) and identical fluid with barite (C75 X1.4 B SW) in Figure 55. These fluids are otherwise identical, though the latter contains a decent amount of barite. As the result sand content increased from 1.50% to 2.00%. It is still recommended to

control density by addition of weighting material rather than drill cuttings. For comparison the fluid with the highest cutting concentration, 150g/350 ml, C150 X1.2 SW had a significantly higher sand content equal to 3.50%.

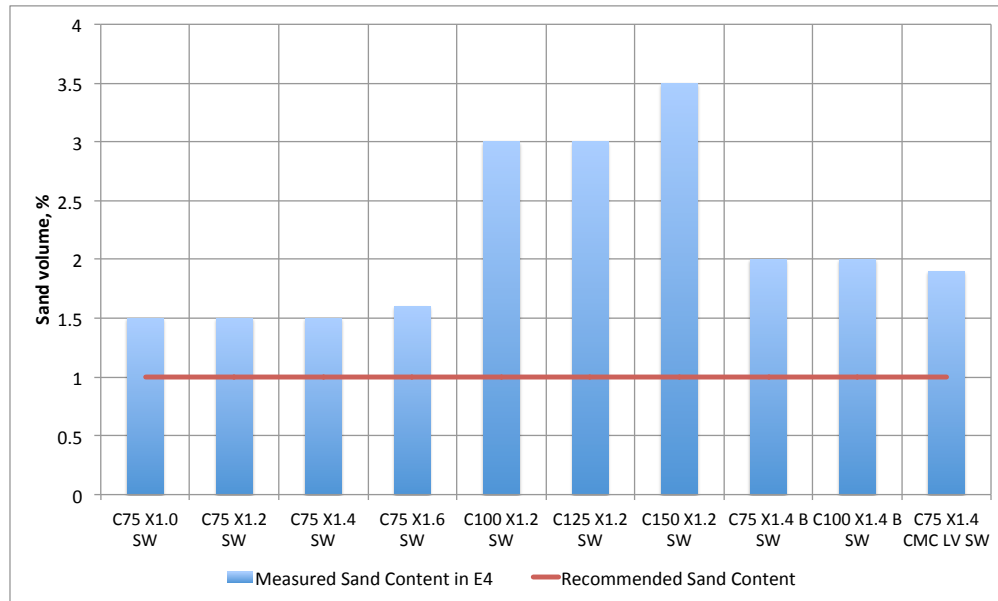


Figure 55. Sand content of the SW based muds containing cuttings and xanthan (experiment E4)

Addition of fluid loss control material resulted in increased sand content as well. For comparison, spud mud containing fluid loss agent, C75 X1.4 CMC LV SW, had sand content equal to 1.90%, which is higher than sand content of the identical mud without fluid loss agent, C75 X1.4 SW (1.50%) as shown in Figure 55. It is therefore recommended to avoid unnecessary application of fluid loss control when one does not expect permeable formations to be encountered. This is beneficial from the economic point of view as well since it would result in a cheaper spud mud.

9.2 Chemical Properties

Important chemical properties such as chloride content, CEC/bentonite content, pH, calcium and magnesium content, lime content and fluid alkalinity were measured in the cases with stable mud compositions containing cuttings and xanthan gum polymers. This chapter provides analysis of the obtained results and explains how these parameters influence the characteristics of spud muds.

9.2.1 Chloride Content

This test is a standard API test, which was performed to roughly estimate salt content of the designed drilling fluids. Chloride content has very high influence on clay performance in water since high chloride concentrations hinder swelling of clay minerals. In this regard all fresh water based stable drilling fluids, containing cuttings and xanthan gum in experiment E2 were tested for chloride content to reveal a correlation between the concentration of cuttings and chloride (Table 15). The results obtained during the testing of the four spud mud compositions with increasing cutting concentration (75g, 100g, 125g and 150g per 350 ml water) in E2

demonstrated the highest degree of linearity with the linear correlation coefficient equal to 0.9920 (when forcing intercept to be equal to 0). The measured values and the generated linear curve are shown in Figure 56.

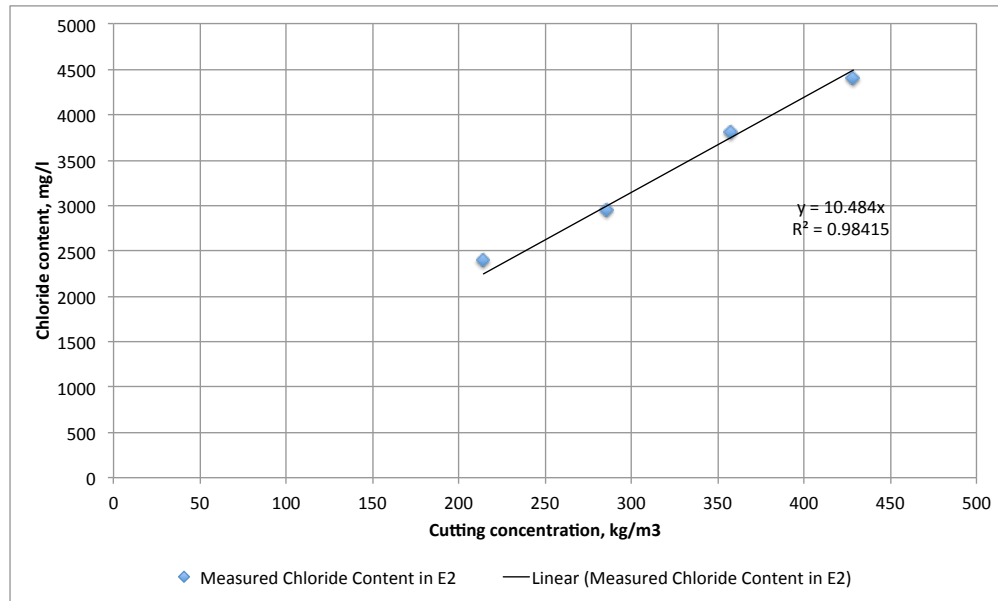


Figure 56. The chloride content of the designed freshwater-based spud muds containing cuttings and xanthan as a function of cutting concentration (E2)

It was mentioned in Section 4.2.2 that osmotic swelling accounted for about 80 to 90% of the total swelling in Na-montmorillonite. When chloride content of water is high, concentration of ions near the crystal surface and the surrounding water will be approximately the same and osmotic swelling will not be promoted. Even in the case with the lowest cutting concentration (75 g per 350 ml water) the resulting chloride content was equal to 2400 mg/l. According to Skjeggstad (1989) chloride concentration of water should not exceed maximum limit of 5000 mg/l during hydration of bentonite. Otherwise, this will result in a poor swelling of clay minerals. Though the value stated by Skjeggstad is still greater than the highest chloride content measured and equal to 4400 mg/l, the designed drilling fluids contained treated drill cuttings, which were not pure bentonite. Based on this information it was concluded that these chloride concentrations were too high to promote hydration of possibly present clay minerals. This is probably one of the reasons and explains the poor swelling behavior and unsatisfactory rheological profile observed in the experiments with simple water-cuttings slurries (E1) and the aging experiment (E3).

As soon as drill cuttings were mixed with fresh water, the salinity significantly increased and hindered any further swelling and hydration of present clay minerals. Basically, one was dealing with a salt solution even when using fresh water as the base fluid. This consideration was the main reason to design similar spud mud compositions based on SW. The chloride test results obtained in the experiment with SW based fluids (E4) demonstrated a similar behavior as can be seen when

referring to Table 21 and Table 22. However, in this case the registered values were elevated by approximately 18400 mg/l on average due to much higher chloride content of SW used as base fluid.

The reason for the resulting high chloride content of the designed drilling fluids lies in the composition of OBM. These drill cuttings had been recovered after drilling with OBM (Section 5.2), while in Section 3.3.2 it was mentioned that the water phase of OBM is actually a salt solution with the salt content reaching up to 35%.

9.2.2 CEC and Bentonite Content

MBT was conducted on most of the spud mud compositions in E2 and E4 to identify approximate amount of active clays/bentonite in the treated drill cuttings. These muds consisted of drill cuttings and xanthan gum polymer and the active clay amount as the function of cutting concentration was studied. Moreover, these tests were meant to provide a firm foundation for deriving the conclusions about the rheological behavior of the mixed fluids.

Based on the results of MBTs and the correlation given in Appendix B approximate amounts of bentonite in the designed fluids were calculated. These are reflected in Figure 57 and Figure 58 together with the two designed reference fluids levels. Freshwater-based drilling fluids in Figure 57 had increasing drilling cuttings concentration from 75 g up to 150 g per 350 ml water in the increments of 25 g. Thus, there is a corresponding increase of absolute active clay content as well. On the other hand, the first four fluids compositions in Figure 58 had identical amounts of cuttings equal to 75 g per 350 ml, while only xanthan gum concentration was adjusted. Therefore the active clay content was also constant here. The cuttings content increased for the last three fluids in Figure 58 in the increments of 25g per 350 ml. Here the active clay content increased with increasing cutting concentration.

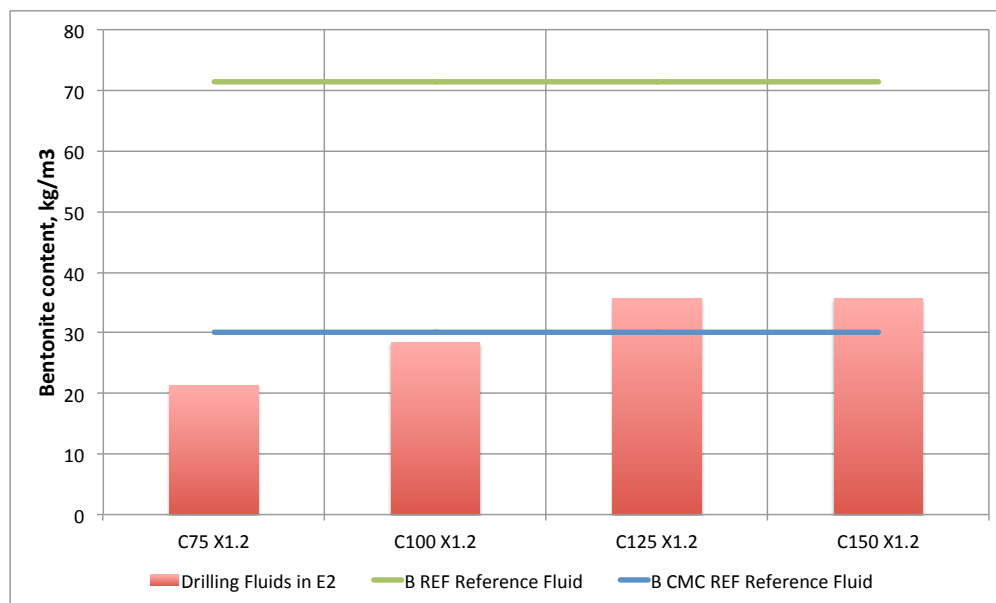


Figure 57. The bentonite content of the freshwater based spud muds with cuttings and xanthan gum (E2)

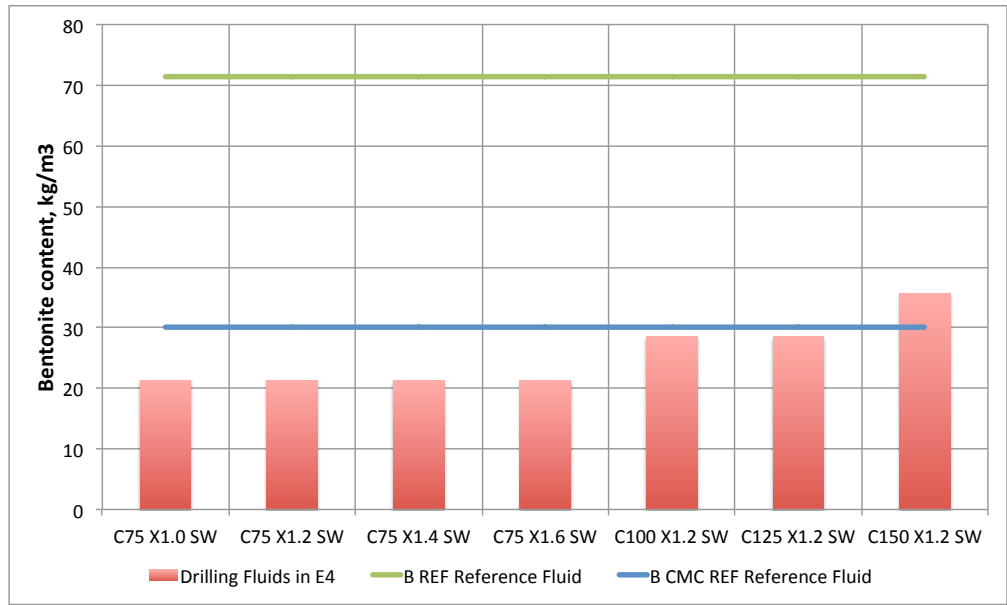


Figure 58. The bentonite content of the SW based spud muds containing cuttings and xanthan gum (E4)

Bentonite contents of the stable muds shown in Figure 57 and Figure 58 were significantly lower than that of B REF fluid. Moreover, the drill cutting concentrations in the designed fluids were 3, 4, 5 and 6 times higher than the bentonite concentration of the B REF spud mud. Based on this it was concluded that even high concentrations of drill cuttings would not compensate for the low clay content. In addition to this, excessively large concentrations would result in unnecessarily high fluid density (Section 9.1.1).

It was determined that approximately 10% of the treated drill cuttings material was active clay minerals or bentonite. This can be seen when comparing bentonite amount from MBT and drill cuttings concentrations in the designed fluids as shown in Table 23.

Table 23. The comparison of the bentonite content and drill cuttings concentration in the designed fluids

	Calculated bentonite content, kg/m ³	Drill cuttings concentration, kg/m ³
E2 experiment (freshwater-cutting-xanthan)	21.4	214.3
	28.5	285.7
	35.6	357.1
	35.6	428.6
E4 experiment (SW-cutting-xanthan)	21.4	214.3
	28.5	285.7
	28.5	357.1
	35.6	428.6

Though the obtained data is not 100% perfect due to the uncertainties in the measurements a distinct trend is observable. This batch of drill cuttings contained rather low amounts of active clay minerals. Furthermore, high chloride content resulting when mixing cuttings and water (Section 9.2.1) would totally hinder

hydration/swelling of these clay minerals. These two reasons provide a good explanation of the poor viscous properties obtained in experiment E1 with simple water-cutting slurries. Likewise, these are the reasons for the absence of hydration during the aging experiment (E3). Moreover, as mentioned in Section 3.2.2 yield stress and gel strength of a fluid occurs due to electrical interaction between particles. Zeta potential of the particles were studied as well and covered in detail in Section 9.3.1. It is worth mentioning that any increase in drill cutting concentration would result in an increase in chloride concentration as well, which will hinder hydration of clays even more. This resulted in the closed loop situation. However, this observation is not a general rule as it strongly depends on the composition of the recovered drill cuttings. As stated in Section 4.2.2 osmotic swelling, which is mainly responsible for swelling of clay minerals, occurs only in montmorillonites with monovalent balancing ions. In addition to its low active clay content, these clay minerals of treated drill cuttings might be of the Ca^{2+} type, which are incapable of notable hydration. Additionally, it was mentioned in Section 5.1.2 that the smectite content of subsurface formations at the Gullfaks field could be significantly high. There is a high chance that cuttings from this or any other smectite rich area would behave differently, though this statement has to be tested in a laboratory.

On the other hand, the bentonite amount of the designed spud mud was comparable to that of the reference fluid containing CMC polymer (B CMC REF). Therefore, it was decided to stabilize the designed fluids by addition of a polymer. As the results in Section 8 demonstrated the xanthan gum biopolymer was the only appropriate type of polymer for this application.

9.2.3 Other Chemical Properties

Other chemical properties as pH, Ca^{2+} and Mg^{2+} content, lime content and alkalinity have less significant influence on the drilling fluid characteristics and these were collected for presentation in a separate chapter of this work.

In all the designed drilling fluids pH values were quite high, varying from 10.1 to a maximum of 11.8. It is common in the drilling fluid industry to increase pH of a fluid by addition of sodium hydroxide. In this case this would not be required due to the high pH value of the designed compositions. Effect of pH on pure water-cuttings slurries was tested by adding varying sodium bicarbonate concentrations to the designed simple water-cuttings slurries in E1. The obtained pH reduction had no effect on the rheological properties of the mixtures. Based on this, it was concluded that pH of the mixtures had no influence on the rheological behavior of the fluid.

It is common in the industry to add biocide in the case of polymer based drilling fluids. However, at high pH values (over 10-11) this is not required. Moreover, according to the MI-Swaco (2004) biocide is required only in low salinity brines. When using SW as the base fluid this is therefore not necessary. Xanthan gum polymers may hydrolyze at high pH values as well according to MI-Swaco (2004). However, this effect was not observed even in the case with the highest measured pH equal to 11.8 (as observed with C150 X1.2 fluid). Furthermore, when SW was used as the base fluid, pH values of the designed muds reduced to approximately

10.1-10.2 from 11.1-11.8. Keeping in mind that pH is the logarithm of the hydrogen concentration with the base equal to 10 this corresponds to a significant decrease. This reduction might have occurred due to the sodium bicarbonate, which was present in the SW composition. This compound acted like a buffer and reduced the pH value. According to Skjeggstad (1989) pH should be higher than 10 to avoid steel corrosion and bacterial degradation. In the conclusion about pH measurements, it is important to mention that the measured pH values of the stable SW based spud muds were in the acceptable range.

Relatively high pH of the designed fluids follows from the presence of lime in OBM from which treated drill cuttings are recovered. As mentioned in Section 3.3.2 lime is normally added to OBM to activate the surfactants. For this purpose lime contents of the cuttings/xanthan containing spud muds were measured in the experiments with freshwater (E2) and SW (E4). The results obtained in E2 were of more interest in this regard as fresh water was used as a base fluid and the measured lime content comes entirely from drill cuttings. Though these tests did not demonstrate a high degree of linearity as in the case with the chloride content measurements (Section 9.2.1), there were two decent trends observable. As shown in Figure 59, which summarizes the results obtained from E2 and E4, lime concentration increased for every increase in the cutting concentration. Here the concentration of the muds shown in Figure 59 varied from 75 g per 350 ml water (C75 X1.2) to 150 g per 350 ml water (C150 X1.2) with the increment of 25g.

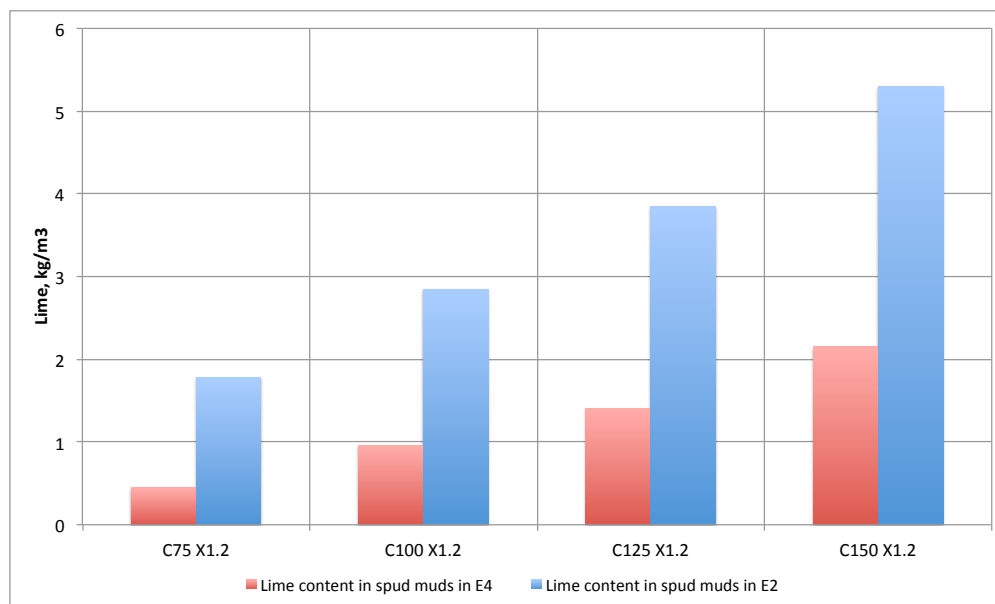


Figure 59. The lime content in the designed cuttings/xanthan containing spud muds (E2 corresponds to the freshwater-based muds and E4 to - the SW based)

Additionally, lime concentrations of the corresponding SW based spud muds in E4 were significantly lower than those of the similar water based fluids in E2. As the standard API test measures the amount of sulfuric acid to reach the equilibrium point for phenolphthalein indicator (pH=8.3), any reduction in pH will result in the

corresponding reduction of lime concentration in mud. It was already mentioned in this section that pH values of SW based muds were lower than the pH of the identical freshwater based fluids due to SW acting as a buffer in this case. This explains the lower lime content of SW based spud muds.

Lime added to OBM contributes not only with OH^- ions, but with Ca^{2+} ions as well. Moreover, calcium chloride salt is often added to OBM to avoid osmosis (Section 3.3.2). Therefore, calcium ions were expected to be present in the designed drilling fluids and the appropriate API tests were carried out. The results of E2, where freshwater/cuttings/xanthan gum spud muds were tested showed that the designed spud muds contained insignificant amount of Mg^{2+} ions. As shown in Table 15, in three of four cases Mg^{2+} ions concentration was equal to 12 mg/l, while it was equal to 0 mg/l in one case (C150 X1.2 SW). Since these results are obtained from volumetric titration of filtrate, such low values can be regarded as negligible due to the uncertainty in measurements. Due to this the values in the line total hardness as calcium in Table 15 are regarded as true calcium ion concentrations in E2. The obtained Ca^{2+} tests results in E2 demonstrated very high linearity with the coefficient of correlation equal to 0.9909 (applying least squares method and forcing intercept to be equal to 0) as shown in Figure 60.

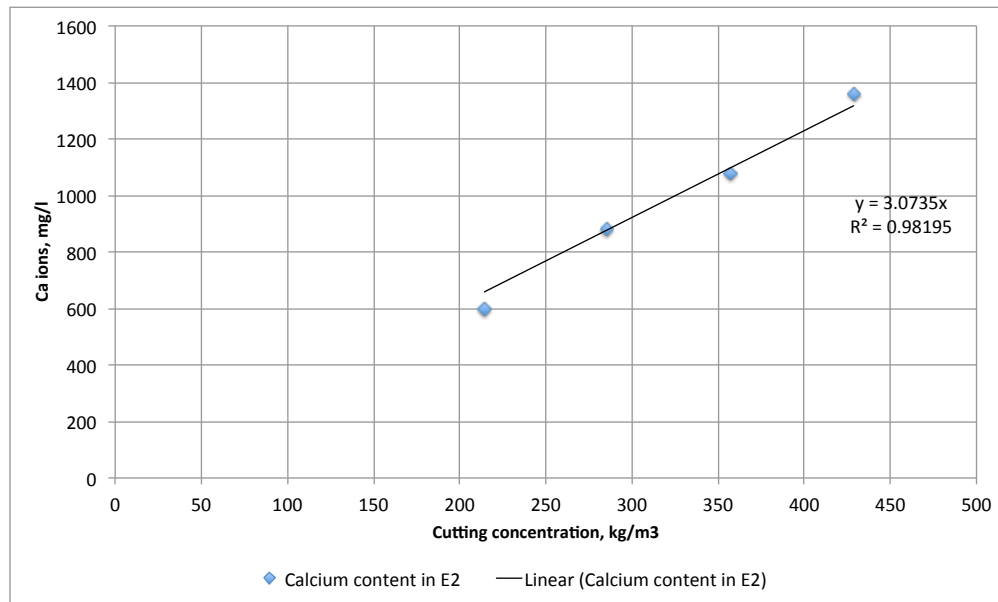


Figure 60. The Ca^{2+} concentration as a function of cuttings content of the freshwater-based spud muds containing cuttings and xanthan

Even small amounts of Ca^{2+} ions in drilling fluids may have destructive effect on swelling abilities of clay minerals. Skjeggstad (1989) mentions that concentration of calcium ions in water used to hydrate bentonite should not exceed 200 mg/l. It is shown in Table 15 and in Figure 60 that even at the lowest tested drill cuttings concentration equal to 75 g per 350 ml water, calcium content was equal to 600 mg/l, which significantly exceeded the limit stated by Skjeggstad. This is yet

another reason for the absence of swelling/hydration in addition to high chloride content and low amount of active clays as stated in Section 9.2.1 and Section 9.2.2.

When considering the Ca^{2+} and Mg^{2+} test results in the experiments with SW based fluids containing cuttings and xanthan gum (E4) a similar trend was observable. Nevertheless, here the absolute values of calcium ion concentrations were higher than those measured in E2. This happened since calcium and magnesium ions were as well present in SW used here as base fluid. As was shown in Table 21 and Table 22 Ca^{2+} concentration varied from 2620 mg/l to 3640 mg/l depending on the cutting concentration. Every increase in cutting concentration resulted in a corresponding increase in the Ca^{2+} amount. On the other hand, more significant amounts of Mg^{2+} ions were measured when using SW as base fluid instead of freshwater, though the values were still low on an absolute scale. These magnesium ions were considered to come entirely from SW as the obtained values were rather spread and no correlation could be seen when comparing Mg^{2+} concentrations of different spud muds in Table 21 and Table 22. The fact that measured magnesium ions concentrations were rather low is in correspondence with literature. Mg^{2+} ions deposit out from the solution as magnesium hydroxide at pH 9.5-10 (Skjeggstad, 1989) and thus, high numbers were not expected, given that pH values of the designed muds were higher than 10.

Alkalinity measurements are performed to identify ion types that can neutralize H^+ ions present in acids. It is mentioned in Appendix B that these measurements are of acceptable accuracy for simple drilling fluids without thinners. Carbonate and bicarbonate ions are undesirable in a drilling fluid and this problem is often referred to as carbonate contamination. This is especially a problem for bentonite-based fluids as the control of main rheological parameters may become challenging (Skjeggstad, 1989). Given that the designed spud mud compositions cannot be classified into the bentonite-based mud group, this problem is of less importance in this case. Moreover, measured P_f values were equal to 0 for all spud mud compositions consisting of water, cuttings, xanthan gum, barite and CMC Lo-Vis. This means that filtrate contains neither OH^- ions nor CO_3^{2-} ions. M_f values demonstrated a correlation with increasing cutting concentration of a drilling fluid. In the case with the freshwater-based cuttings/xanthan spud muds in E2 these values increased from 0.55 ml to 0.80 ml of 0.01 M H_2SO_4 with increasing cutting concentration. When SW was used as the base fluid for the same compositions in E4 M_f increased from 0.40 ml to 0.70 ml of 0.01M H_2SO_4 . Skjeggstad (1989) mentions that before the M_f value becomes as high as 5 ml, no significant carbonate contamination exists. In this regard it was concluded that the measured filtrate alkalinity is well within the acceptance range.

9.3 Rheological Properties

Rheological properties of a drilling fluid are the most essentials and considered to be the most important during the design process of a new fluid composition. These properties are as well directly dependent on the chemical composition of the fluid. Due to this rheological properties of the designed drilling fluids are discussed after

having covered physical and chemical properties. The performance of drill cuttings and the selected polymers, the effect of polymer and drill cuttings concentration on the rheological properties of the fluids as well as temperature effects are discussed in details in this section.

9.3.1 Performance of Drill Cuttings in Fresh Water

The results of the experiments with simple water-cutting slurries (E1) (reflected in Table 13) and the hydration experiment (E3) (reflected in Table 16) demonstrated that this batch of thermo-mechanically treated drill cuttings was incapable of yielding required rheological properties. High chloride content and low content of active clay minerals in the material were considered to be the two main reasons for this behavior as described in Section 9.2.1 and Section 9.2.2. The designed simple water-cuttings mixtures in E1 and E3 had extremely low gel strength and yield stress values. Moreover, in some cases these values were as low as 0. This can be seen when studying GEL 10s and τ_0 lines of Table 13 and Table 16. Since the presence of charged particles is essential for the electrical interaction between them and hence the development of gel structures, zeta potentials of the drill cuttings and the bentonite were measured using an AcoustoSizer II instrument available at the University of Stavanger. For the drill cuttings the measured zeta potential was equal to -7.6 mV, while that of the bentonite sample was equal to -35 mV (software generated reports of zeta potential measurements are shown in Figure E-1 and Figure E-2 provided in Appendix E). According to Hanaor et al. (2012) and Greenwood and Kendall (1999) particles with high absolute zeta potential values form more stable colloidal suspensions since the repulsive forces between particles are dominating. On the other hand, when zeta potential is low, van der Waals forces start to dominate and particles tend to agglomerate and settle. Zeta potential of the drill cuttings were significantly lower than that of the bentonite sample. The value of -7.6 mV is rather close to zero and most likely van der Waals forces were dominating in the water-cuttings slurries resulting in unstable suspensions. Moreover, according to the results provided in Section 6.1.4 particles as large as 100 microns were present in the cuttings as well. As mentioned in Section 8.1 severe sag effect of drill cuttings was observed in the experiment with water-cuttings slurries due to the high concentration of heavy particles. This means that heavy and approximately neutrally charged drill cutting particles were incapable of yielding required rheological properties when simply mixed with water.

9.3.2 Effect of CMC and PAC Polymers on Rheological Properties

CMC Hi-Vis and PAC polymers were initially considered as stabilizing agents for the designed simple water-cuttings slurries in E1. As it can be seen from the results presented in Table 14 these polymers were only partially successful for this application. Here the increased concentration of CMC Hi-Vis polymers yielded improved high shear rate viscosity. However, low shear rate viscosity and gel strength values of the designed fluids were still insignificant. Furthermore, yield point values calculated using the Herschel Bulkley model, τ_0 , were equal to 0.511 Pa in four of five cases presented, while in case of the C75 CMC1.3 drilling fluid the same value was equal to 0 Pa. Effect of polymers on the rheological properties of the

fluids can as well be seen in Figure 61, where the corresponding viscosity curves of the fluids presented in Table 14 are plotted in the same diagram.

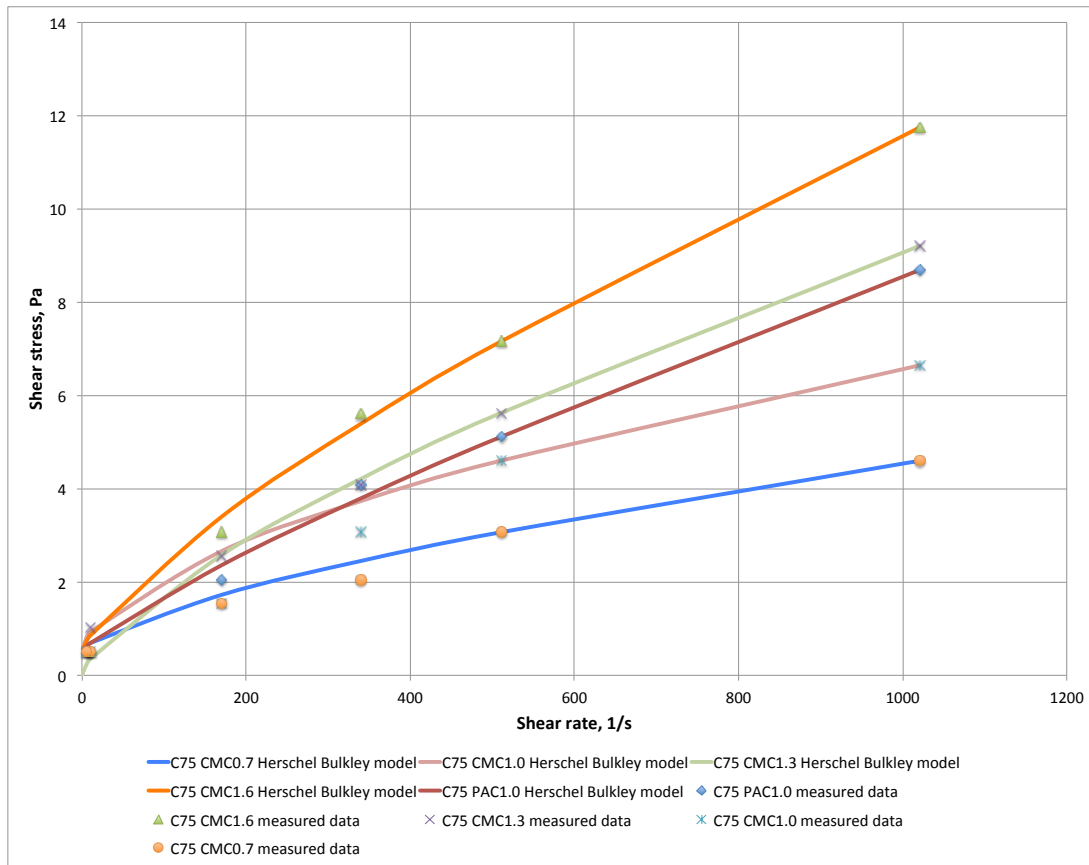


Figure 61. The effect of CMC and PAC polymers concentration on the rheological properties of the designed freshwater-based spud muds with the cuttings concentration equal to 75 g per 350 ml water

The plotted curves almost coincide at shear rate values less than 100 s^{-1} , while there is an observable increasing deviation between the plotted lines with increasing shear rate values. Comparing shear stress values at 1022 s^{-1} of C75 CMC0.7 and C75 CMC1.3 fluids an increase by a factor of two is seen. This means that approximately doubling of CMC Hi-Vis concentration results in double as high shear stress value at 1022 s^{-1} . However, this was not the case for shear stress readings at the low end of the viscosity curves shown in Figure 61. Most of the measured shear stress values of CMC/PAC containing fluids shown in Figure 61 at 3 and 6 RPM coincided and were equal to 0.511 Pa with an only exception of C75 CMC1.3 fluid. Shear stress for the latter fluid was equal to 1.02 Pa at 6 RPM though this could occur due to the uncertainty in the measurements.

Another important aspect found was that PAC polymer yielded better rheological properties than CMC Hi-Vis when added in equal concentrations to the same water-cutting slurries. Comparing the fluids with equal polymer concentrations, 1 g per 350 ml water, CMC containing fluid C75 CMC1.0 (pink line) and PAC containing fluid

C75 PAC1.0 (red line) on the chart it can be seen that the latter fluid demonstrated higher shear stress values.

CMC and PAC based fluids presented in Table 14 had relatively high value of the power law index, n . This is an indication of poor shear thinning properties, which are observable as well when studying viscosity curves presented in Figure 61 since the curves are rather linear. Consistency indexes, K , for all fluid compositions in Table 14 were contrary quite low regardless of the applied type of polymer and its concentration. As mentioned in Section 3.2.2 consistency index provides information about fluid viscosity at low shear rates. This means that when CMC and PAC polymers were used as stabilizing agents, the obtained fluids were neither capable of suspending solids at low shear rates nor of yielding good gel and thixotropic properties. Thus, it was concluded that CMC and PAC polymers were not suited well for this application.

9.3.3 Effect of Xanthan Gum on Rheological Properties

Xanthan gum biopolymer was tested as well as a stabilizing agent for water-cuttings slurries. The results of the experiment with xanthan gum and fresh water based drilling fluids (E2), reflected in Table 15 demonstrated that this polymer type could provide required rheological properties to the designed fluid compositions.

Several improvements were observed when xanthan gum was added to the water-cuttings slurries instead of CMC and PAC. This can be seen when comparing fluids with equal cuttings and polymer concentrations as shown in Figure 62. Here C75 X1.0 is a xanthan gum based mud, while C75 CMC1.0 and C75 PAC1.0 are CMC and PAC based fluids respectively. Concentration of cuttings was equal to 75 g per 350 ml water and concentration of polymer was equal to 1 g per 350 ml water for all fluids. Nevertheless, rheological properties of the xanthan-based spud mud were significantly better than those of the CMC and PAC based muds. Yield point of C75 X1.0 calculated from the Herschel Bulkley model was equal to 1.53 Pa, which is three times higher than that of the other two fluids.

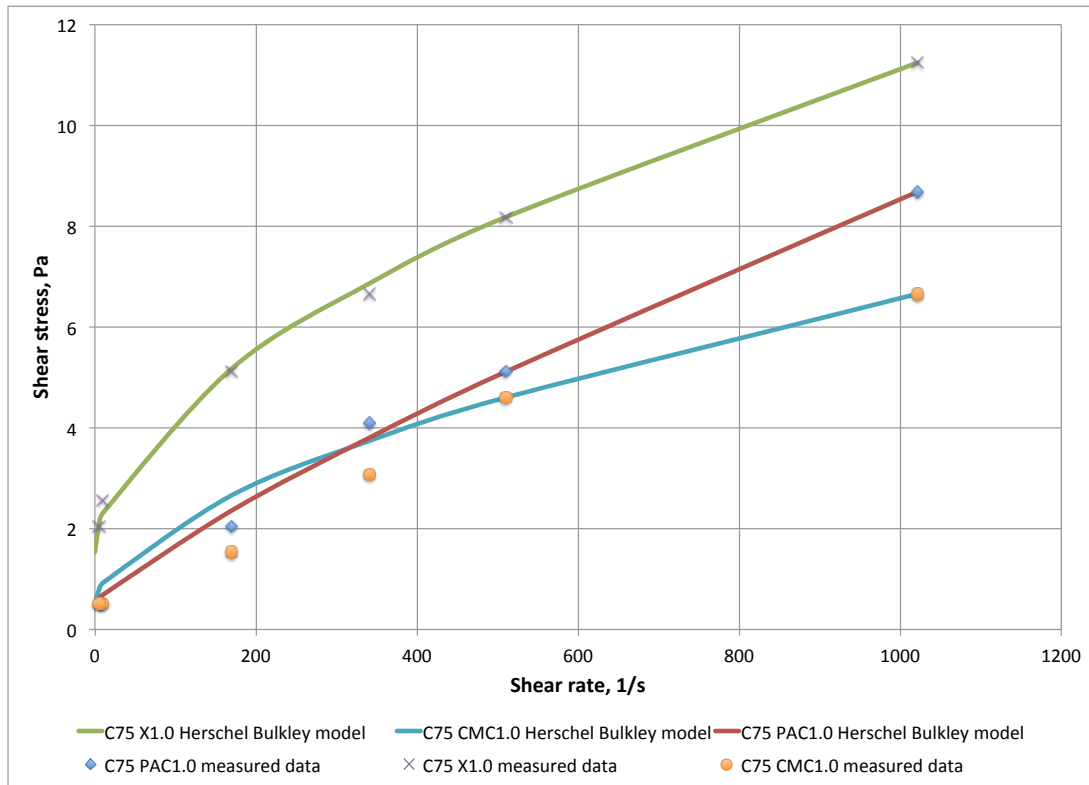


Figure 62. The effect of xanthan gum, CMC and PAC polymers on the rheological properties of the designed freshwater-based spud muds with the cuttings concentration equal to 75 g per 350 ml water

Similar trend is observable when comparing YP values based on the Bingham model for these fluids in Table 14 and Table 15 as the YP increased to 5.11 Pa with addition of xanthan gum. For comparison YP of CMC and PAC based fluids were equal to 2.56 Pa and 1.53 Pa respectively. Significant increase in gel strength was observed as well. Gel strength after 10s of the spud mud containing xanthan gum was equal to 5, which is five times greater than the gel strengths of CMC/PAC based fluids. Xanthan gum based drilling fluid had the best shear thinning properties as well with the lowest among these three fluids power law index equal to 0.55 and significantly higher consistency index equal to 0.22 Pa·sⁿ (Table 15). PV values of C75 X1.0, C75 CMC1.0 and C75 PAC1.0 drilling fluids were equal to 6 cP, 4 cP and 7 cP respectively. This means that the selected polymer types have little influence on PV of the designed fluid, leading to the conclusion that xanthan gum could significantly improve low shear rate viscosity and gel properties without jeopardizing the requirement of low PV of spud muds.

It was of interest to study the effect of xanthan gum concentration since this polymer provided better rheological properties to the fluids. Four different biopolymer concentrations were mixed in the experiment with xanthan and freshwater-based fluids (experiment E2). Fluids containing 1/1.2/1.4/1.6 g of xanthan gum per 350 ml water were prepared in E2. The cutting concentrations were kept constant in the mixtures and were equal to 75 g per 350 ml water. These fluids are referred to as C75 X1.0/1.2/1.4/1.6 respectively depending on the

corresponding polymer concentration. The viscosity curves of these fluids presented in Figure 32 through Figure 36 (including the B CMC REF standard reference fluid to enable overall evaluation of performance of the fluids) are plotted for comparison in one diagram in Figure 63. As it is seen from Figure 63 increased biopolymer concentrations had very limited influence on the PV of the fluids, as this value was slightly increased with increasing polymer concentration (Table 15) and curves are quite parallel to each other. Even for the highest polymer concentration this value was equal to 8 cP, which is acceptable for spud mud application. On the other hand, yield stress value τ_0 increased with increasing xanthan gum concentration. When xanthan concentration was increased from 1 g to 1.6 g per 350 ml of water, τ_0 increased from 1.53 Pa to 5.11 Pa. This is a significant change as the yield stress increased more than 3 times.

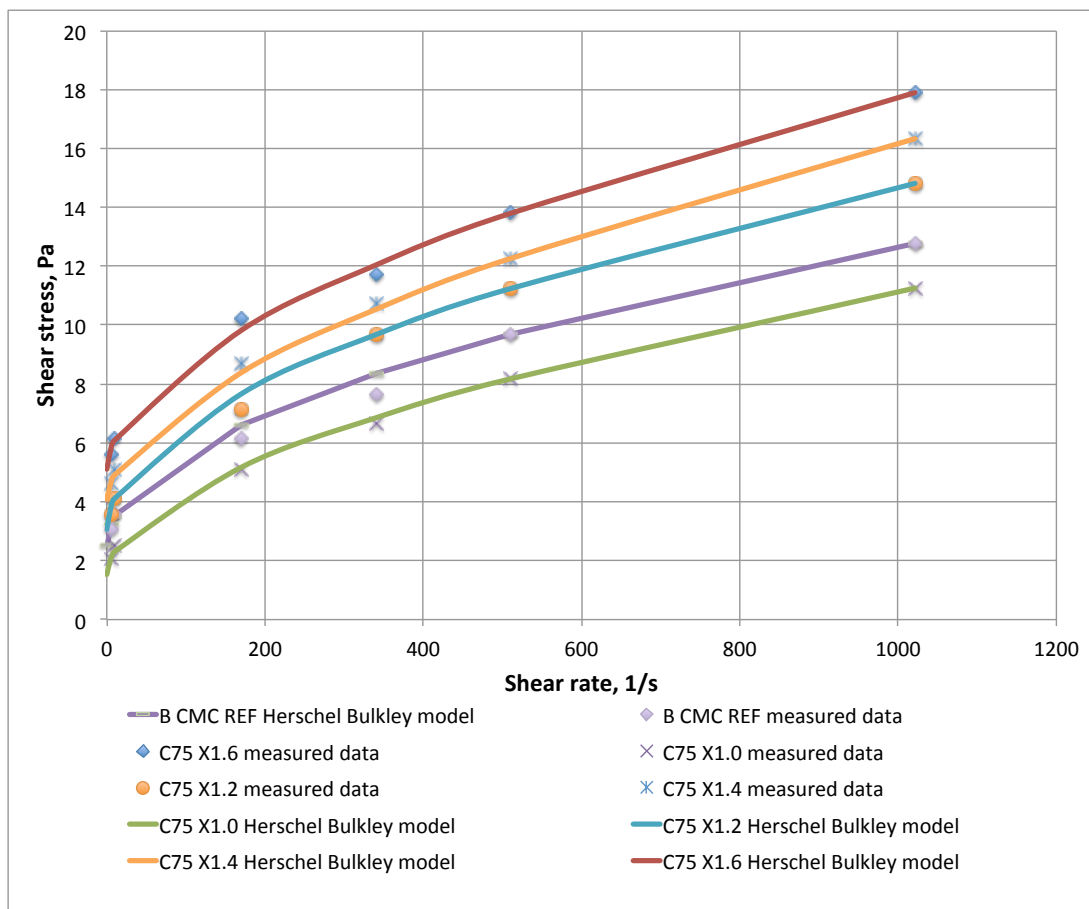


Figure 63. The effect of the increasing xanthan gum concentration on the rheological properties of the freshwater-based spud muds with the cuttings concentration equal to 75 g per 350 ml water

Ten seconds gel strength of the fluids presented in Figure 63 were as well quite high, equal or even slightly higher than the Fann viscometer reading at 6 RPM. The designed xanthan gum containing fluids quickly built good gel structure and were as well capable of suspending solid particles. On the other hand, gel structures were easy to break by simple agitation and initial rheological properties were restored after a short mixing period.

Identical spud mud compositions were designed using SW as the base fluid in experiment E4. Here the same cutting concentration equal to 75 g per 350 ml SW and xanthan gum concentrations equal to 1/1.2/1.4/1.6 g per 350 ml SW were used. The resulting fluids are referred to as C75 X1.0/1.2/1.4/1.6 SW depending on the corresponding xanthan concentration. The effect of xanthan concentration in these SW based fluids can be studied when plotting the respective viscosity curves of the fluids presented in Figure 40 through Figure 43 in one diagram as shown in Figure 64 (here viscosity curves are shown together with the B REF standard reference fluid).

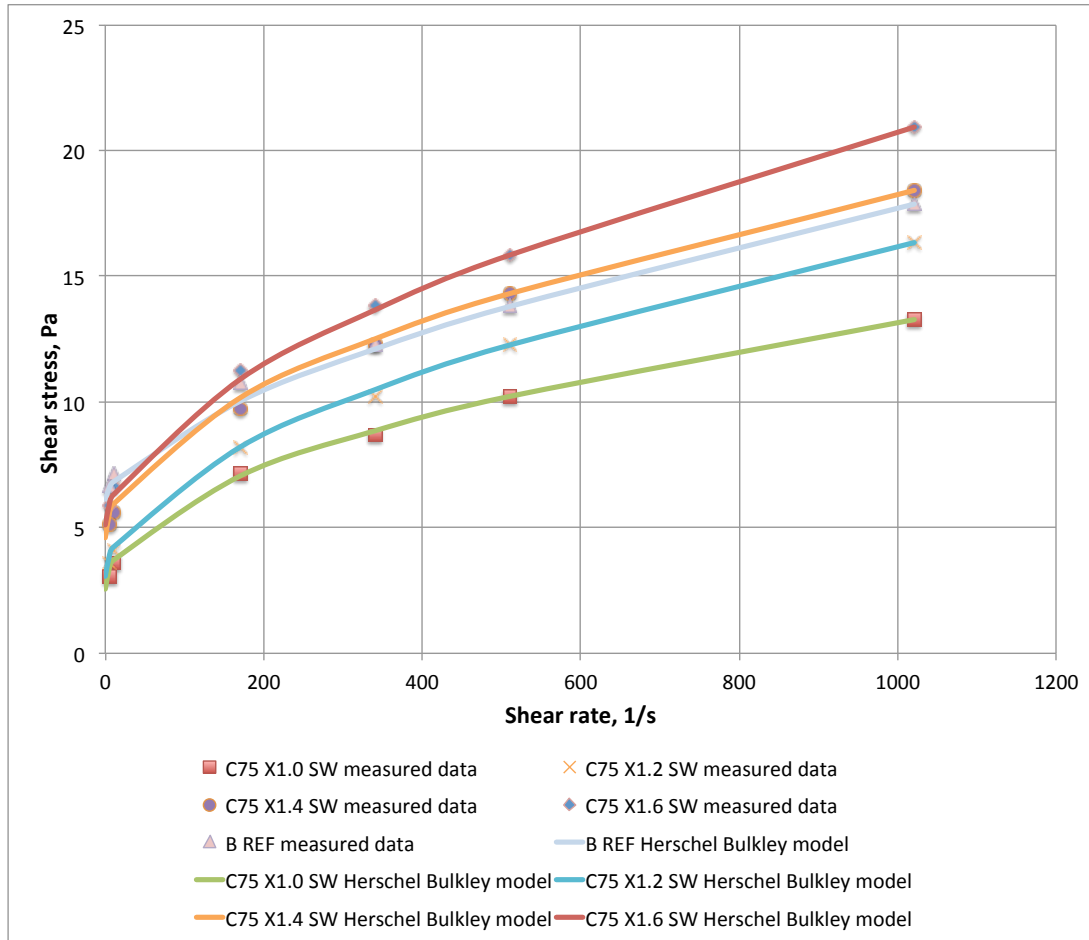


Figure 64. The effect of the increasing xanthan gum concentration on the rheological properties of the SW based spud muds with the cuttings concentration equal to 75 g per 350 ml water

Significant increase in the YP of the fluids calculated based on the Herschel Bulkley model was obtained here as well. The Herschel Bulkley model YP of C75 X1.0 SW fluid with the lowest xanthan concentration was equal to 2.56 Pa, while the same value for C75 X1.6 SW spud mud with the highest xanthan concentration was equal to 5.11 Pa, which corresponds to an increase of approximately 100%. Moreover, comparing the Herschel Bulkley YP values of identical freshwater and SW based spud muds, containing xanthan gum, one can see that these values are quite similar independently of the base fluid type. The same applies to GEL 10 s measurements,

which were slightly higher than 6 RPM reading for these four SW based spud muds shown in Figure 64. This observation supports the expectations that YP and gel strengths of the designed fluids depend mainly on the concentration of biopolymer. On the other hand, PV values of the SW based muds (E4) were slightly higher than the PV values of the identical freshwater-based drilling fluids (E2). This can be seen as well when comparing two similar fluid compositions C75 X1.6 and C75 X1.6 SW with equal cutting and xanthan gum content as shown in Figure 65. Here the Herschel Bulkley model YP for both fluids were equal to 5.11 Pa, while the PV of the latter was 2 cP higher. Given that the number of solid particles in these fluids were approximately equal (same concentrations were used) PVs were expected to have similar values as well. This deviation occurred most likely due to the different mixing procedures of these fluids. As it was mentioned in Section 7.3.4 the Silverson L4RT-A mixer was used during the experiments with SW based fluids, while a standard Hamilton mixer was used during the experiments with freshwater. The former develops higher shear rates than the latter during mixing, which results in a larger number of smaller particles yielding higher PV. It is important to keep in mind this observation with regards to field implementation. Shear rates developed in mud mixing tanks are not very high, however, when the fluid is pumped through bit nozzles it will be exposed to significantly higher shear rates. Due to this rheological properties of the mixed fluid may slightly change after one complete circulation. However, based on the experimental observations this alteration might only affect the PV of the fluids.

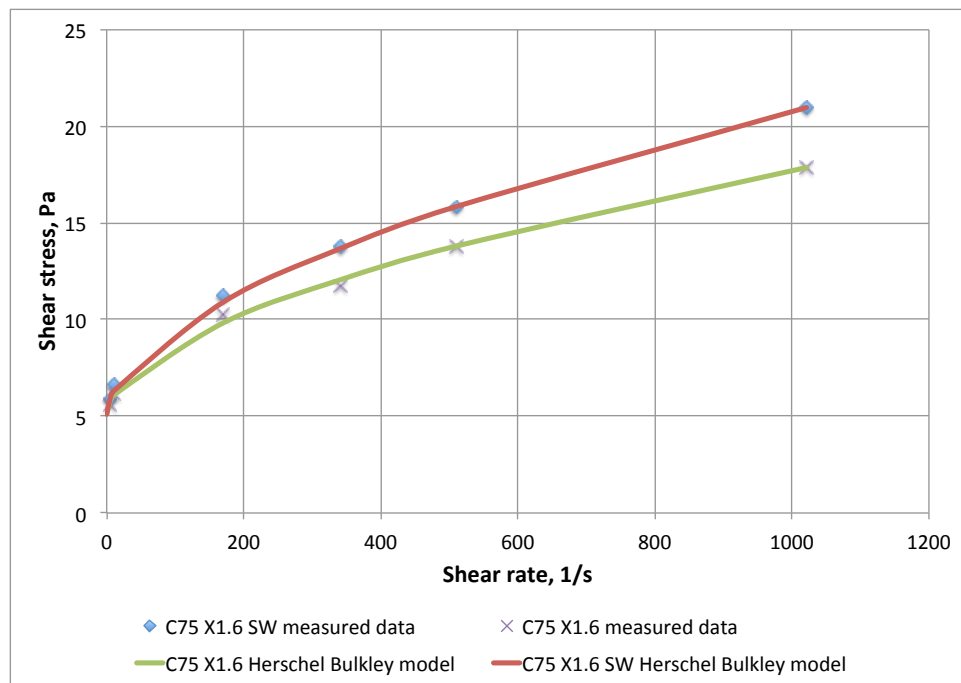


Figure 65. The comparison of the rheological properties of the freshwater-based mud C75 X1.6 and the identical SW based mud C75 X1.6 SW

Another important observation regarding how different polymer types influenced the rheological properties of the designed fluids could be made when comparing

power law indexes, n , and consistency indexes, K , of the fluids containing CMC, PAC and xanthan (Table 14, Table 15 and Table 17). As it was pointed out in Section 9.3.2 fluid compositions with CMC or PAC polymers had relatively high n values and very low K values. On the other hand, spud muds containing xanthan gum (regardless of the base fluid type) had lower values of power law indexes, approximately equal to 0.50. Additionally, K values for the biopolymer-based fluids increased significantly to approximately 0.20-0.40 Pa·s ^{n} . This means that, xanthan gum is capable of improving shear-thinning properties of simple water-cutting slurries designed in E1 as well as providing significantly better low shear rate viscosity. Last, but not least it is important to emphasize that addition of biopolymers resulted in a stable drilling fluid composition as well. The results presented in Table 16 demonstrated that even after being aged for 10 days C75 X1.2 mud had the same rheological properties as earlier.

9.3.4 Effect of Solids Concentration on Rheological Properties

Discussion of how solid particles affected rheological properties of the designed stable xanthan gum containing fluids was of interest after having thoroughly considered effects of biopolymer concentration. During the experiments three different solid compounds were added to the designed spud muds: cuttings, barite and CMC Lo-Vis. Though the effect of cutting concentration on the rheological properties of the fluids was of the main interest, the influence of other solid particles on the fluids behavior will be discussed here as well.

Effect of cutting concentration on the designed fluids can be quickly studied when plotting viscosity curves of four spud muds with increasing cuttings concentration in one diagram. This includes freshwater-based spud muds with xanthan gum, where concentrations of cuttings were equal to 75/100/125/150 g per 350 ml water respectively. The polymer concentration was kept constant equal to 1.2 g per 350 ml water. These fluids are referred as C75 X1.2, C100 X1.2, C125 X1.2 and C150 X1.2 where the number standing after the “C” indicates the amount of cuttings present in the mud in g per 350 ml water. The viscosity curves of these fluids presented in Figure 34, Figure 37, Figure 38 and Figure 39 are compared here in one diagram as shown in Figure 66.

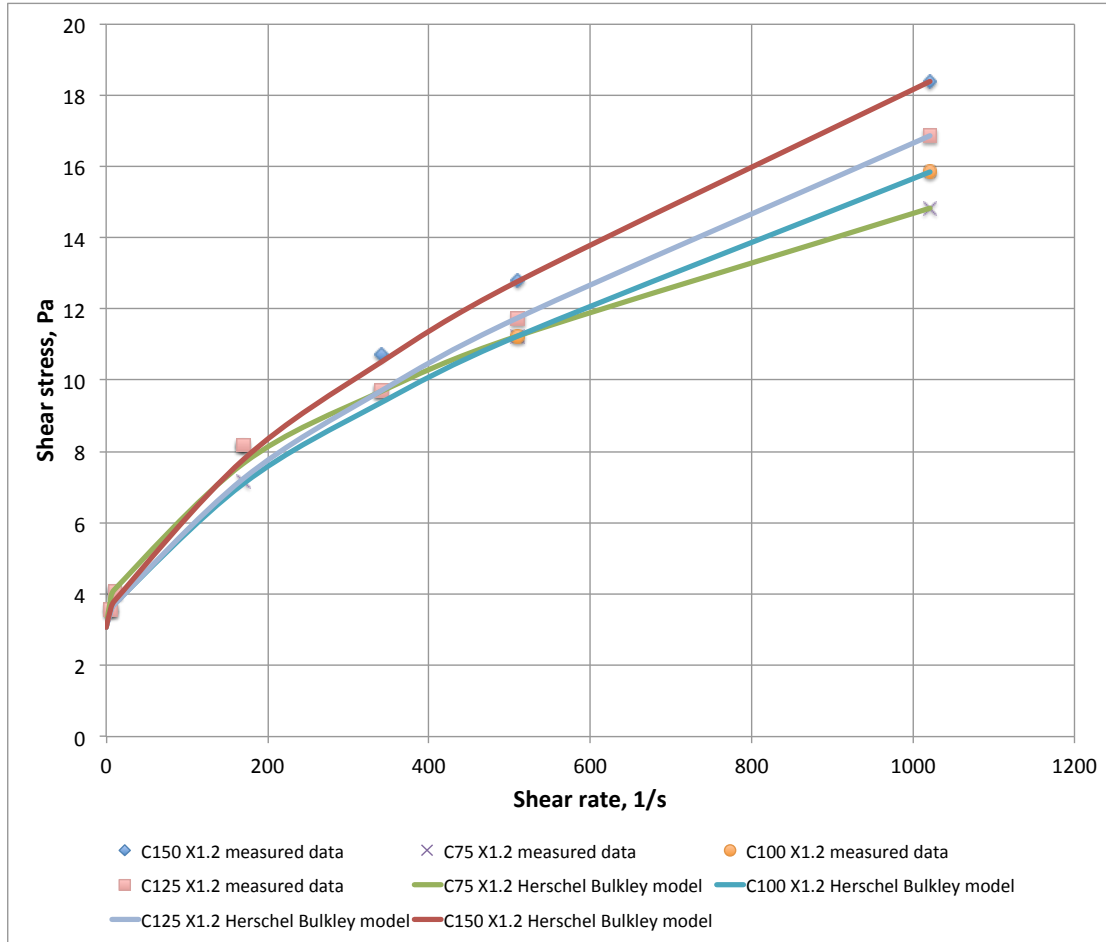


Figure 66. The effect of the increasing cuttings concentration on the rheological properties of the freshwater-based spud muds containing cuttings and xanthan with the concentration equal to 1.2 g per 350 ml water

As it can be seen from Figure 66 viscosity curves for these fluids are quite coinciding for shear rate values lower than 200 s^{-1} . However, curves start to diverge at higher shear rates. This graphical behavior is an indication of the two following aspects: increased cutting concentration contributes to increased PV and it does not affect YP of the designed fluids significantly. This statement is as well supported by the results of the viscosity measurements presented in Table 15. For these four mentioned freshwater-based spud muds, YP calculated based on the Herschel Bulkley model, τ_0 , was exactly the same equal to 3.07 Pa, while PV increased regularly for every increase in cutting concentration. This trend is visually shown in Figure 67. Similarly to the yield stress the 10s gel strength values were not affected by increasing cuttings concentration either as these values were approximately constant and equal to either 8 or 9 for these four fluids.

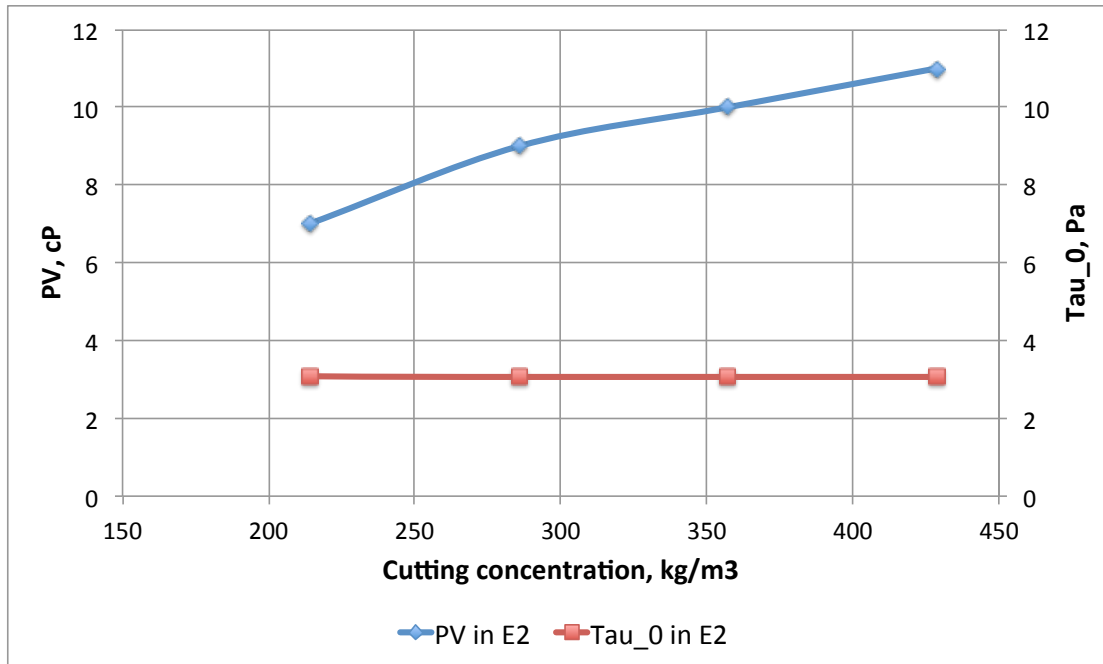


Figure 67. PV and τ_0 variation with the increasing cuttings concentration for the freshwater-based spud muds

When cutting concentration was increased in the similar SW based fluids identical effect on the rheological properties was observed in experiment E4 meaning that PV increased with increasing cutting concentration. Here the identical SW based muds were mixed using the same xanthan concentration equal to 1.2 g per 350 ml SW. The cutting concentration was equal to 75/100/125/150 g per 350 ml SW. These fluids are referred to as C75 X1.2 SW, C100 X1.2 SW, C125 X1.2 SW and C150 X1.2 SW, where the number after “C” corresponds to the cutting concentration. The effect of cutting concentration on these SW based muds can be studied when plotting the corresponding viscosity curves in one diagram as shown in Figure 68. The results of rheological measurements of these fluids were given in Table 17 and Table 18. The curves become more divergent at higher shear rates in Figure 68 indicating greater PV values with increasing cutting concentration. Here PV increased from 8 cP to 12 cP with increasing cuttings concentration. A minor increase in the Herschel Bulkley YP and gel strengths with increasing cutting concentration of the mentioned fluids was registered during testing (Table 17 and Table 18). However, these changes were in order of 1 Pa and might have occurred due to the uncertainty in the measurements.

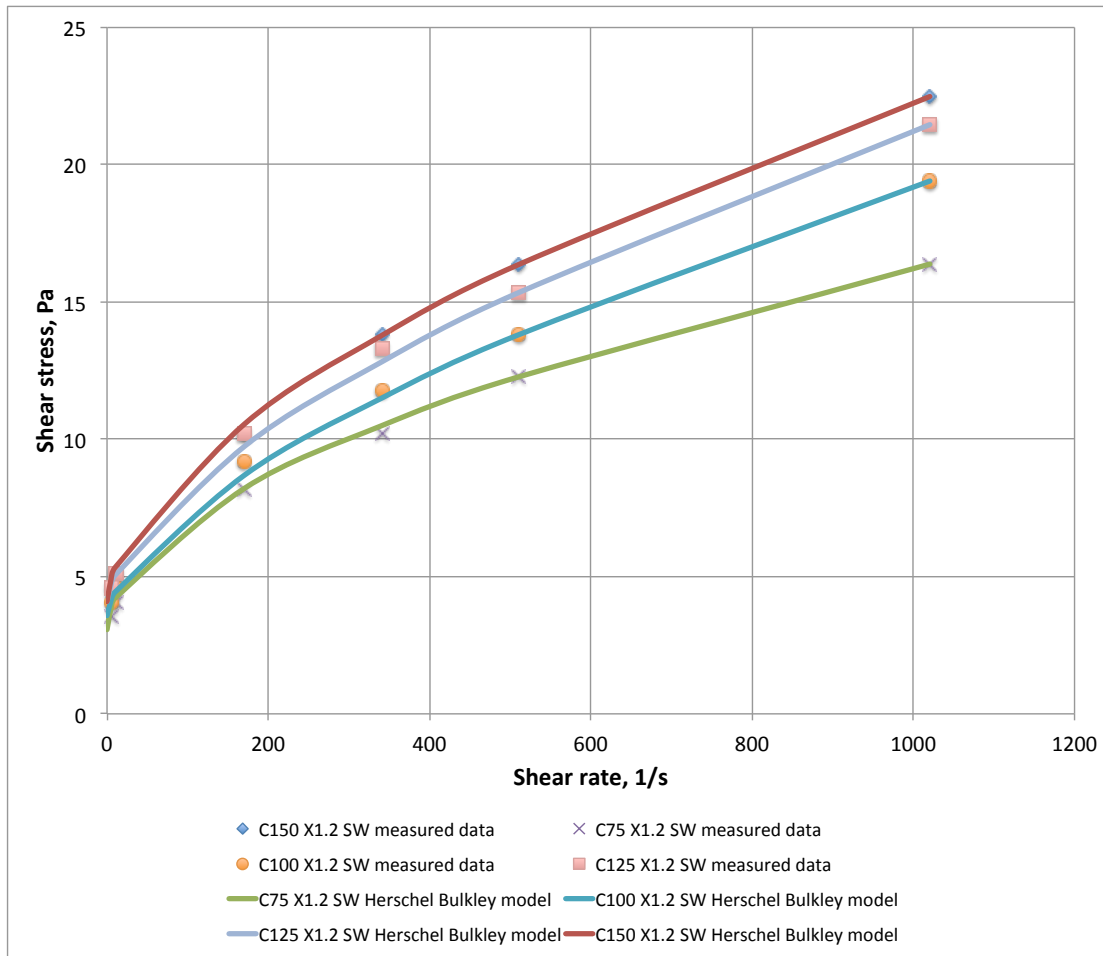


Figure 68. The effect of the increasing cuttings concentration on the rheological properties of the SW based spud muds containing cuttings and xanthan with the concentration equal to 1.2 g per 350 ml water

The presented statements and discussion support the conclusions made based on the results of simple water-cuttings slurry testing (E1) and the aging experiment (E3) and discussed in Section 9.3.1. Due to their neutral nature, high chloride content and low amount of active clay minerals these drill cuttings were incapable of contributing to significantly better rheological properties. Increased cutting concentration led only to a decent increase in PV, while YP remained unchanged.

Increase of cutting concentration from 75 g per 350 ml water to 150 g per 350 ml water resulted in a higher power law index n and the reduction of K value approximately by the factor of 2. This can be seen when comparing n and K values of C75 X1.2 fluid with C100 X1.2, C125 X1.2 and C150 X1.2 muds shown in Table 15. Here the n value increased from 0.52 to approximately 0.65, while the K value reduced from 0.31 Pa·s ^{n} to approximately 0.15 Pa·s ^{n} with increasing cutting concentration. This trend was observable with the identical SW based fluids as well (Table 17 and Table 18). Based on these observations it can be concluded that higher drill cutting concentration is undesirable from several points of view. Higher

cutting content in fluids would lead to higher PV, while YP will remain unchanged. Moreover, increased cutting content results in worse shear-thinning properties as n values increased with increasing concentration. In addition to the worsened low shear rate viscosity, as K values of the fluids reduced with increasing cutting concentration, this would lead to unnecessary high fluid density.

Barite was added to one of the designed SW based drilling fluid compositions to increase its density to 1.30 SG. This fluid contained initially 150 g of cuttings and 2.8 g of xanthan gum per 700 ml SW and is referred as C75 X1.4 SW. The resulting barite containing fluid is referred to as C75 X1.4 B SW. When 177.6 g of barite were added, the PV of the fluid increased by 50% from 8 cP to 12 cP due to the higher solid content (Table 17 and Table 18). However, other parameters as τ_0 , n and K values remained approximately unchanged. YP calculated based on the Herschel Bulkley model increased from 4.55 Pa to 5.11 Pa with addition of barite. Gel strengths after 10 seconds increased indistinguishably from 11 to 12. Slight increase in the YP and the gel strength might have occurred due to the significantly increased solid content as well, which made the system more dense, hence promoting closer interaction between the particles (Skjeggstad, 1989). Thus, as it was expected, addition of barite to the drilling fluid resulted in a significant increase of PV, while other parameters remained approximately unchanged. This observation is in line with the similar conclusion made regarding the cutting concentration as well. s

Moreover, one more fluid composition containing barite was prepared during the experiments. However, here the initial cutting content was slightly higher and equal to 200 g per 700 ml SW, while the amount of xanthan was still equal to 2.8 g per 700 ml SW. Therefore, less barite was required to reach the density of 1.30 SG and 136.1 g of barite were added. The resulting fluid is referred to as C100 X1.4 B SW. As shown in Table 18, the two barite containing fluids had quite similar viscometer readings and hence calculated properties. Based on this observation it can be concluded that fluid density can be increased both by using treated drill cuttings as well as barite. However, when large increase of density is required it is recommended to use barite due to its higher density (4.2 SG while cuttings had 2.5 SG). Otherwise, this would result in a significant increase of PV due to the higher solid content and more severe foaming due to the higher amount of surfactants, which are present in treated cuttings. Comparison of the viscosity curves of barite free C75 X1.4 SW and barite containing C75 X1.4 B SW, C100 X1.4 B SW fluids is shown in Figure 69.

When 2 g of CMC Lo-Vis were added to the C75 X1.4 SW drilling fluid as a fluid loss agent, PV of the fluid increased as well, while other rheological parameters remained approximately unchanged. This can be seen when comparing the respective results in Table 17 and Table 18. The new CMC Lo-Vis containing spud mud is referred as C75 X 1.4 CMC LV SW. The comparison of the viscosity curves of these fluids is shown in Figure 70.

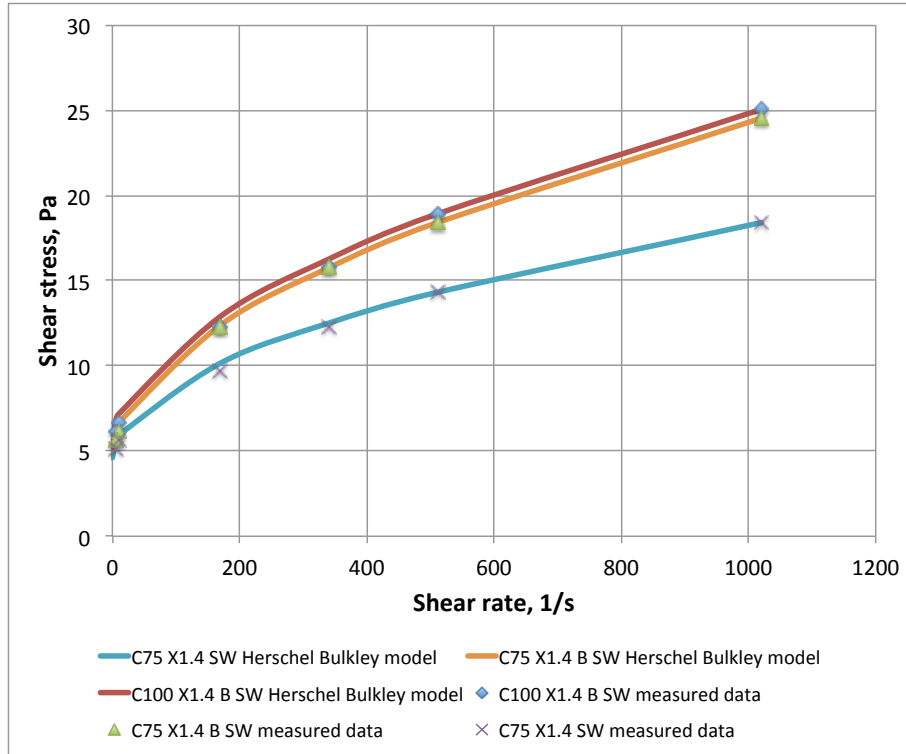


Figure 69. The effect of barite on the rheological properties of spud mud C75 X1.4 SW containing cuttings and xanthan

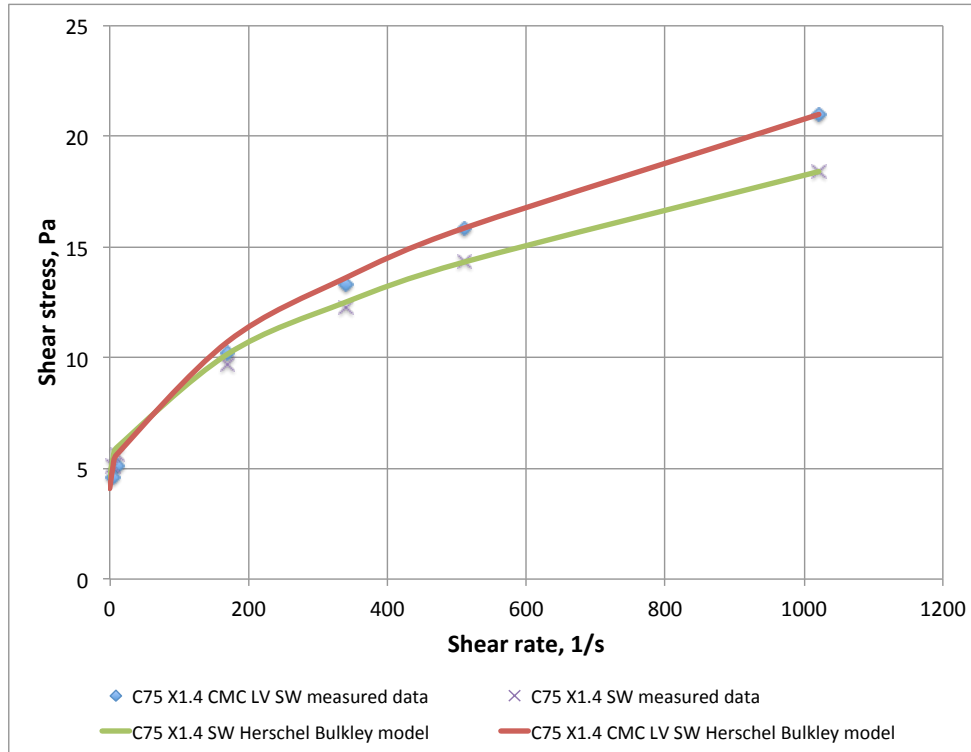


Figure 70. The effect of CMC Lo-Vis fluid loss agent on the rheological properties of spud mud C75 X1.4 SW containing cuttings and xanthan

9.3.5 Effect of Temperature on Rheological Properties

The temperature effect on the rheological properties of the designed SW based fluids was studied by conducting the same Fann viscometer measurements at 50°C using a thermo cup in the experiment with stable SW based fluids (E4). This analysis was of interest since temperature increases as drilling continues deeper into the ground. At the depth of 1500 m (relatively to seabed) the temperature in the well may become 49°C high, assuming that the average geothermal gradient is equal to 3°C per 100 m and the seabed temperature in the North Sea is equal to 4°C. Even though spud muds are used for drilling of relatively shallow top holes, in some cases a 26" hole can reach these depths. Even though during drilling the mud is cooled due to a continuous pumping process, during pumping breaks the temperature of the mud will approach the geothermal gradient in the well. The effect of temperature on the rheological properties of the fluid can be studied by comparing the two viscosity curves of the same fluid (C75 X1.4 SW) measured at 20°C and 50°C as shown in Figure 71. The comparison of the viscosity curves at two different temperatures of other designed spud muds would look similarly as the diagram in Figure 71. Due to this the diagram is provided for only one fluid here. Green line in Figure 71 corresponds to Fann readings at a lower temperature, and thus the fluid had a higher PV and a slightly higher YP value.

The overall observation is that the increase in temperature resulted in a slight decrease of PV for 8 of the 10 designed fluids. On the other hand, very minor changes were observed in Bingham model YP and τ_0 values. Though reductions of the Bingham model YP values were observed in 8 of the 10 designed fluids the magnitudes of these changes were really low in the order of 10% of the initial values.

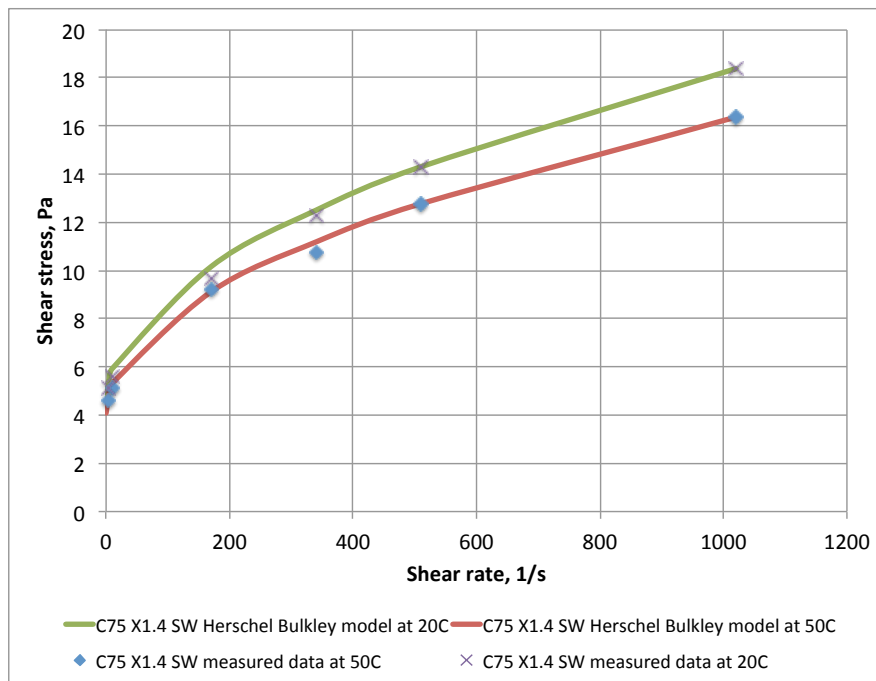


Figure 71. The temperature effect on the rheological properties of the SW based spud mud C75 X1.4 SW containing cuttings and xanthan (at 20°C and 50°C)

The changes in the Herschel Bulkley model YP , τ_0 , with the temperature were of a minor magnitude. The power law and consistency indexes of the designed fluids changed in an uneven manner. For some of the fluids these values reduced, while for other compositions an increase was observed. In some cases these values were kept approximately unchanged. Given that these alterations were of a smaller magnitude and that the models are not perfect, these variations may be neglected in a bigger picture. This means that n and K values may be regarded as unaffected by temperature changes. On the other hand, the most important observation can be made about the AV of the fluids. A reduction in the order of 1 to 3.5 cP was observed during fluid testing at the elevated temperature, which is in line with expectations that liquid viscosity should reduce at higher temperatures.

9.4 Economical Aspects of the New Spud Mud Concept

Economical aspects of the introduced concept of spud mud with application of treated drill cuttings is studied in this chapter as the economical side of any development in the oil industry is often considered as the most important one. It is important to emphasize that approximate costs of the designed drilling fluids will be studied here. When dealing with oil contaminated drill cuttings operators have three possibilities for waste handling: treatment and deposition in an onshore facility, re-injection into wells drilled for this purpose and TCC technology introduced in Section 5.2 (Saasen et al., 2014). The economical and other sides of these three options are beyond the scope of this work. However, if an operator selects the TCC to treat oil-contaminated cuttings, the recovered treated cutting material will cost nothing for the operator. Therefore, only the costs of other additives as polymers and barite were included in the calculations. These calculations are approximate and not exact, just to provide an insight into the economical aspects of this development and are based on the assumed market prices given in Table 24.

Table 24. The assumed market prices for the materials used in laboratory testing

Material	Price, NOK/kg
Bentonite	2.8
Barite	1.7
Xanthan gum	40
CMC	30

Since SW based drilling fluids are the most relevant for an offshore application these have been considered for price estimation. The fluids with the lowest and the highest polymer concentrations (1 g and 1.6 g per 350 ml SW) were analyzed to provide a price range depending on polymer concentration. Spud muds containing CMC Lo-Vis and barite were studied as well as these fluids were the most complex ones. Prices of standard bentonite reference fluids used in the experiments were estimated for comparison as well. It is important to emphasize that prices are given in NOK per 1 m³ of prepared spud mud. For example, mixing of C75 X1.0 SW drilling fluid in 1 m³ of SW would result in a total volume of 1.094 m³. For this reason the total price of the components for this mud was divided by 1.094 to obtain the price

of 1 m³ of this spud mud. The estimated prices shown in Table 25 were calculated using three significant numbers.

Comparison of the prices of the C75 X1.6 SW spud mud with the highest cutting concentration and the conventional bentonite mud (B REF) shows that the introduced spud mud has a price in the same range and may as well become cheaper under some circumstances. However, as it was stated in Section 8.4 C75 X1.6 SW fluid had higher filtrate loss than the B REF fluid.

Table 25. The approximate prices for the drilling fluids designed in the experimental part

C75 X1.0SW, NOK/m ³ mud	C75 X1.6SW, NOK/m ³ mud	C75 X1.4 B SW, NOK/m ³ mud	C100 X1.4 B SW, NOK/m ³ mud	C75 X1.4 CMC LV SW, NOK/m ³ mud	B REF, NOK/m ³ mud	B CMC REF, NOK/m ³ mud
105	167	512	421	224	190	142

When drilling through permeable formations it would be necessary to add fluid loss agents to the designed spud mud. In this case, the price would become higher than that of the standard bentonite mud as the C75 X1.4 CMC LV SW mud containing fluid loss agent costs 224 NOK/m³ mud. On the other hand, much higher amounts of barite would be required to increase the density of the B REF mud up to 1.30 SG. According to theoretical calculations 388 kg/m³ of barite would be needed for this purpose. This means that the B REF fluid with a specific density equal to 1.30 SG would cost approximately 766 NOK/m³ mud. This value is significantly higher than the estimated prices of C75 X1.4 B SW and C100 X1.4 B SW barite containing spud muds, which have the same density. Thus, based on this approximate economical analysis the designed drilling fluids have comparable prices with the standard bentonite spud muds and for some applications may even become cheaper under given circumstances.

10 Conclusion

The possibility of application of thermo-mechanically treated drill cuttings as an alternative to bentonite in spud muds was investigated by extensive laboratory testing. The results of the performed experiments demonstrated that:

- This batch of treated drill cuttings was incapable of yielding required physical and rheological properties when simply mixed with fresh water or SW
- Poor rheological properties of water-cutting slurries were observed due to the high chloride content of the mixture resulting when cuttings are added to water
- When drill cuttings were used simply as a replacement for bentonite in adequate concentrations desired rheological properties were not achieved. This happened due to the rather low active clay content of the treated cuttings (approximately 10% of total drill cutting mass)
- Significant foaming occurred when cuttings were mixed with water due to the rests of surfactants present in the cutting material. Two types of antifoam were tested to combat this problem and the Delfoam V14 by MI-Swaco was successful for this application
- This batch of treated cutting material was incapable of hydration even at long time intervals of 10 days, which allows SW to be used as the base fluid
- Only xanthan gum (unlike CMC and PAC polymers) allowed design of a spud mud with rheological properties similar to that of a standard bentonite mud
- 2.86 kg/m³ of CMC Low-Vis can be sufficient under given circumstances to reduce API filtrate loss to 10 ml
- The designed stable drilling fluid compositions in E4 were as well capable of suspending heavy barite particles, which can be used as a weighting agent
- The higher temperature equal to 50°C affected mostly PV and AV of the fluids.

Overall, the stable composition of spud mud fluid was developed as the result of this experimental work. These drilling fluids consisted mainly of treated drill cuttings, xanthan gum and SW or freshwater used as the base fluid. Some spud muds contained barite as a weighting agent and CMC Lo-Vis a filter loss agent.

Economical aspects of the proposed design were considered as well. It was revealed that economical benefits depend on the specific conditions. However, the designed spud muds may cost significantly less than the standard bentonite mud when barite is added to increase the fluid density.

The future testing of the designed spud muds at onshore small-scale facilities are of interest to evaluate whether the designed fluids can be applied on a field scale as well.

11 References

- Aadnoy, B.S. 2010. *Modern Well Design*, second edition. Chapter 2, Rock Mechanics, pp. 9-14 and Chapter 5, Casing Design, p. 136. Leiden, The Netherlands: CRC Press/Balkena
- Alder H.L. and Roessler, E.B. 1977. *Introduction to Probability and Statistics*, sixth edition. Chapter 12, Regression and Correlation p. 230. USA: W.H. Freeman and Company
- API RP 13B-1, Recommended Practice Standard Procedure for Field Testing Water-Based Drilling Fluids, first edition. 1990. Washington, DC: API.
- ASME. 2005. *Drilling Fluids Processing*, Chapter 5, Tank Arrangement, p. 94. Oxford, UK: Elsevier.
- Azar, J.J. and Robello Samuel, G. 2007. *Drilling Engineering*, Chapter 2, Drilling Fluids, pp. 46 and 70. Tulsa, Oklahoma: PennWell Corporation.
- Boggs, S.Jr. 2009. *Petrology of Sedimentary Rocks*, first edition. Chapter 1 Origin, classification, and occurrence of sedimentary rocks, pp. 3-8 and Chapter 6 Mudstones and Shales, pp. 194-220. New York: Cambridge University Press.
- Bourgoyne, A.T., Chenevert, M.E. and Millhein, K.K. 1986. *Applied Drilling Engineering*, Vol. 2, 41-42. Richardson, Texas: Textbook Series, SPE.
- Burrafato, G. and Miano, F. 1993. Determination of the Cation Exchange Capacity of Clays by Surface Tension Measurements. *Clay Minerals* **28** (3): 475-481.
- Caenn, R., Darley, H.C.H. and Gray, G.R. 2011. *Composition and Properties of Drilling and Completion Fluids*, 6th edition. Chapter 1, Introduction to Drilling Fluids, pp. 1-26; Chapter 3, Equipment and Procedures for Evaluating Drilling Fluid Performance, pp. 107-111; Chapter 4, Clay Mineralogy and the Colloid Chemistry of Drilling Fluids, pp. 136-168; Chapter 5, The Rheology of Drilling Fluids, pp. 180-182, 243, Chapter 11; Drilling Fluid Components, pp. 537-546. Gulf Professional Publishing, Waltham.
- Chilingarian, G.V. and Vorabutr, P. 1983. *Drilling and Drilling Fluids*. Chapter 6, Drilling Fluid Additives Other Than Clays, p. 264. Amsterdam: Elsevier.
- Datta, B.K., Saasen, A., Hafenbrädl, F.O., et al. 2007. Norwegians Develop New Method to Measure Shaker Screen Performance. *Oil and Gas J.* Nov. 19 2007, pp. 37-46.
- Framnes, E. 1992. *Plattformtyper og Boreutstyr*. Vett & Viten A/S. Chapter 3, p. 47.

- Greenwood, R. and Kendall, K. 1999. Selection of Suitable Dispersants for Aqueous Suspensions of Zirconia and Titania Powders using Acoustophoresis. *Journal of the European Ceramic Society* **19** (4): 479-488. DOI: [http://dx.doi.org/10.1016/S0955-2219\(98\)00208-8](http://dx.doi.org/10.1016/S0955-2219(98)00208-8)
- Grim, R.E. 1968. *Clay Mineralogy*, 2nd edition. Appendix Chemical Analysis, pp. 575-582. McGraw-Hill Book Company. 596.
- Hanaor, D., Michelazzi, M., Leonelli, C., et al. 2012. The Effects of Carboxylic Acids on the Aqueous Dispersion and Electrophoretic Deposition of ZrO₂. *Journal of the European Ceramic Society* **32** (1): 235-244. DOI: <http://dx.doi.org/10.1016/j.jeurceramsoc.2011.08.015>
- Hendricks, S.B. and Jefferson, M.E. 1938. Structure of Kaolin and Talc-Pyrophyllite Hydrates and Their Bearing on Water Sorption of the Clays. *Am. Mineral.* **23**: pp. 863-875.
- Hendricks, S.B., Nelson, R.A. and Alexander, L.T. 1940. Hydration Mechanism of the Clay Mineral Montmorillonite Saturated with Various Cations. *Journal of the American Chemical Society* **62**: pp. 1457-1464
- Horiba. 2012. A Guidebook to Particle Size Analysis. https://www.horiba.com/fileadmin/uploads/Scientific/eMag/PSA/Guidebook/pdf/PSA_Guidebook.pdf (downloaded 11 March, 2014)
- Huang, L., Yu, M., Miska, S.Z. et al. 2011. Modeling Chemically Induced Pore Pressure Alterations in Near Wellbore Region of Shale Formations. Paper SPE 149415 presented at the SPE Eastern Regional Meeting, Columbus, Ohio, 1st October. <http://dx.doi.org/10.2118/149415-MS>
- Jones, T.G.J., Hughes, T.L. and Tomkins, P. 1989. The Ion Content and Mineralogy of a North Sea Cretaceous Shale Formation. *Clay Minerals* **24**: 393-410. DOI: <http://dx.doi.org/10.1180/claymin.1989.024.2.15>
- ISO 13320:2009, Particle Size Analysis – Laser Diffraction Methods. 2009.
- IPT, Institute of Petroleum Technology. 2012. "Øvinger i Bore- og Brønnvæsker" (compendium in the undergraduate drilling fluid course). University of Stavanger.
- Khodja, M., Khodja-Saber, M., Canselier, J.P. et al. 2012. Drilling Fluid Technology: Performances and Environmental Considerations.
- Kirkness, A. and Garrick, D. 2008. Treatment of Nonaqueous-Fluid-Contaminated Drill Cuttings – Raising of Environmental and Safety Standards. Paper SPE 112727 presented at the IADC/SPE Drilling Conference, Orlando, Florida, 4-6 March. DOI: <http://dx.doi.org/10.2118/112727-MS>

- Lovdata. 2010. *Activity Regulations (Forskrift om utføring av aktiviteter i petroleumsvirksomheten)*, http://lovdata.no/dokument/SF/forskrift/2010-04-29-613?q=aktivitetsforskrift* (accessed 25 January, 2014)
- MI-Swaco. 2010. *Data Sheet, Bentonite OCMA*.
https://app.econline.com/documents/msds/285_2376860.pdf (accessed 1 March, 2014)
- MI-Swaco. 2004. *Product Sheet, Duo-Vis Plus NS*.
http://www.slb.com/~media/Files/miswaco/product_sheets/duo-vis_plus_ns.ashx (accessed 1 March, 2014)
- Murray, A.J., Kapila, M., Ferrari G., et al. 2008. Friction-Based Thermal Desorption Technology: Kashagan Development Project Meets Environmental Compliance in Drill-Cuttings Treatment and Disposal. Paper SPE 116169 presented at the SPE Annual Technical Conference and Exhibition, Denver, Colorado, 21-24 September. DOI: <http://dx.doi.org/10.2118/116169-MS>
- Norrish, K. 1954. The Swelling of Montmorillonite. *Discussions of the Faraday Society* **18**: pp. 120-134.
- Prothero, D.R. and Schwab, F. 2004. *Sedimentary Geology: An Introduction to Sedimentary Rocks and Stratigraphy*, second edition. Chapter 1, Sedimentary Processes and Products, pp. 2-16 and Chapter 6 Mudrocks, pp. 99-109. New York: W.H Freeman and Company.
- Ratnayake, C., Biplab, K.D., Saasen, A., et al. 2008. Prediction of Pressure Drop at the Entry Section from Top Discharge Blow Tank in a Pneumatic Conveying System, *Particulate Science and Technology* **26**: 451-459. DOI: <http://dx.doi.org/10.1080/02726350802367639>
- Saasen, A., Jødestøl, K., Furuholt E., et al. 2014. CO₂ and NO_x Emissions from Cuttings Handling Operations. Paper SPE 169216 presented at the SPE Bergen One Day Seminar, Bergen, Norway, 2nd April.
- Schlumberger Oilfield Glossary, <http://www.glossary.oilfield.slb.com/>, (accessed 22 January 2014)
- Shaw, D.B. and Weaver, C.E. 1965. The Mineralogical Composition of Shales. *Journal of Sedimentary Petrology* **35** (1): 213-222.
DOI: <http://dx.doi.org/10.1306/74D71221-2B21-11D7-8648000102C1865D>
- Skjeggstad, O. 1989. *Boreslamteknologi*. Alma Mater Forlag AS. Chapter 1-6, 7.6, 9.2, 10 and 13.5.
- Statoil. 2010. *Activity Program, Drilling, Well NO 6608/10-K-2 H&AH*.

- Stojanovic, Z. and Markovic, S. 2012. Determination of Particle Size Distributions by Laser Diffraction.
- Sympatec. 2014. *HELOS Particle Size Analysis with Laser Diffraction*.
<https://www.sympatec.com/EN/LaserDiffraction/HELOS.html> (accessed March 11, 2014)
- The Norwegian Oil and Gas Association. Recommended Guidelines for Waste Management in the Offshore Industry, Revision 2. 2004. Sandnes, Norway: Norwegian Oil and Gas Association.
- Time, R.W. 2009. Two-Phase Flow in Pipelines. Course Compendium with Matlab Examples and Problems. Department of Petroleum Engineering, University of Stavanger.
- Torbjørnsen, K. 1994. *Borevæsketeknologi*. Vett&Viten. Chapter 1, pp. 14-29.
- TWMA. 2012. *Data Sheet, TWMA Tørrstoff*.
- Wilkinson, M., Haszeldine, R.S. and Fallick, A.E. 2006. Jurassic and Cretaceous Clays of the Northern and Central North Sea Hydrocarbon Reservoirs Reviewed. *Clay Minerals* **41**: 151-186. DOI:
<http://dx.doi.org/10.1180/0009855064110197>
- Yaalon, D.H. 1961. Mineral Composition of the Average Shale. *Clay Minerals* **5**: 31-36. DOI: <http://dx.doi.org/10.1180/claymin.1962.5.27.05>
- Zhao, L.A., Jin, Q.E., Long, A.H., et al. 1992. The Spectrophotometric Determination for Cation Exchange Capacity of Clay. Paper SPE 25303.

Appendix A. Paper Accepted for the Nordic Rheology Conference

This Appendix presents the paper, which has been written based on this master thesis work and accepted for the presentation at the Nordic Rheology Conference to be held in Reykjavik, Iceland on the 12-14 August, 2014.

Application of Thermo-Mechanically Treated Drill Cuttings as an Alternative to Bentonite in Spud Muds

Farid Taghiyev¹, Arild Saasen^{1,2} and Helge Hodne¹

¹ University of Stavanger, Stavanger, Norway

² Det Norske Oljeselskap AS, Oslo, Norway

ABSTRACT

The possibility of applying thermo-mechanically treated drill cuttings as a replacement for bentonite in spud muds was investigated by carrying out an extended laboratory study. A total number of 28 drilling fluid compositions, including two standard reference spud mud fluids, were prepared and tested in accordance with the API 13B-1 practices. As a result, stable drilling fluid compositions with the application of treated drilling cuttings were developed. The designed muds had satisfactory fluid properties comparable to that of drilling fluids conventionally used in the industry.

INTRODUCTION

Drilling fluids play a central role in the drilling of exploration and development wells as the success of the project and its cost depends significantly on the type of fluids selected¹. Moreover, drilling fluids perform a number of tasks, which actually enable the drilling process. Providing primary pressure control in the well, performing cuttings transport to the surface, cooling and lubricating the bit are just some examples of the drilling fluid functions.

Spud mud is a concept commonly used in the industry to describe a drilling fluid used to drill top sections of the wells. These fluids should possess good rheological properties to compensate for low fluid

velocities due to large flow areas. Today spud muds are prepared offshore by mixing pre-hydrated bentonite with seawater. Bentonite (mainly smectite mineral) is often the only additive in these fluids and acts as a viscosifier and filter loss agent. In some cases a native mud can be used instead of a bentonite mud. In these cases, fresh water is used to drill the top sections and the required properties are achieved while drilling. This happens because 75% of the drilled formations are shales², which may contain smectite that viscosify the fluid. Therefore, it was of interest to investigate the possibility of preparing native mud at the installation by mixing treated drill cuttings with water³. This application would as well turn drill cuttings, what is today considered as waste into a recycled material.

THERMO-MECHANICAL CUTTINGS CLEANING TECHNIQUE

According to the Norwegian Regulations oil contaminated drill cuttings cannot be discharged offshore unless the oil content of the cuttings is less than 10 g of oil per kilogram of dry mass⁴. Due to these regulations drill cuttings can either be treated and deposited onshore in a filling facility, re-injected into wells drilled for this purpose or treated using a thermo-mechanical cuttings cleaner (TCC)⁵. TCC is a technology, which has already been successfully field-tested on the UK

Continental Shelf⁶. The basic principle of this technology is indirect thermal sorption⁷. Here drill cuttings are fed into a series of rotary mills, where significant amounts of heat are released due to the intense friction between the cuttings and the mill. This heat is high enough to evaporate the water and oil phases, which are recovered in a condenser section. Moreover, cleaned cutting material is produced as a result of this process. Material recovered after a treatment in a TCC was used in this work.

EXPERIMENTS

Sample preparation

During the laboratory research 28 different fluid compositions were mixed. The materials used in the experiments include: freshwater, artificial seawater (SW)³, thermo-mechanically treated drill cuttings, bentonite, polyanionic cellulose (PAC), carboxymethyl cellulose (CMC) both Hi-Vis and Lo-Vis, xanthan gum and barite.

The prepared samples also include two commonly used reference fluids: a bentonite spud mud (B REF) and a bentonite/CMC mud (B CMC REF). These compositions are shown in Table 1.

Table 1. Compositions of the reference fluids used during the experiments

Component	Sample	
	B REF	B CMC REF
Bentonite, g	25	10.5
CMC Hi-Vis, g	-	0.7
Na ₂ CO ₃ , g	-	0.7
Water, ml	350	

The prepared fluid compositions with drill cuttings can be divided into three groups: water-cuttings slurries, water-cuttings slurries and polymers (either CMC or PAC) and water-cuttings slurries and xanthan gum. In the names of the prepared fluids the letters represent a specific

component, while the following number reflects the concentration of this component in grams per 350 ml of water. In the following C stands for cuttings, X for xanthan, B for barite and CMC LV for CMC Lo-Vis. CMC and PAC abbreviations were used unchanged.

The simple freshwater-cuttings slurries prepared initially are summarized in Table 2.

Table 2. Compositions of simple water-cutting slurries

Component	Sample			
	C75	C100	C125	C150
Cuttings, g	75	100	125	150
Water, ml	350			

Initially CMC and PAC polymers were tested as stabilizing agents and fluid loss agents. Various amounts of CMC and PAC were added to the C75 slurry (Table 2). The compositions of the resulting fluids are shown in Table 3. As the obtained results using these polymers were unsatisfactory an additional study was carried out where xanthan gum was used instead of the CMC or PAC polymers. The xanthan containing muds are summarized in Table 4. Spud mud compositions presented in Table 4 were prepared both with fresh and SW as base fluids (C75 X1.4 B, C100 X1.4 B and C75 X1.4 CMC were prepared with SW only).

Most of the designed compositions were mixed using a standard Hamilton Mixer. The drill cuttings were slowly added to the water and mixed at a low speed for 12 minutes. Significant foaming of the fluids was observed. Ten drops of antifoam (Delfoam V14) were added and agitated manually with a spoon since mixer agitation resulted in a vortex drawing in more air.

In the cases where polymers were added as well, the drill cuttings were mixed for 10 minutes before adding polymers and mixing for 10 more minutes. Ten drops of antifoam were added after each mixing was commenced. At the later stages of the

Table 3. Compositions of the water-cuttings slurries with either CMC or PAC polymers

Component	Sample				
	C75 CMC0.7	C75 CMC1.0	C75 CMC1.3	C75 CMC1.6	C75 PAC1.0
Cuttings, g	75	75	75	75	75
CMC Hi-Vis, g	0.7	1.0	1.3	1.6	-
PAC, g	-	-	-	-	1.0
Na ₂ CO ₃ , g	0.7	0.7	0.7	0.7	-
Water, ml	350				

Table 4. Compositions of the water-cuttings slurries with xanthan gum polymer

Component	Sample									
	C75 X1.0	C75 X1.2	C75 X1.4	C75 X1.6	C100 X1.2	C125 X1.2	C150 X1.2	C75 X1.4 B	C100 X1.4 B	C75 X1.4 CMC
Cuttings, g	150	150	150	150	200	250	300	150	200	150
Xanthan, g	2.00	2.40	2.80	3.20	2.40	2.40	2.40	2.80	2.80	2.80
CMC LV, g	-	-	-	-	-	-	-	-	-	2.00
Barite, g	-	-	-	-	-	-	-	178	136	-
Water, ml	700									

experiments larger volumes were required and the fluids were mixed using a Silverson L4RT-A mixer.

Testing procedures

The testing of the prepared fluid compositions was carried out in accordance with the API 13B-1 recommended practices⁸. Rheological measurements were carried out using an automated Fann viscometer.

RESULTS

The original study included full scale testing of the designed fluid compositions, including determination of rheological, physical and chemical properties³. In the following rheological results are presented and discussed in details (shear rates are given in RPM and shear stresses in lb/100 ft²).

Reference fluids

Two reference fluid compositions commonly used in the industry were mixed and tested prior to the start of the main

experiments. This was done to achieve an approximate guideline for what range of rheological properties that should be achieved. The obtained results are presented in Table 5.

The Herschel-Bulkley model (H-B) was used for the calculations as this model provided the best data matching for most of the fluids based on the linear correlation coefficient³. In the tables τ_0 is a fluid's yield stress, n stands for the power law index and K stands for the consistency index.

Table 5. Reference fluids results

Fann reading	B REF	B CMC REF
600	35	25
300	27	19
200	24	15
100	21	12
6	14	7
3	13	6
Gel 10s	14	10
H-B		
τ_0 , Pa	6.13	2.56
n	0.616	0.514
K, Pa·s ⁿ	0.164	0.290

Water-cuttings slurries

As shown in Table 6 the prepared water-cuttings slurries presented in Table 2 did not demonstrate the required rheological properties. Moreover, the mixtures had low gel strength and low shear rate viscosities regardless cuttings concentration. Even cuttings concentrations six times higher than that of bentonite in B REF did not yield desired results.

Table 6. Water-cuttings slurry results

Fann Reading	C75	C100	C125	C150
600	5	8	11	14
300	4	5	7	10
200	3	3	5	9
100	2	2	4	7
6	1	2	3	3
3	1	1	2	2
Gel 10s	0	1	2	3
H-B				
τ_0 , Pa	0.511	0	0.511	0.511
n	0.415	0.678	0.737	0.530
K, Pa·s ⁿ	0.115	0.0373	0.0310	0.168

These simple fluids were incapable of suspending large solid particles. Quick and severe separation of the solid phase was observed even after few minutes of static fluid condition.

A separate study was performed to evaluate whether the hydration time influenced the cuttings behaviour in water. Identical samples as presented in Table 2 were mixed and aged for 10 days at ambient conditions. Water and solid phases were totally separated and a soft “foam cap” floated on top. The slurries were re-mixed, however, no improvements in rheological properties were observed. The Fann viscometer measurements showed identical results as in Table 6. The material was incapable of hydrating even after a long enough exposure to fresh water.

Water-cuttings slurries and polymers

CMC Hi-Vis and PAC polymers were tested initially as stabilizing agents to obtain better low shear rate viscosity, gel strength and solid suspension. The obtained results are shown in Table 7. Viscosity curves are shown in Fig. 1. (H-B model assumption). However, addition of these polymers to the existing slurries only resulted in a partial improvement. As it can be seen from Table 7, shear stresses at high shear rate values increased significantly with increasing polymer concentration. On the other hand, low shear rate viscosity and gel strength remained unchanged. Moreover, τ_0 calculated using H-B model assumption, was equal to either 0.511 Pa or 0 Pa for the presented fluids, which is unacceptable. The designed fluids were still not capable of suspending heavy particles and large solid particles deposited quickly.

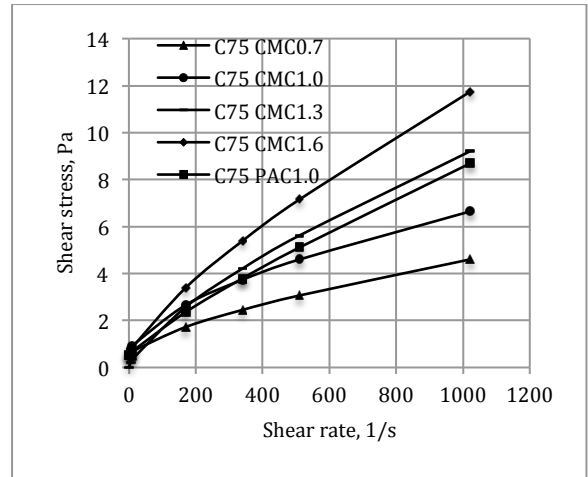


Figure 1. Viscosity curves of fluids presented in Table 7

The power law indexes, n and consistency indexes, K were as well unsatisfactory. High n values indicate poor shear thinning qualities of the fluid, which is as well observable in Fig. 1 as the curves are quite linear. Furthermore, particularly low K values indicate poor low shear rate viscosity and solid suspension ability. Based on the presented results it was concluded that CMC and PAC polymers were not suitable for this

Table 7. Results of the water-cuttings slurries with either CMC or PAC polymers

Fann Reading	C75 CMC0.7	C75 CMC1.0	C75 CMC1.3	C75 CMC1.6	C75 PAC1.0
600	9	13	18	23	17
300	6	9	11	14	10
200	4	6	8	11	8
100	3	3	5	6	4
6	1	1	2	1	1
3	1	1	1	1	1
Gel 10s	1	1	1	1	1
H-B					
τ_0 , Pa	0.511	0.511	0	0.511	0.511
n	0.678	0.585	0.710	0.759	0.830
K, Pa·s ⁿ	0.0374	0.107	0.0671	0.0586	0.0260

application.

Water-cuttings slurries and xanthan gum

Xanthan gum was tested as a stabilizing agent for the designed water-cuttings slurries (Table 2). Freshwater based slurries with xanthan polymers demonstrated improved viscous properties and similar compositions were tested using SW as a base fluid (Table 4). Since the obtained results were quite similar regardless of the base fluid type, and SW based fluids are more relevant for an offshore application, only these SW based fluid results are presented in Table 8.

Spud mud compositions with xanthan gum as a stabilizing agent demonstrated satisfactory viscous properties and significant improvements were observed compared to the simple water-cuttings slurries and CMC/PAC based slurries. This can be seen when comparing fluids with equal concentrations of xanthan (C75 X1.0), CMC (C75 CMC1.0) and PAC (C75 PAC 1.0) in Table 7 and Table 8. It is important to emphasize that xanthan based muds were able to suspend large cuttings and heavy barite particles and no segregation was documented. Furthermore, low shear rate viscosity increased significantly by the addition of xanthan. Here the τ_0 value increased by the factor of 5. Increasing

xanthan gum concentration resulted in higher gel strengths as well. Even though the fluids developed quite strong gel structures with time, these were easy to break. According to the results presented in Table 8, xanthan based spud muds had significantly better shear thinning properties, as the calculated n values were lower than those in Table 7 when comparing the compositions with equal polymer concentrations. Moreover, K values increased by the factor of several magnitudes, which is in line with the observations made regarding gel strength and low shear rate viscosities.

Another important observation can be made when comparing the results in Table 8 and the reference fluid testing results in Table 5. C75 X1.4 fluid demonstrated quite similar behaviour to the B REF fluid as the main rheological properties were of a comparable range. Moreover, C75 X1.0 spud mud demonstrated approximately the same viscous qualities as B CMC REF in Table 5. So, τ_0 values of both fluids had equal values, while n and K values were approximately the same. These observations indicate, that the xanthan gum polymer is well suited for this application and the properties of the fluid can be adjusted by varying xanthan gum and cuttings' concentration.

Table 8. Results of the spud muds with xanthan gum polymer

Fann Reading	C75 X1.0	C75 X1.2	C75 X1.4	C75 X1.6	C100 X1.2	C125 X1.2	C150 X1.2	C75 X1.4B	C100 X1.4B	C75 X1.4 CMC
600	26	32	36	41	38	42	44	48	49	41
300	20	24	28	31	27	30	32	36	37	31
200	17	20	24	27	23	26	27	31	31	26
100	14	16	19	22	18	20	20	24	24	20
6	7	8	11	13	9	10	10	12	13	10
3	6	7	10	11.5	8	9	9	11	12	9
Gel 10s	7	8	11	12.5	9	10	10	12	12	11
Gel 10m	10	11	14	15	12	14	15	13	14	14
H-B										
τ_0 , Pa	2.56	3.066	4.60	5.11	3.58	4.09	4.09	5.11	5.62	4.09
n	0.485	0.530	0.507	0.562	0.632	0.628	0.585	0.547	0.547	0.521
K, Pa·s ⁿ	0.372	0.337	0.412	0.323	0.199	0.225	0.320	0.438	0.438	0.458

An aging test of the C75 X1.2 fluid was conducted as well to test the stability of the designed fluid. The mud was stored at ambient conditions for 10 days, re-mixed and tested by the Fann viscometer. The obtained results were exactly the same as the initial measurements meaning (Table 8) that the designed fluid was stable as well.

DISCUSSION

Performance of drill cuttings in water

As the results in Table 6 demonstrate simple replacement of bentonite with treated drill cuttings did not provide the desired results. Viscous properties were unsatisfactory with 10s gel strength values as low as 0. High chloride and Ca²⁺ content in the resulting mixtures and low amount of active clay minerals are considered the main reasons for this behaviour. Both chloride and Ca²⁺ are present in the cuttings material as it is recovered after drilling with oil-based mud, which contains these compounds. Standard chloride tests were carried out and the amount varied from 2400 mg/l to 4400 mg/l depending on the cuttings concentration³. Chloride content has important influence on the swelling of clay

minerals and high chloride amounts hinder osmotic swelling of Na⁺ montmorillonite, which accounts for 90% of total swelling. Skjeggstad⁹ mentions that bentonite should be pre-hydrated in water with chloride content less than 5000 mg/l. Although this value is higher than those measured in the experiments, keeping in mind that drill cuttings are not pure bentonite material, the existing chloride content could be sufficient to hinder the hydration. Furthermore, Skjeggstad emphasized that Ca²⁺ concentrations of the water used for pre-hydration should not exceed 200 mg/l since divalent ions can bind two clay crystals together and hinder hydration. Calcium tests were as well carried out on the designed fluids and Ca²⁺ content varied from 600 mg/l to 1360 mg/l depending on the cuttings concentrations³. Even at the lowest cuttings concentration the resulting value was 3 times higher than that stated by Skjeggstad. Yet another reason for poor hydration performance was the low amount of active clay minerals. Standard methylene blue tests⁸ were carried out to identify the active clay content. Approximately 10% of the total cuttings mass was comprised by active clay minerals based on these test results³

meaning that 10 times higher concentration of cuttings would be required to achieve similar fluid parameters to the B REF fluid. However, higher cuttings concentrations would result in undesired high fluid density and even higher chloride and calcium content leading to a closed loop situation.

Gel strength and yield stress of the fluid depend on the electrical interactions between particles⁹. This requires the presence of charged particles. Zeta potential measurements were carried out on cuttings particles using an AcoustoSizer II and the result was equal to -7.6 mV while that of bentonite particles was equal to -35 mV. High absolute zeta potential values result in stable suspensions, when at low values van der Waals forces start to dominate yielding particle deposition¹⁰. Thus, the relative neutrality of the cuttings particles can describe the quick solid settling observed in the experiments.

Effect of xanthan gum concentration

Xanthan gum was the only polymer among the selected types, which provided the required rheological properties. As it is seen from Table 8, τ_0 and gel strength values increased with increasing xanthan concentration for each spud mud composition. The comparison of viscosity curves is shown in Fig. 2.

As it can be seen from Fig. 2 increased polymer concentrations resulted in a shift in the viscosity curves towards higher shear stress values, meaning that gel strength and yield stress depend mainly on the xanthan concentration.

The B REF and the C75 X1.4 fluids have quite similar viscosity curves (Fig. 2) meaning that addition of xanthan gum can provide required properties to the water-cuttings slurries.

Effect of cuttings concentration

Effect of cuttings concentration on the rheological properties of stable fluids can be

studied by comparing respective parameters of the fluids in Table 8.

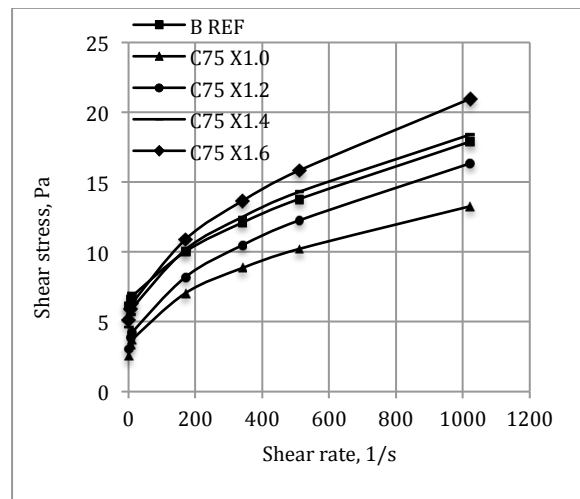


Figure 2. Effect of xanthan gum concentration

At low shear rate values, where electrical interaction between the particles dominates, very minor increase in shear stresses was observed. Thus, the τ_0 value and gel strengths were affected to a minor degree with increasing cuttings concentration. On the other hand, more severe increase in high shear rate viscosity was observed. Increased concentration of electrically neutral drill cuttings particles contributed to higher friction between the fluid components (solid particles and water molecule), hence leading to increased shear stress values. This observation was in line with expectations, as drill cuttings were not capable of altering low shear rate viscosity of the fluids when simply added to water. However, a slight increase in τ_0 values was registered due to the mass effect. Increased cuttings concentration resulted in more dense fluids, where particles interact closer with each other, thus causing higher τ_0 . This is in line with the description given by Skjeggstad⁹, where he mentions that τ_0 may slightly increase with increase solid content of the fluid.

Increased drill cuttings concentration had as well an undesired effect on n and K

values. This can be seen when comparing respective values of C75 X1.2 fluids with C100/125/150 X1.2 fluids. This resulted in increased n values, meaning that fluids became less shear thinning. Moreover, K values slightly reduced with increased cuttings concentration, yielding reduced low shear rate viscosity.

CONCLUSION

Performance of treated drill cuttings in water was investigated to study the possibility of using the material as a replacement of bentonite. The results of the experiments revealed that simple replacement of bentonite by cuttings did not yield desired rheological properties. High chloride and calcium ion content of the mixtures and low active clay content of the material were considered as the main reasons. Moreover, the material was as well incapable of hydrating even after long enough exposure to fresh water.

Stable drilling fluid compositions were, however, developed as the result of this experimental work. Xanthan gum polymers qualified as a stabilizing agent suitable for this application and modified water-cuttings slurries with xanthan gum had similar to the standard spud muds rheological properties. CMC and PAC polymers were, on the other hand, not suitable for this application.

REFERENCES

1. Caenn, R., Darley, H.C.H., Gray, G.R. (2011) "Composition and Properties of Drilling and Completion Fluids". Chapter 1, p.1. Gulf Professional Publishing, Waltham
2. Huang, L., Yu, M., Miska, S.Z. et al. (2011), "Modeling Chemically Induced Pore Pressure Alterations in Near Wellbore Region of Shale Formations". Paper SPE 149415 presented at the SPE Eastern Regional Meeting, Columbus, Ohio, 1st October.
3. Taghiyev, F. (2014), "Application of Thermo-Mechanically Treated Drill Cuttings as an Alternative to Bentonite in Spud Mud". Master thesis, University of Stavanger, Norway.
4. Lovdata (2010), "Activity Regulations", http://lovdata.no/dokument/SF/forskrift/2010-04-29-613?q=aktivitetsforskrift* (accessed 25 January, 2014)
5. Saasen, A., Jødestol, K., Furuholt, E. et al. (2014), "CO₂ and NO_x Emissions from Cuttings Handling Operations". Paper SPE 169216 presented at the SPE Bergen One Day Seminar, Bergen, Norway, 2nd April.
6. Kirkness, A. and Garrick, D. (2008), "Treatment of Nonaqueous-Fluid-Contaminated Drill Cuttings – Raising of Environmental and Safety Standards". Paper SPE 112727 presented at the IADC/SPE Drilling Conference, Orlando, Florida, 4-6 March.
7. Murray, A.J., Kapila, M., Ferrari, G. et al. (2008), "Friction-Based Thermal Desorption Technology: Kashagan Development Project Meets Environmental Compliance in Drill-Cuttings Treatment and Disposal". SPE Paper 116169 presented at the SPE ATCE, Denver, Colorado, 21-24 September.
8. American Petroleum Institute (1990), API RP 13B-1, "Recommended Practice Standard Procedure for Field Testing Water-Based Drilling Fluids", Washington DC: API.
9. Skjeggstad, O. (1989), "Drilling Fluid Technology (Boreslamteknologi)", pp. 33, 41, 43 and 45. Alma Mater Forlag AS.
10. Greenwood, R. and Kendall, K. (1999), "Selection of Suitable Dispersants of Aqueous Suspensions of Zirconia and Titania Powders using Acoustophoresis ", *J. of the European Ceramic Soc.*, **19**, 479-488.

Appendix B. Drilling Fluid Testing Procedures

The designed spud mud compositions were tested for physical and chemical properties in accordance with the API recommendations (API, 1990). Physical testing of drilling fluids included determination of density, viscosity, gel strength, filter loss and sand content.

Density

Fluid density was measured by a mud balance, which consisted of a cup and a counterbalance located on the opposite sites of the equipment to balance each other (Figure B-1). The mud entirely filled the designated cup, however, all mud rests left on the surface of the cup were wiped off to achieve exact results. The Halliburton mud balance was used in case of trapped air in the drilling fluid. Here the slurry in the mud cup was pressurized with a plunger to compress the air and significantly reduce its effect on the measured value.

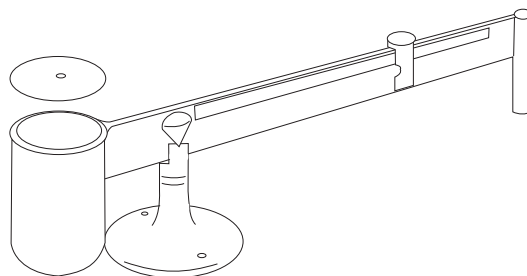


Figure B-1. Mud balance used for density determination (from IPT, 2012)

Viscosity and Gel Strength

The viscosity of the fluids was evaluated using direct-indicating viscometer in accordance with the API standard (API, 1990). Fann viscometer VG 35 was used to determine fluid's rheological properties. For the most stable compositions these properties were determined both at the ambient conditions using a standard cup and at 50°C using a thermo cup. The viscometer was calibrated based on the Bingham model so that PV and YP could be directly determined from measurements (Section 3.2.2).

Fann VG 35 measures shear stress in the fluid generated by the combination of static and rotating concentric cylinders. The rotor could rotate at 600, 300, 200, 100, 6 and 3 RPM thus generating different shear rates. The drilling fluid entrained between the cylinders acts as the transfer media, so the rotor can exert a force on the static cylinder. This force produces a torque on the inner cylinder, which rotates it and its movement is registered on the dial. This movement is used to determine the shear stress under different shear rates. The shear rate is measured in s^{-1} rather than in RPM (Section 3.2.2) and the conversion was obtained by multiplying the RPM value by 1.7023 (IPT, 2012). The shear stress was converted to Pa by multiplying the Fann viscometer reading by the factor of 0.511.

Gel strength was reported as 10 s gel and 10 min gel, which correspond to the gel strength after the fluid has been static for 10 seconds and 10 minutes respectively. This measurement was performed by a direct-indicating viscometer in accordance with the API procedures as well (API, 1990).

Filter Loss

This test was carried out to determine how much fluid could be lost into a permeable formation under static conditions during drilling and to evaluate filter cake properties. The test was performed using a standard API filter press, which operated at the ambient temperature and 100 ± 5 psi pressure. Filter loss was reported in ml of filtrate after 30 minutes.

Sand Content

According to API all particles larger than 74 microns in dimensions are classified as sand particles (API, 1990). Sand content in a drilling fluid was determined by means of 200-mesh sieve, measuring tube and a funnel (Figure B-2). The volume percent of the particles, which could not pass through the sieve, was determined directly by reading off the value on the measuring tube.

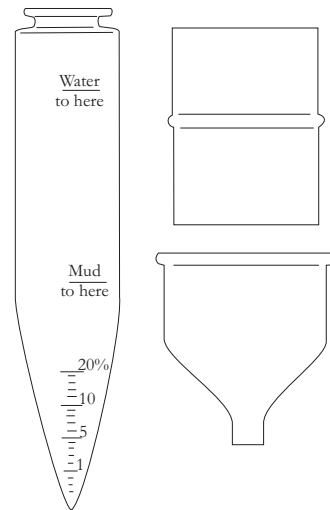


Figure B-2. The standard equipment for sand content test (from IPT, 2012)

Chemical testing of a drilling fluid included determination of approximate CEC value using MBT, pH value, chloride content, total hardness as calcium, Ca^{2+} ions concentration, Mg^{2+} ions concentration, filtrate alkalinity and lime content in mud. These tests were carried out to yield a better understanding of the observed phenomena and to provide a firm foundation for deriving the conclusions.

CEC Determination

CEC reflects the activity of clay minerals to exchange the ions adhered to the surface (Section 3.2.5). This test was conducted to obtain a very rough estimate of the active clay content in the prepared drilling fluids and allowed comparison of bentonite content in the reference muds and in the cuttings-based mud systems.

A short literature study was performed to identify the best method to determine CEC of clay minerals. API (1990), Burrafato and Miano (1993) and Zhao et al. (1992) described several different measurement techniques for this purpose. Though the mentioned methods may provide quite exact results, it is commonly accepted in the petroleum industry to measure the CEC of the clay particles by means of MBT in accordance with the API standard, which was implemented.

According to the API standard (API, 1990) all organic material, which may react with methylene blue had to be removed by treatment of the mud with hydrogen peroxide and sulfuric acid. However, when having a mixture of water and clay/cuttings material only, this step may be omitted. Methylene blue was then added to the mixture in 0.5 cm³ increments and one drop of the mixture was transferred to filter paper until a stable blue ring developed around the solids on the filter paper. Based on the test result the approximate amount of bentonite in the sample was estimated using the correlation provided by API (1990) (Eq. B-1):

$$\text{Bentonite equivalent, kg/m}^3 = \frac{14.25 V_{MB}}{V_M} \quad (\text{Eq. B-1})$$

where, V_{MB} is consumed methylene blue volume in cm³ and V_M is mud volume in cm³.

pH Value

The concept of pH was introduced in this thesis in Section 3.2.4, where detailed theoretical description of it was given. This measurement was carried out by a pH electrode calibrated in accordance with the API standards (API, 1990).

Chloride Content

This test was carried out to determine concentration of Cl⁻ ions in the mud filtrate, which had been obtained during the API filter loss test. The concentration of chloride ions was of interest for this work, as too high concentrations would hinder the hydration of possible active clays present. The main principle for determination was titration using 0.0282N solution of AgNO₃. Here chromate ions were used as indicator, as these would react with silver ions after all Cl⁻ ions had been precipitated from the solution. This resulted in the change of color of the solution from yellow to orange-red. Chloride content was calculated based on the amount of silver nitrate consumed according to Eq. B-2 (API, 1990):

$$[Cl^-] = \frac{1000 \cdot V_{AgNO_3}}{V_{filtrate}} \quad (\text{Eq. B-2})$$

where, $[Cl^-]$ is concentration of chloride ions in filtrate in mg/l, V_{AgNO_3} is volume of nitrate consumed in ml and $V_{filtrate}$ is volume of filtrate used in the analysis in ml.

Total Hardness as Calcium

Hardness in mud filtrate occurs due to the presence of Ca^{2+} or Mg^{2+} ions. The total hardness is reported normally only as Ca^{2+} ions concentration in filtrate. The amount of metal ions was determined by titration in the presence of the indicator where ethylenediaminetetraacetic acid (EDTA) was used as acid (sometimes salts of EDTA are as well used for titration). The acid and the indicator react with metal ions and create complex compounds. At the equilibrium point the free indicator would be present in the solution and the color change would be observed. The total hardness as calcium was calculated based on the EDTA amount consumed using Eq. B-3 (API, 1990):

$$[Ca_{total}^{2+}] = \frac{400 \cdot V_{EDTA}}{V_{filtrate}} \quad (\text{Eq. B-3})$$

where, $[Ca_{total}^{2+}]$ is total hardness as calcium in filtrate in mg/l and V_{EDTA} is volume of EDTA consumed in ml.

Ca^{2+} Ions Concentration

The concentration of Ca^{2+} ions in the filtrate was determined using similar procedure as for determination of total hardness as calcium. However, in this case 1 ml of 8M NaOH solution was added to the diluted filtrate sample to increase the pH value of the solution to 12-13. It is reported that at this pH value Mg^{2+} ions are removed from the mixture by precipitating as $Mg(OH)_2$ (API, 1990) and further titration with EDTA will measure only Ca^{2+} ions. After the titration with EDTA was concluded, Ca^{2+} ions concentration could be calculated using Eq. B-3.

Mg^{2+} Ions Concentration

Concentration of Mg^{2+} ions in the solution was calculated by finding the difference between total hardness as calcium value and Ca^{2+} ions concentration. The concentrations needed to be converted into mole/l and the difference was multiplied by the atomic weight of Mg^{2+} ion. As the approximate atomic weight of Ca^{2+} ion is equal to 40, while that of Mg^{2+} ion to 24, the total concentration of the latter in the filtrate can be found according to Eq. B-4 (API, 1990):

$$[Mg^{2+}] = 0.6 \cdot ([Ca_{total}^{2+}] - [Ca^{2+}]) \quad (\text{Eq. B-4})$$

where, $[Mg^{2+}]$ is concentration of magnesium ions in mg/l and $[Ca^{2+}]$ is calcium ion concentration as determined from Ca^{2+} chemical test.

Filtrate Alkalinity

The filtrate alkalinity test was conducted to identify the type of anions that contributed to the filtrate's pH value. This test is rather simple, but according to API (1990) provides good results on mud systems without thinners (no thinners were implemented in this work). Here two titrations using 0.01M H₂SO₄ on diluted with 25 ml distilled water filtrate samples were performed, first using phenolphthalein as indicator and then using methyl orange on the same sample. The former has equilibrium point at pH=8.3 while the latter one at pH=4.3. The alkalinity is reported as P_f and M_f values, which correspond to the amount of acid consumed to reach the corresponding pH values. As the color change of indicators was obvious pH measurements were not performed during the tests. Based on the recorded P_f and M_f concentration of the anions present in the filtrate were calculated as given in Table B-1 (API, 1990).

Table B-1. The correlations for determination of OH⁻, CO₃²⁻ and HCO₃⁻ ions concentration in mud filtrate

	[OH ⁻], mg/l	[CO ₃ ²⁻], mg/l	[HCO ₃ ⁻], mg/l
P _f =0	0	0	1220M _f
2P _f <M _f	0	1200P _f	1220(M _f - 2P _f)
2P _f =M _f	0	1200P _f	0
2P _f >M _f	340(2P _f - M _f)	1200(M _f - P _f)	0
P _f =M _f	340M _f	0	0

Lime Content in Mud

The content of lime in the new drilling fluids was of interest since drilling cuttings supplied by TWMA were recovered after drilling with an OBM, where lime had been added to activate surfactants (Section 3.3.2). The lime content was determined by titration of diluted filtrate sample (1ml of filtrate was diluted with 49 ml of water) with 0.01M H₂SO₄ using phenolphthalein as indicator. The color change at the equilibrium was not easily observable and the equilibrium point was verified by pH measurements with a pH-meter to yield more exact results. Mud alkalinity is reported as P_m, which is the volume of sulfuric acid consumed. The total lime content in mud was estimated according to Eq. B-5 (API, 1990):

$$[Ca(OH_2)] = 0.742 \cdot (P_m - F_w \cdot P_f) \quad (\text{Eq. B-5})$$

where, [Ca(OH)₂] is estimated lime concentration in kg/m³ and F_w is water fraction of mud, which is calculated as shown in Eq. B-6:

$$F_w = \frac{V_{water}}{V_{mud}} \quad (\text{Eq. B-6})$$

where, V_{water} is the volume of water in mud and V_{mud} is the total mud volume.

Appendix C. Rheological Models

Viscometer measurements were used to build drilling fluid consistency curves by implementation of different model approximations. Rheological models were first introduced in Section 3.2.2. The Bingham, Power Law and Herschel-Bulkley models were considered for generating viscosity curves.

Bingham Model

PV, YP and AV were directly determined by the viscometer measurements at 600 and 300 RPM using the Bingham model according to Eq. C-1, Eq. C-2 and Eq. C-3 (API, 1990):

$$PV = \theta_{600} - \theta_{300} \quad (\text{Eq. C-1})$$

$$YP = 0.511 \cdot (2 \cdot \theta_{300} - \theta_{600}) \quad (\text{Eq. C-2})$$

$$AV = \frac{\theta_{600}}{2} \quad (\text{Eq. C-3})$$

where, PV is plastic viscosity in cP, YP is yield point value in Pa, AV is apparent viscosity in cP, θ_{600} and θ_{300} are the viscometer readings at 600 and 300 RPM respectively.

Power Law Model

Power law index, n, and consistency index, K, as used in the power law model were calculated according to Eq. C-4 and Eq. C-5 (Azar and Robello Samuel, 2007):

$$n = 3.32 \cdot \log \frac{\theta_{600}}{\theta_{300}} \quad (\text{Eq. C-4})$$

$$K = \frac{\theta_{600}}{\dot{\gamma}_{600}^n} = \frac{\theta_{300}}{\dot{\gamma}_{300}^n} \quad (\text{Eq. C-5})$$

where, $\dot{\gamma}_{600}$ and $\dot{\gamma}_{300}$ are shear rates at 600 and 300 RPM respectively expressed in s^{-1} .

Herschel-Bulkley Model

The same parameters (n and K) were calculated, however, differently for Herschel-Bulkley model. The so-called zero gel strength was calculated first as shown in Eq. C-6 (from IPT, 2012).

$$\theta_0 = 2 \cdot \theta_3 - \theta_6 \quad (\text{Eq. C-6})$$

where, θ_0 is zero gel strength in $^\circ$, θ_3 and θ_6 are 6 and 3 RPM readings on the viscometer respectively in $^\circ$.

The power law and consistency indexes for Herschel-Bulkley model were calculated according to Eq. C-7 and Eq. C-8 (from IPT, 2012):

$$n = 3.32 \cdot \left(\frac{\theta_{600} - \theta_0}{\theta_{300} - \theta_0} \right) \quad (\text{Eq. C-7})$$

$$K = 0.511 \cdot \left(\frac{\theta_{600} - \theta_0}{\gamma_{600}^n} \right) = 0.511 \cdot \left(\frac{\theta_{300} - \theta_0}{\gamma_{300}^n} \right) \quad (\text{Eq. C-8})$$

The yield stress of the drilling fluid in Pa is calculated by multiplying zero gel strength, which is measured in degrees by the factor of 0.511 (Eq. C-9).

$$\tau_0 = 0.511 \cdot \theta_0 \quad (\text{Eq. C-9})$$

where, τ_0 is the yield stress in Pa.

Coefficient of Correlation

The coefficient of correlation based on the least square method was calculated for all designed spud mud systems in E1, E2, E3 and E4. This was done in order to identify the model, which described the measured data best. The model, which yielded the highest coefficient of correlation, was used to build the viscosity curve of the fluid. These equations are slightly modified versions of the equations presented by Alder and Roessler (1977) and provide the same result. For the Bingham model the measured values were used directly in the equation for the coefficient of correlation due to the linearity of the model (Eq. C-10):

$$R = \frac{n \cdot \sum \dot{\gamma} \cdot \theta - \sum \dot{\gamma} \cdot \sum \theta}{\sqrt{[n \cdot \sum \dot{\gamma}^2 - (\sum \dot{\gamma})^2] \cdot [n \cdot \sum \theta^2 - (\sum \theta)^2]}} \quad (\text{Eq. C-10})$$

where, R is correlation coefficient, n is number of measurements taken by Fann VG 35 viscometer, $\dot{\gamma}$ is shear rate in s^{-1} and θ is shear stress in Pa.

On the other hand, the power law and the Herschel-Bulkley models were linearized by taking the logarithm of the both sides of Eq.4 and Eq.5. The coefficients of correlation for these two models were calculated according to Eq. C-11 and Eq. C-12.

$$R = \frac{n \cdot \sum \log \dot{\gamma} \cdot \log \theta - \sum \log \dot{\gamma} \cdot \sum \log \theta}{\sqrt{[n \cdot \sum (\log \dot{\gamma})^2 - (\sum \log \dot{\gamma})^2] \cdot [n \cdot \sum (\log \theta)^2 - (\sum \log \theta)^2]}} \quad (\text{Eq. C-11})$$

$$R = \frac{n \cdot \sum \log \dot{\gamma} \cdot \log (\tau - \tau_0) - \sum \log \dot{\gamma} \cdot \sum \log (\tau - \tau_0)}{\sqrt{[n \cdot \sum (\log \dot{\gamma})^2 - (\sum \log \dot{\gamma})^2] \cdot [n \cdot \sum (\log (\tau - \tau_0))^2 - (\sum \log (\tau - \tau_0))^2]}} \quad (\text{Eq. C-12})$$

where, τ is shear stress in Pa and τ_0 is yield stress in Pa calculated by Eq. C-9.

Appendix D. Correlation Coefficients of the Measured Viscometer Data

The coefficient of linear correlation of each rheological model based on the least squares methods were calculated using Eq. C-10, Eq. C-11 and Eq. C-12 presented in Appendix C to identify the model describing the measured points best. These coefficients are shown in Table D-1, which summarizes all designed fluids in the experiments.

Table D-1. The summary of the linear correlation coefficients based on the different rheological models

Fluid type	Bingham plastic	Power law	Herschel Bulkley
B REF	0.9722	0.9808	0.9965
C75	0.9653	0.9756	0.9790 ³
C100	0.9838	0.8824	0.8824
C125	0.9940	0.9348	0.9480
C150	0.9519	0.9965	0.9920
C75 CMC0.7	0.9899	0.9830	0.9910 ³
C75 CMC1.0	0.9848	0.9761	0.9809 ³
C75 CMC1.3	0.9943	0.9862	0.9862
C75 CMC1.6	0.9895	0.9932	0.9958 ³
C75 PAC1.0	0.9932	0.9866	0.9909 ³
B CMC REF	0.9764	0.9828	0.9952
C75 X1.0	0.9744	0.9916	0.9955
C75 X1.2	0.9681	0.9873	0.9968
C75 X1.4	0.9707	0.9874	0.9972
C75 X1.6	0.9679	0.9867	0.9967
C100 X1.2	0.9730	0.9895	0.9975
C125 X1.2	0.9782	0.9894	0.9976
C150 X1.2	0.9812	0.9880	0.9980
C75 X1.0 SW	0.9555	0.9961	0.9960
C75 X1.2 SW	0.9667	0.9929	0.9973
C75 X1.4 SW	0.9648	0.9885	0.9976
C75 X1.6 SW	0.9689	0.9885	0.9964
C100 X1.2 SW	0.9667	0.9929	0.9973
C125 X1.2 SW	0.9736	0.9904	0.9981
C150 X1.2 SW	0.9740	0.9891	0.9985
C75 X1.4 B SW	0.9646	0.9921	0.9985
C100 X1.4 B SW	0.9713	0.9870	0.9996
C75 X1.4 CMC LV SW	0.9660	0.9918	0.9995

³ Since τ_0 was equal to 3 and 6 RPM readings the coefficient of correlation was calculated based on four measurements only

Appendix E. Zeta Potential Measurement Reports



Generated from: AcoustoSizer II v3.27

GENERAL DATA Measurement Time: Tue, 11 February 2014 16:21:16 Background Data: Not used Thermal Properties: Not used		Analyse Time: Tue, 11 February 2014 16:31:00 Std Calibration Time: Tue, 11 February 2014 14:58:06	
PARTICLE DATA ID: kaolinite (aluminosilicate) Density: 2.6 g/mL Concentration: 0.28 wt% Dielectric Const.: 2.5 Specific Heat: J/(kg.K) Thermal Cond.: W/(m.K) Thermal Expan. Coeff.: (10 ⁻⁴)/K Speed of Sound: m/s Intrinsic Atten. Coeff. (a): ((10 ⁻¹⁹),np.s ² /m) Intrinsic Atten. Expon. (n):		SOLVENT DATA ID: Water Density: 0.9979 g/mL Dielectric Const.: 80.4 Specific Heat: J/(kg.K) Thermal Cond.: W/(m.K) Thermal Expan. Coeff.: (10 ⁻⁴)/K Speed of Sound: 1483 m/s Intrinsic Atten. Coeff. (a): ((10 ⁻¹⁹),np.s ² /m) Intrinsic Atten. Expon. (n):	
SIZE & CHARGE ANALYSIS Distribution Function: Lognormal ESA Size Analysis (µm): d50 = 0.217 Atten. Size Analysis (µm): d50 = -1,000 Zeta Potential: -35 mV Smoluchowski Zeta Potential: -17 mV Median ka: 16.2		ENVIRONMENTAL DATA pH: 10.37 Conductivity: 0.0283 S/m Temperature: 21.6 C	
COMMENT No comment entered		d85 = 0.240 d85 = -1,000 d15 = 0.196 d15 = -1,000 Fit error = 30.0% Fit error = -1.0%	

Figure E-1. Zeta potential measurement of the bentonite sample



Generated from: AcoustoSizer II v3.27

GENERAL DATA Measurement Time: Wed, 12 March 2014 11:54:56 Background Data: Not used Thermal Properties: Not used		Analyse Time: Wed, 12 March 2014 11:59:50 Std Calibration Time: Wed, 12 March 2014 10:41:55	
PARTICLE DATA ID: SiO ₂ (quartz) Density: 2.5 g/mL Concentration: 1.5 wt% Dielectric Const.: 4.5 Specific Heat: J/(kg.K) Thermal Cond.: W/(m.K) Thermal Expan. Coeff.: (10 ⁻⁴)/K Speed of Sound: m/s Intrinsic Atten. Coeff. (a): ((10 ⁻¹⁴).np.s ²)/m Intrinsic Atten. Expon. (n):		SOLVENT DATA ID: Water Density: 0.9977 g/mL Dielectric Const.: 80.4 Specific Heat: J/(kg.K) Thermal Cond.: W/(m.K) Thermal Expan. Coeff.: (10 ⁻⁴)/K Speed of Sound: 1491.2 m/s Intrinsic Atten. Coeff. (a): ((10 ⁻¹⁴).np.s ²)/m Intrinsic Atten. Expon. (n):	
COMMENT Final total testing		ENVIRONMENTAL DATA pH: 4.57 Conductivity: 0.0914 S/m Temperature: 22.9 C	
SIZE & CHARGE ANALYSIS Distribution Function: Lognormal ESA Size Analysis (µm): d50 = 2.220 Atten. Size Analysis (µm): d50 = -1.000 Zeta Potential: -7.6 mV Smoluchowski Zeta Potential: -1.6 mV Median ka: 298.9		d85 = 0.504 d15 = -1.000 d85 = 9.768 d85 = -1.000 Fit error = 47.2% Fit error = -1.0%	

Figure E-2. Zeta potential measurement of the cuttings sample